

27712

NATIONAL LIBRARY
OTTAWA



BIBLIOTHÈQUE NATIONALE
OTTAWA

NAME OF AUTHOR... THOMAS MICHAEL MORROW.....

TITLE OF THESIS... FREQUENTAL HAIL SAMPLES
..... from ALBERTA HAILSTORMS.....

UNIVERSITY.... UNIVERSITY OF ALBERTA.....

DEGREE FOR WHICH THESIS WAS PRESENTED... MASTER OF SCIENCE

YEAR THIS DEGREE GRANTED... 1976.....

Permission is hereby granted to THE NATIONAL LIBRARY
OF CANADA to microfilm this thesis and to lend or sell copies
of the film.

The author reserves other publication rights, and
neither the thesis nor extensive extracts from it may be
printed or otherwise reproduced without the author's
written permission.

(Signed). Michael Morrow.....

PERMANENT ADDRESS:

11339-76 AVENUE.....

Edmonton Alberta.....

T6G 0K3.....

DATED: 23 JUN 1976

NL-91 (10-68)

INFORMATION TO USERS

THIS DISSERTATION HAS BEEN
MICROFILMED EXACTLY AS RECEIVED

This copy was produced from a microfiche copy of the original document. The quality of the copy is heavily dependent upon the quality of the original thesis submitted for microfilming. Every effort has been made to ensure the highest quality of reproduction possible.

PLEASE NOTE: Some pages may have indistinct print. Filmed as received.

Canadian Theses Division.
Cataloguing Branch
National Library of Canada
Ottawa, Canada K1A ON4

AVIS AUX USAGERS

LA THESE A ETE MICROFILMEE
TELLE QUE NOUS L'AVONS RECUE

Cette copie a été faite à partir d'une microfiche du document original. La qualité de la copie dépend grandement de la qualité de la thèse soumise pour le microfilmage. Nous avons tout fait pour assurer une qualité supérieure de reproduction.

NOTA BENE: La qualité d'impression de certaines pages peut laisser à désirer. Microfilmée telle que nous l'avons reçue.

Division des thèses canadiennes
Direction du catalogage
Bibliothèque nationale du Canada
Ottawa, Canada K1A ON4

THE UNIVERSITY OF ALBERTA

SEQUENTIAL HAIL SAMPLES

FROM ALBERTA HAILSTORMS

by

THOMAS MICHAEL MORROW

A THESIS

SUBMITTED TO THE FACULTY OF GRADUATE STUDIES AND RESEARCH

IN PARTIAL EULFMENT OF THE REQUIREMENTS FOR THE DEGREE

OF MASTER OF SCIENCE IN METEOROLOGY

DEPARTMENT: Geography

EDMONTON, ALBERTA

SPRING, 1976

THE UNIVERSITY OF ALBERTA
FACULTY OF GRADUATE STUDIES AND RESEARCH

The undersigned certify that they have read, and
recommended to the Faculty of Graduate Studies and Research,
for acceptance, a thesis entitled.....
.....
.....
.....
submitted by Thomas Michael Morrow
in partial fulfilment of the requirements for the degree of
Master of Science
in Meteorology.

Edward Dobrowolny

Supervisor

E. H. G. M. G. L.

External Examiner

Date 14 April 1976

ABSTRACT

A method of collecting sequential samples of falling hail was developed and used during the summers of 1973 and 1974. The collectors were mesh screens and had collecting apertures of 0.75 m^2 and 0.58 m^2 , respectively. The collected hailstones were stored in polyethylene bottles, plastic breakers or plastic bags. The collectors were operated from vans working in conjunction with the Alberta Hail Project. Samples were obtained from three storms in 1973 and six storms in 1974.

Several methods of analyzing the collected hailstones for hailstone numbers and size distributions were evaluated. The most commonly used technique was to count and measure manually photographs of the collected hailstone samples. Size distributions produced by this method gave results similar to those obtained from hailpads, and different to a greater extent from those obtained from photographs of the hail lying on the ground.

The resulting size distributions could be described by several density functions or distribution functions. An exponential density function

$$N(D) \delta D = 28,239 e^{-2.00 \delta D}$$

provided the best description of the size distribution of the hail collected during the two years. The function varied from year to year. It was

$$N(D) \delta D = 38.967 e^{-3.8D} \delta D$$

in 1973 and

$$N(D) \delta D = 6.427 e^{-1.8D} \delta D$$

in 1974. Exponential density functions of flux density and hailstone concentration were also calculated, and compared with values found in the literature. A Log-normal distribution was obtained for the collected hail. The Log-normal distribution compared well with other Log-normal distributions found in the literature when the hailstones considered were restricted to those with diameters greater than or equal to 0.5 cm. A power-law size distribution of the form

$$C(D) = k D^{-\alpha}$$

was tried. The values for α varied from 0.13 to 7.1, with a value of approximately 3 for the 1971 hailstones greater than or equal to 0.5 cm only.

Three sets of hailstone samples from three differing hailstorms were selected for a time-dependent analysis. Time changes of size spectra, hailstone flux, hailstone concentration, hailstone mean and median size, and variance from an exponential distribution were studied. The largest hailstones fell during the time of greatest hailstone flux. The size spectra of the samples were

most nearly exponential during the times of greatest hailstone flux.

A simple anisshaft model was developed to predict upper-air hailstone concentrations by extrapolating backwards in time the hailstone concentrations at the ground calculated from the collected samples. The model was applied to samples collected from a large hail storm of 19 August 1974. The model indicated that the hail may have accumulated in the lower part of the updraft, and that the collected hailstones possibly came from two separate hail cells.

ACKNOWLEDGMENT

Many people shared in the creation of this thesis. To them I wish to extend my appreciation.

Dr. E. P. Lozowski, my supervisor, willingly provided moral and financial support throughout these long years. In addition, his clear reasoning and red pens restrained and guided my somewhat erratic flights of fancy in a rational direction.

Drs. R. B. Charlton, A. D. Hage and S. R. Heinelt, other members of the Division of Meteorology, offered helpful advice and intelligent questions, which did not always receive intelligent answers.

Dr. G. G. Goyer of the Alberta Hail Project served as a member of my examining committee.

My fellow students, Alastair Beattie, Lawrence Cheng, Myron Cleskiw, Geoff Strong and Peter Wrenshall, assisted in the collection of the hail samples under the adverse conditions of Alberta hailstorms.

Dr. W. Davis and Norman Tsang of the Department of Computing Science provided their particle counting computer system for the analysis of the 1973 samples.

The Departments of Mechanical and Civil Engineering of the University of Alberta provided cold-room facilities.

The staff of the Alberta Hail Project provided accommodation and equipment in the field as well as expert radio direction in the pursuit of hailstorms.

This experiment was carried out with the financial support of the Atmospheric Environment Service of Canada.

TABLE OF CONTENTS

	PAGE
ABSTRACT	iv
ACKNOWLEDGMENT	vii
LIST OF TABLES	x
LIST OF FIGURES	xi
CHAPTER	
1. INTRODUCTION	1
1.1. Size Distributions	1
1.2. Time-varying Properties of Falling Hail	4
2. FIELD OPERATIONS	6
3. METHODS OF ANALYSIS	15
4. SIZE DISTRIBUTIONS	27
4.1. Exponential Distributions	27
4.2. Log-normal Distributions	40
4.3. Power Law Distributions	46
5. TIME-VARYING PROPERTIES OF FALLING HAIL	51
5.1. Variation of Size Distributions with Time	51
5.2. Variation of Other Parameters with Time	55
5.3. Statistical Significance	68
6. HAILSHAFT MODELING	76
7. SUMMARY AND RECOMMENDATIONS	81
7.1. Summary	81
7.2. Recommendations	84

BIBLIOGRAPHY

87

APPENDIX I.	SAMPLING PROBLEMS	96
APPENDIX II.	MELTING OF FALLING HAIR SPOTS	95
APPENDIX III.	DETAILS OF INDIVIDUAL HAIR SPOT SAMPLES	101
APPENDIX IV.	LOG-NORMAL DISTRIBUTIONS FOR INDIVIDUAL HAIR SPOTS	111
APPENDIX V.	SIZE, FLUX DENSITY AND CONCENTRATION SPECTRA OF SEQUENTIAL HAIR SAMPLES	114

LIST OF TABLES

TABLE	PAGE
1 Comparison of the two sequential sampling systems	12
2 Summary of the useful sequential information samples	14
3 Comparison of the sample masses obtained by weighing and from measured shapes	19
4 Comparison of three hail size distribution sampling techniques made on 12 August 1974	21
5 Comparison of sample measurements obtained by autocorrelation photographic images of hailstones and by measuring their longest dimensions with vernier calipers	22
6 Parameters of the best-fitting cumulative exponential distribution for hailstone samples collected from individual storms	33
7 Distribution parameters for individual sampling locations	43
8 Least-squares fits for log-normal hail size distributions at individual sampling locations	45
9 Least-squares fits for power-law distributions of subsets of the coaggregations of hailstone samples	50
10 Correlation coefficient R between number flux and mean diameter for three sets of storm samples	61
11 Correlation coefficient P between number flux and maximum diameter for three sets of storm samples	63
A1 Radius of a melting hailstone at the ground level after falling from the freezing level	98
A2 Liquid water content produced in the wake of a melting hailstone	99

LIST OF FIGURES

FIGURE	PAGE
1. 1973 Sampling System	7
2. 1974 Sampling System	9
3. Cumulative size distributions of hailstone samples obtained in three different ways	11
4. Reconstruction of the cumulative size distribution of a hail sample taken from the ground near Foremost, Alberta on 22 July 1974	22
5. Size distribution of a hail sample measured by the computerized line scanning system and by hand measurement of the photographic images	24
6. Hailstone size distributions for all sequential samples collected during 1973 and 1974	29
7. Oscillation of accumulative experimental distribution caused by the superposition of several distributions with different characteristics	32
8. Hailstone size distributions for years 1973 and 1974 individually	34
9. Hailstone size distributions at single sampling points in individual storms 1973 and 1974	36
10. Size distributions of all sequential hail samples for the storms of 1973 and 1974 plotted on log-logial axes	41
11. Power law distributions of hailstones collected in 1974	48
12. Hailstone concentration vs. time and diameter, 9 July 1974	55
13. Hailstone concentration vs. time and diameter, 24 June 1974	54
14. Hailstone concentration vs. time and diameter, 18 August 1974	56
15. Number flux as a function of time	59

CHAPTER	TOPIC	PAGE
16	Mean of the size distribution at 80° time	6.0
17	Mean and median diameter at 80° time	6.1
18	Verification of the validity of the method of estimation for the distribution	6.1
19	Value of the beta function exponent and distribution function at different times	6.2
20	Distribution curves at A and C from different times	6.2
21	Arrival distribution in terms of fibre length for the final field	6.3
22	Experiments on initial concentration of seed particles for the final field	6.4
23	The effect of medium on a cumulative exponential distribution	6.4
24	Half-time size distribution at 80° time and the points in individual stages, 18.75 and 19.25 mm for normal law	6.5

CHAPTER I. INTRODUCTION

During the summers of 1973 and 1974 the author was employed by Dr. E. P. Tozer of the University of Alberta to assist in the operation of various field experiments performed in conjunction with the Alberta Hail Project (ALHAP). The work presented here resulted from the sequential hail sampling experiment performed during the two summers. This investigation covers three main areas:

1. the size distributions of the collected hail samples
2. the time-varying properties of the sequential samples
3. modelling the hailfall using the parameters of the collected hail samples.

Because the internal structure of the collected sample was not determined, whether or not the collected particles were actually hailstones also remained undetermined. For this study, the author applies the word "hail" to precipitation consisting of frozen water and disregards the differences between hail, frozen raindrops and graupel. This approach therefore sidesteps the question of whether hailstones smaller than 0.5 cm in diameter actually occur.

1.1. Size Distributions

Several attempts have been made to describe the size distribution of hail by a mathematical relation. The most prevalent

description is an exponential relation of the form

$$N(D) \delta D = N_0 e^{-\Delta D} \delta D \quad (1)$$

where

$N(D) \delta D$ is the number of particles in a diameter interval $D-\delta D$ to D

N_0 is the y-axis intercept of the resulting curve

Δ is the negative slope

D is the diameter.

Equation 1 also applies to rainfall (Marshall and Palmer, 1948).

Exponential distributions for Alberta hail are given by

Douglas (1960, 1965, 1964). His samples were collected in wire mesh baskets and stored in freezers after the end of the hailfall. This collection method may have resulted in the melting off some of the smaller hailstones in his samples. Equation 1 in Douglas' case was

$$N(D) \delta D = 40 e^{-2.93 D} \delta D \quad (2)$$

Luffam and MacLain (1960) give an exponential distribution for hailstones from a severe hailstorm in England. The sizes were obtained from photographs of the hail lying on the ground after the passage of the storm. They give a value of

$\Delta = 2.15 \text{ cm}^{-1}$ for their distribution.

Pedder and Malivoire (1975) obtained sequential hail samples from a Swiss hailstorm. The hailstone sizes were taken from a photograph of 30 seconds of hail collected on a foam rubber pad.

The mean distribution for the hailstones collected from this one storm was found to be

$$N(D) \delta D = 12 e^{-0.42D} \delta D \quad (3)$$

Log-normal distributions are also applied to hail collections.

Barge and Isaac (1973) give log-normal distributions for a sample of hailstones taken from Alberta hailstorms in the summer of 1969. Since they were mainly interested in the shape features of the hailstones, their sample consisted mainly of large hailstones. In their paper, they also presented the data used in Douglas' exponential distributions in a log-normal form.

Another distribution encountered in the literature is a power law distribution of the form

$$C(D) = k D^{-\alpha} \quad (4)$$

where

$C(D)$ is the concentration of the hail in the diameter interval $D - \delta D$ to D

D is the diameter.

Examples can be found in Auer (1972) for hail and graupel from convective cloud systems over the High Plains, and Marwitz (1972) for hail and graupel near a thunderstorm gust front.

1.2 Time-varying Properties

Although hailfall characteristics change greatly with time, some authors (List et al., 1968; Charlton and List, 1972) model hailstorms as steady state phenomena. Douglas (1963) recognizes the problem in his discussion of size distributions: "The major source of error is likely to lie in the assumption that the size distribution remains invariant throughout the period of hailfall. Such invariance is most unlikely..."

Williams and Douglas (1963) report the observed differences in three parameters; rain/hail sequence, occurrence of largest hail, and continuity of hail. Because their results were derived from Alberta Hail Studies (ALHAS) hailcard reports, they were able to examine spatial variations as well as time variations.

Pell (1971) discusses the change with time and space of six hail parameters deduced from ALHAS hail card data. His results apply to the entire history of a hailstorm rather than being restricted to one point, so his conclusions do not relate directly to this study. He concludes that "...Alberta hailstorms seem to be most intense in their youth, becoming more and more dissipated as they pass middle age".

Ulrich (1971) derived the two parameters, Λ and N_0 , of an assumed exponential distribution along with the maximum diameter from Doppler radar spectra of falling hail. He states that the total hailstone concentration for all sizes decreased from 1000 m^{-3} to 10 m^{-3} and the median diameter increased from about 0.1 cm to about 4.0 cm during a period of observation of 8.5

minutes. With regard to N_o and Λ , he says "...the temporal behavior of N_o and Λ implies a size distribution which gradually broadens to hailstones of larger diameters and for which the number of smallest diameter stones is decreasing."

A sequential hail sampling experiment similar in concept to the one reported in this work was performed by Federer and Waldvogel (1975) in Switzerland. They were able to detect the passage of several hail cells during their collecting. Their results show that "of an exponential distribution showed an increasing trend during the course of the storm."

Wisner et. al. (1972) present a time-dependent model of a hail-bearing cloud, in which they state, "...a steady state assumption is appropriate until the formation of hail in the cloud." The model assumes exponential raindrop and hailstone size distributions at all times and employs extensive parameterization of the microphysics. One of the properties was a vertical profile of hail concentration as a function of time. This output showed that the initial hail flux was small, rose to a maximum, then decreased to a minimum. The time of the maximum hail flux occurrence was influenced by melting and evaporation terms, but it was usually in the first half of the hail storm lifetime. This theoretical result can be compared with the hail fluxes derived from this field experiment.

CHAPTER 2. FIELD OPERATIONS

The sequential sampling experiment was planned to operate in conjunction with a mobile photography vehicle operated by the University of Alberta in cooperation with the Alberta Hail Project (ALHAP). The sampling experiment ran during the summers of 1973 and 1974. An account of the hail photography experiment has been given by Lozowski et al. (1975).

The truck used during the summer of 1973 was a rented vehicle and modifications to it were not permitted. Consequently, the sampling equipment was of a very makeshift nature. The catcher consisted of a nylon mesh suspended about 70 cm above the ground by a light metal tubing frame (Figure 1). The nylon mesh had openings of about 0.5 cm. The relatively large mesh size was selected to allow rain to drain through quickly. No hail was ever observed to pass through the net. The net tapered to a spout in the center with an orifice diameter of 5 cm. Since any hail approaching that diameter would have destroyed the net, the spout was considered large enough to accomodate most of the hail expected to be encountered. The spout funnelled into the containers used for storage, which will be described later. The area of the collecting aperture was 0.75 m^2 . The slope of the collecting surface was fairly flat, the surface being held in tension by the weight of the spout only. The resulting slackness of the netting prevented any significant bouncing of the

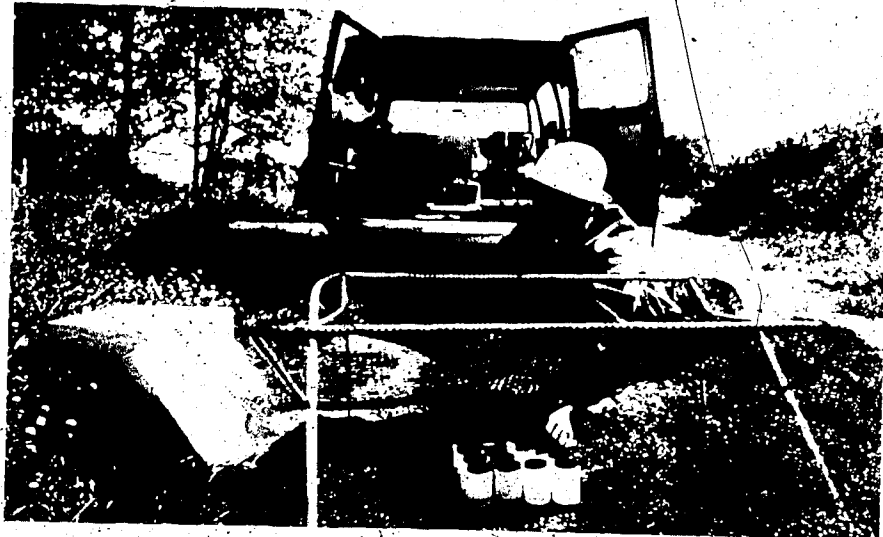


FIGURE 1. The 1975 sequential sampling equipment. In the foreground is the collapsible hail catcher. Below the catcher are several polyethylene bottles containing cooled hexane used to hold the collected hailstones. To the left of the picture is the styrofoam box which stores the sample bottles while in transit. The large white box seen in the back of the van is an extra freezer chest cooled by dry ice.

impacting hail. This catcher was collapsible and was carried along one wall of the van. When a stop was made for sampling or photography, it was set up in a convenient spot near the truck. Sampling could begin within 30 seconds of stopping the truck.

No special effort was made to level the catcher, but it was probably within 5 degrees of horizontal in all sampling situations.

In 1974 the University was supplied with its own truck, to which modifications could be made. The hail catcher was permanently mounted on the roof of the van, with the spout leading to the interior (Figure 2). A similar nylon mesh was used, but with slightly larger openings (0.7 cm) and with a greater percentage of the netting filled in. This material was less desirable than that used the previous year with respect to the opening size and open area, but it was the best available at the time. Because of the permanent mounting of the new catcher, the net had to be stretched tightly to prevent sagging on the roof and accumulation of hail around the spout. Consequently, in order to prevent the hailstones from bouncing out, the net was given a steeper slope. The area of the catcher aperture was 0.58 m^2 and it stood 1 m above the roof of the van and 2.7 m above the ground. The net led to a 7.5 cm opening in the roof and then to a flip-flop gate which could direct the hail to either one of two containers. This gate permitted the rapid changing of the sample containers at accurately controlled times.

Various means were used for storing the samples. The most

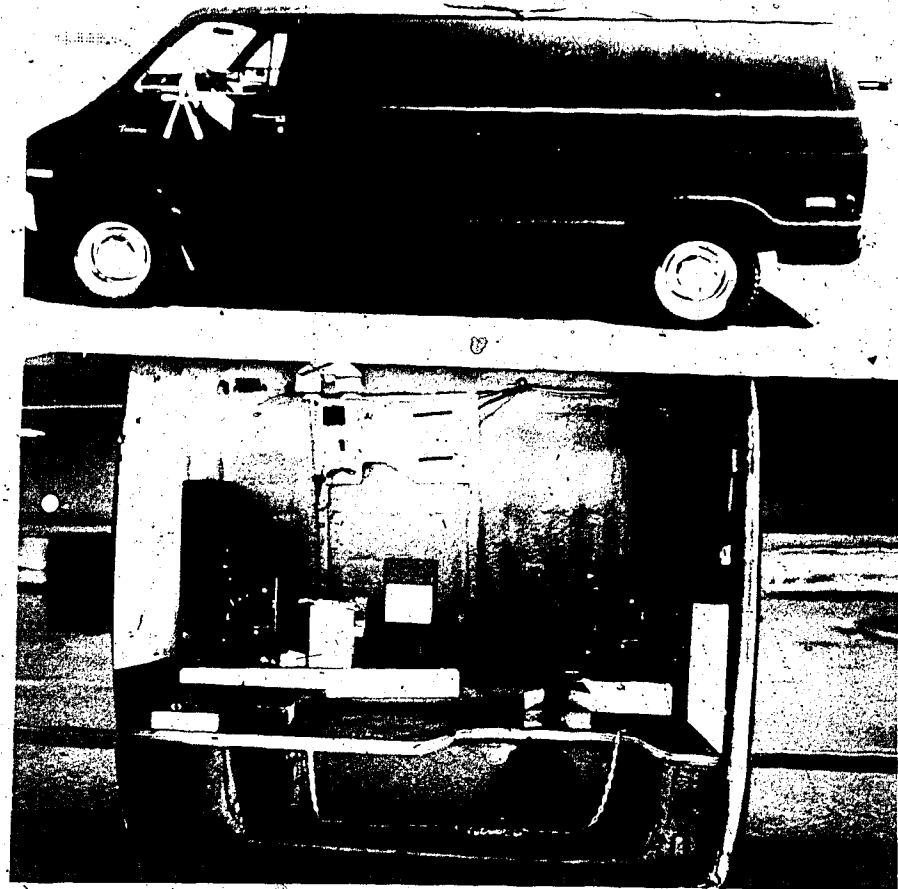


FIGURE 2. The 1974 sequential hail sampling equipment. The top photograph shows the hail catcher permanently mounted on the roof of the van. The lower photograph shows the interior equipment seen through the door on the right side of the van. At the top of the photograph is the catcher drain, with two outputs. Below the drain is a microphone, to the tape recorder. On the left side of the doorway is an electric freezer. The other equipment relates to the hail photography and air sampling equipment.

frequently used method was to collect the hail in 250 ml "polyethylene" bottles containing hexane cooled well below the freezing point of water by dry ice. This method of collection should very rapidly freeze any liquid water in the hailstone thereby preserving the crystal structure and overall mass of the hailstone. This "quenching" of the liquid water distinguished the spongy ice of the hailstone by transforming liquid portions into ice with many fine hairlike bubbles (Knight and Knight, 1968). A few problems were encountered with this method:

Rain water is also collected along with the hail in spite of the holes in the mesh of the catcher, and the rain and hail tend to freeze into a single mass of ice at the bottom of the bottle.

In a heavy shower, the bottle would fill up in about 10 seconds, leaving insufficient time for putting on the lid and storing the bottle before installing another. The hexane evaporates rapidly, and in spite of tight sealing of the bottles, they were frequently dried out when needed. This method was varied

by using 400 ml plastic beakers with cardboard lids supplied by ALUMAP. These were better than the bottles because of their increased capacity and quick lid operation, but the lids did not seal very well and spillage was common. For some storms (notably that of 18 August 1971) plastic bags were used. They had a large capacity, but the spongy ice was not quenched, and collected rainwater tended to melt the hailstones. An attempt was made to separate the rain from the hail in the beakers by inserting squares of metal screen in the beakers at the surface.

of the hexane. The idea was that the hail would collect on the screen, while the rain would sink to the bottom of the beaker and displace the hexane up over the hail. Unfortunately, it did not work that way. The rainwater adhered to the surface of the hailstones, and the result was a frozen mass with a piece of screen imbedded in it.

In both years, the samples were stored in a styrofoam box cooled with dry ice and with a capacity of about 0.1 m^3 . In 1974, the van was also equipped with an electric freezer that was used if the capacity of the box was exceeded.

Although both catchers were successful in collecting sequential samples, they had various disadvantages. The 1973 system was simple and relatively foolproof, but inconvenient and uncomfortable to operate. The 1974 system allowed better timing and faster operation, but the greater complexity increased the chance of mechanical breakdown. The 1973 net could be seen in operation, and interesting hailstones, as well as incipient trouble could be observed. The 1974 net was hidden from view, and could become plugged up or torn without the operator immediately becoming aware of it. The 1973 system required a stationary operating location, while the 1974 system could be operated with the van in motion.

The timing of the sampling was done by wristwatch in 1973, while in 1974 a clock was installed near the output of the catcher. The timepieces were synchronized every few hours with the clock at ALHAP by means of radio time-checks.

The containers were all numbered and the sampling times and numbers were recorded on a tape recorder. The tape recorder broke down a few times, with a resulting loss of the data. The tapes were subsequently transcribed for later reference.

Table 1 compares the two systems.

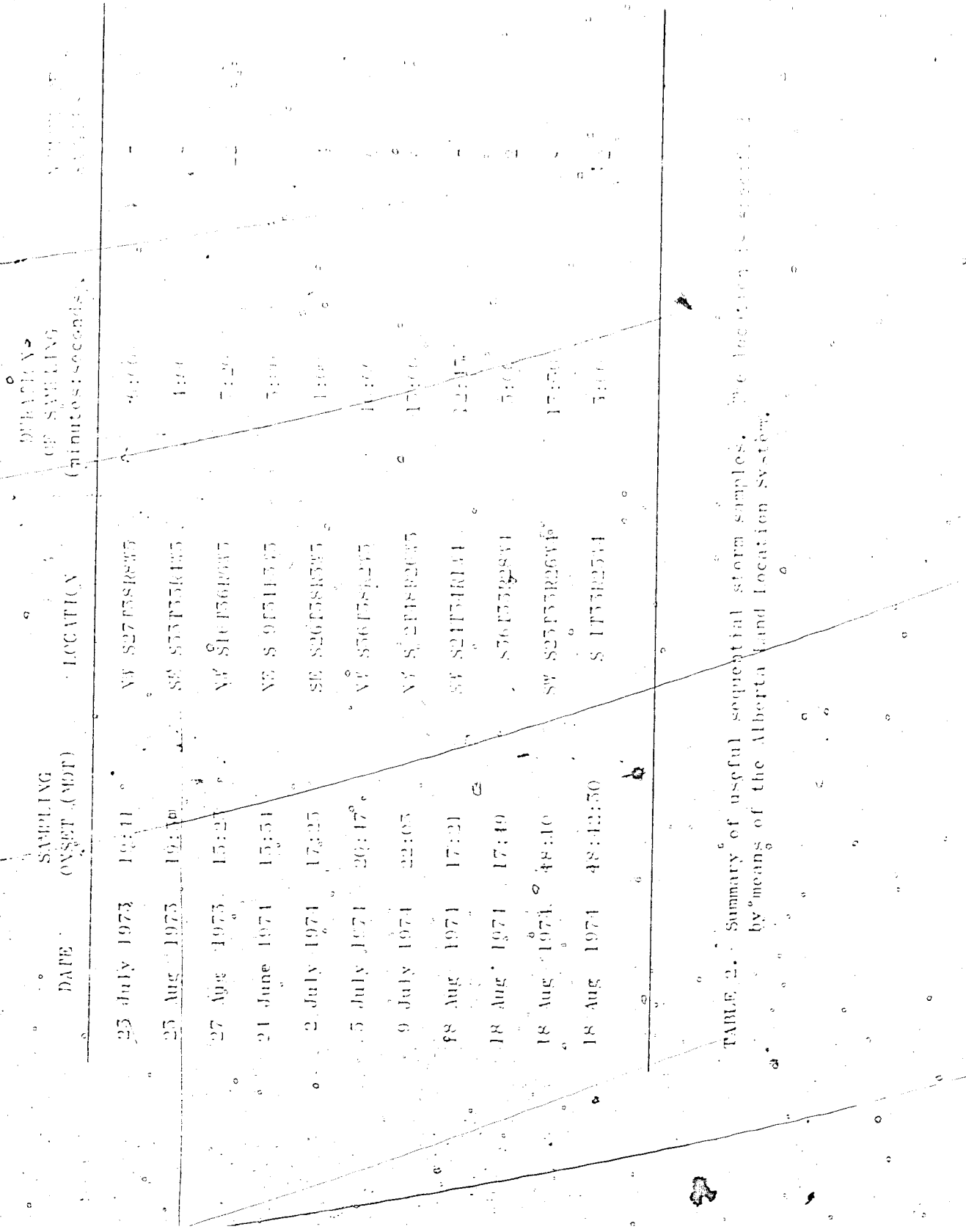
TABLE 1. Comparison of the two sequential sampling systems.

Type	1973 Portable, collapsible	1974 Permanently mounted
Diameter of mesh holes (mm)	5.0	7.0
Area of collecting aperture (m^2)	0.75	0.58
Height of collecting aperture above ground (m)	0.7	2.7
Maximum diameter of collectable hailstone (cm)	5.0	6.0
Time required to switch containers (s)	0.5	0.1
Minimum possible sampling time for one container (s)	15	1
Number of sampling days	6	13
Number of samples collected	58	79

The sampling vehicle used during the two summers operated together with the mobile sampling vehicles of ALHAP. These were directed onto areas of high radar reflectivity as observed on the ALHAP radars. In 1974 the van was also equipped with a radio for monitoring the communications of the seeding aircraft and their controllers. The procedure on a chase was to follow the instructions of the mobile controller at the radar console until the storm was in sight. Subsequently the course of action was determined by the observable features of the storm such as the precipitation shaft, cloud structure, and hail swath.

About 6000 miles were covered in obtaining hail samples during 1973 and 12,000 in 1974. The useful sequential samples are summarized in Table 2.

TABLE 2. Summary of useful sequential storm samples, by means of the Alberta Land Location System.



CHAPTER 3. METHODS OF ANALYSIS

The analysis of the hailstones was carried out in the cold rooms of the Departments of Mechanical and Civil Engineering of the University of Alberta. The sequential samples that were used in the analysis are listed in Appendix 3. The primary objective of the analysis was to measure the numbers and external dimensions of the hailstones in each sample. Several methods were employed in performing these measurements.

The first attempt to determine the size distributions consisted of measuring each hailstone individually. However, holding the hailstones between the fingers melted them significantly and the very large numbers to be processed made this method quite impractical.

The next attempt consisted of photographing each sample spread out on a dark background, and counting and measuring the images. On the suggestion of Geoff Strong (private communication) the facilities of the Department of Computing Science were used for some of the counting. One of the students of the department, Norman Tsang (1971), applied a computerized scanning system to the counting of photographed articles. The procedure involved line scanning an enlarged photograph of the sample with a television camera, followed by digital processing of the video signal. The processed signal was used to reconstruct the photograph on

a monitor. The sensitivity of the system to different light levels from the photograph was adjustable, so that a good representation of the photograph could be obtained. The reconstructed display consisted of a grid of 2000 by 2000 points.

Typically, the area photographed by the film camera was about 0.5 by 0.5 m, with the result that the resolution of the system was about 0.25 mm. The computer generated a number of rectangles, each one being just large enough to enclose a single particle image. The longest dimension of each of these rectangles was determined by the computer and a histogram of the size distribution of these longest sides was printed out. A source of error was introduced by the additional step of photographic enlargement from the negative. The blurring of the images, due to the film grain, added about a 20 percent uncertainty to the measurement of particles with a diameter of 1 mm.

Another major problem was the overlapping of hailstones in the photograph. Since the computer program could not always resolve an overlapped image into two separate hailstones, they were sometimes counted as a single larger hailstone. This prob-

lem was compounded by small ice chips and frost, which reduced the contrast of the photograph. In order to minimize this latter difficulty, most samples to be processed by the computer were sifted by a sieve with a 2 mm mesh size to remove the smaller particles.

This scanning system was used to count most of the samples collected during 1975. The exceptions were those with very few

hailstones which were easily counted and measured by hand, or those where the hailstones were frozen into a block with rainwater and could not be separated. These samples were analyzed by trying to distinguish the individual hailstones on a photograph of the frozen sample and subsequently counting and measuring the images by hand.

There were two major problems with the computerized system.

One is the large error introduced by the inadequate resolution and contrast of the photographs. The other is the arbitrariness of the selection of the sensitivity level for the gray scale, which affected the detection of the small particles and the dimensions of the large hailstones. This system therefore was not employed for the 1974 samples.

The 1974 samples were photographed as before, but the negatives were projected onto a screen and the sizes of the hailstone images were measured by hand. The scale of magnification was adjusted so that the smallest particles of interest (about 2 mm diameter) could be measured with an accuracy of 20 percent.

The hailstones were classified in size intervals of 1 mm.

A ruler was included in all of the photographs to permit an accurate determination of the scale. The dimension measured was the longest linear dimension of the projected image. The reason for this procedure is as follows. A single ellipsoidal hailstone, under the influence of gravity, will most likely assume a position such that its longest dimension is parallel to the flat horizontal surface upon which it lies, and so parallel to the film plane.

The longest dimension is thus easily measured from the photograph.

Further, it was frequently observed that if a hailstone was chipped, the chipping was such that the longest dimension of the hailstone tended to be the most preserved one; and therefore a better representation of the original hailstone than any other dimension. This anisotropic chipping of the hailstones appeared to result from the growth of large ice crystals with their long axes parallel to each other and parallel to the long axis of the hailstone. Since ice will tend to fracture along the boundary of a crystal, chipping on the short axes of hailstones would be possible. Finally, the longest dimension is a representative dimension for deposit and transfer calculations, according to List and Dussault (1967).

The most serious drawback of using the longest dimension as a representative particle diameter is that it gives rise to misleading volume and mass estimates. This error is illustrated in Table 3. The samples were sequential samples from the storm of 18 August 1974 which contained from 10 to 100 hailstones each. The total mass of each sample was both measured directly and also calculated from the photographic distributions using the formula:

$$M = \sum_{k=1}^n N(D_k) \frac{\pi (D - 0.5)^3}{6000} \rho_i \quad (6)$$

where

n = number of millimeter size intervals considered.

$N(D_k)$ = number of hailstones in size interval D_k to D_{k+1} mm.

D_k = image diameter in mm

$\rho_t = 0.89 \text{ g cm}^{-3}$, a typical density for hailstones.

TABLE 5. Comparison of sample masses obtained by weighing and from measured images.

SAMPLE	MEASURED MASS (g)	CALCULATED MASS (g)	VRATIO
0880	53.3	59.8	1.12
0819	12.6	17.8	1.41
0883	4.5	6.1	1.36

The errors are caused chiefly by the nonsphericity of the hailstones, which would lead to an overestimation of the sample mass calculated from the hailstone measurements. The presence of frozen rainwater in the collected samples on the other hand leads to an overestimation of the sample mass obtained by weighing.

Both of these problems were extant on 18 August 1974, so the errors in Table 5 are probably the worst to be expected.

Another comparison of the relation of the longest image dimension to measurements from other sources can be obtained by comparing size distributions of hailstones from the storm of 18

August 1974 which were obtained in several different ways. Data for this comparison came from the hail catcher samples, from hailpads (Strong, 1974), and from photographs of the hail on the ground at the end of the storm. The measurements do not apply to the same hailstones, but to similar samples taken under similar conditions. The samples were separated in space by less than 5 meters, and were of the same 5 minutes of hailfall. Figure 5x

shows the cumulative distributions of the samples, measured by the three methods. Best-fitting straight lines were derived for the graph of the natural logarithms of the cumulative fraction of hailstones against their diameter. Table 4 shows three parameters of these straight lines for the various sampling methods. The hailpad measurements have been converted from dent size to hailstone size using the calibration curve of Strong (1974). Table 11 shows that hailpads and the hail catcher give similar results. Using the longest dimension of a hailstone image as a representative dimension does not appear to result in errors in the size distribution exceeding those involved in the use of hailpads. Photographs of hail on the ground show more extreme differences from hailpads than the catcher samples do, possibly because the photographs were taken after the hail had ceased falling and when it had already melted significantly.

We will now compare size distributions obtained by measuring projected photographs of hail catcher samples with those obtained by measuring the longest dimension of the hailstones directly with calipers. The hailstones were collected from the ground near Trestburg, Alberta on 22 July 1974. Table 5 and Figure 4 compare the two methods of measuring the sample. The results show excellent agreement between the two measuring techniques. The sample consisted of relatively large hailstones. Smaller hailstones would be influenced by melting in the caliper measurements and the discrepancy between the two measuring techniques would be larger.

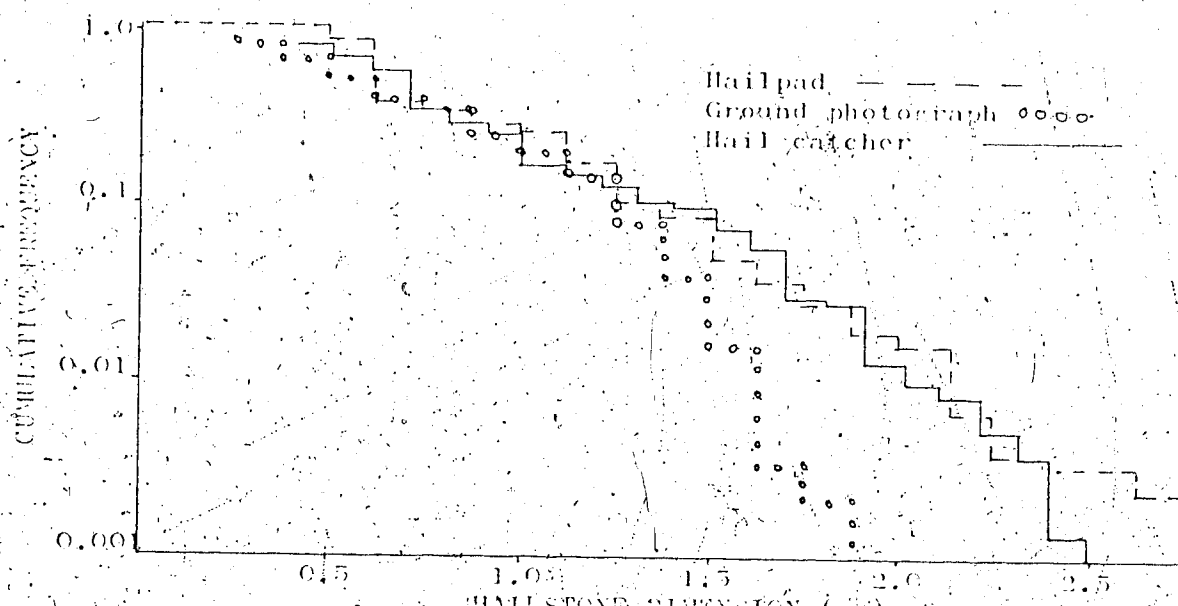


FIGURE 3. Cumulative size distributions of hailstone samples obtained in three different ways. DIMENSION is the hailstone diameter derived from the dent diameter for hailpads, the geometric mean of major and minor axes of the hailstone images for the ground photograph, and the longest dimension for the hail catcher.

Sample technique	Y_0	$M (\text{cm}^{-1})$	s^2
Hailpad	2.55	-2.75	7.02×10^{-5}
Ground photograph	4.93	-3.36	0.102
Hail catcher	2.87	-2.60	5.42×10^{-5}

TABLE 4. Comparison of three hail size distribution sampling techniques used on 18 August 1971. Y_0 is the intercept of the best-fitting straight line with the Y axis. M is the slope of the straight line. s^2 is the variance of the difference between the sample cumulative distribution and the straight line.

	Number of hailstones	Mean diameter (cm)	Standard Deviation (cm)
Band measurement	1810	1.81	0.35
Image measurement	408	1.78	0.39

TABLE 5. Comparison of sample measurements obtained by measuring photographic images of hailstones and by measuring their longest dimensions with vernier calipers.

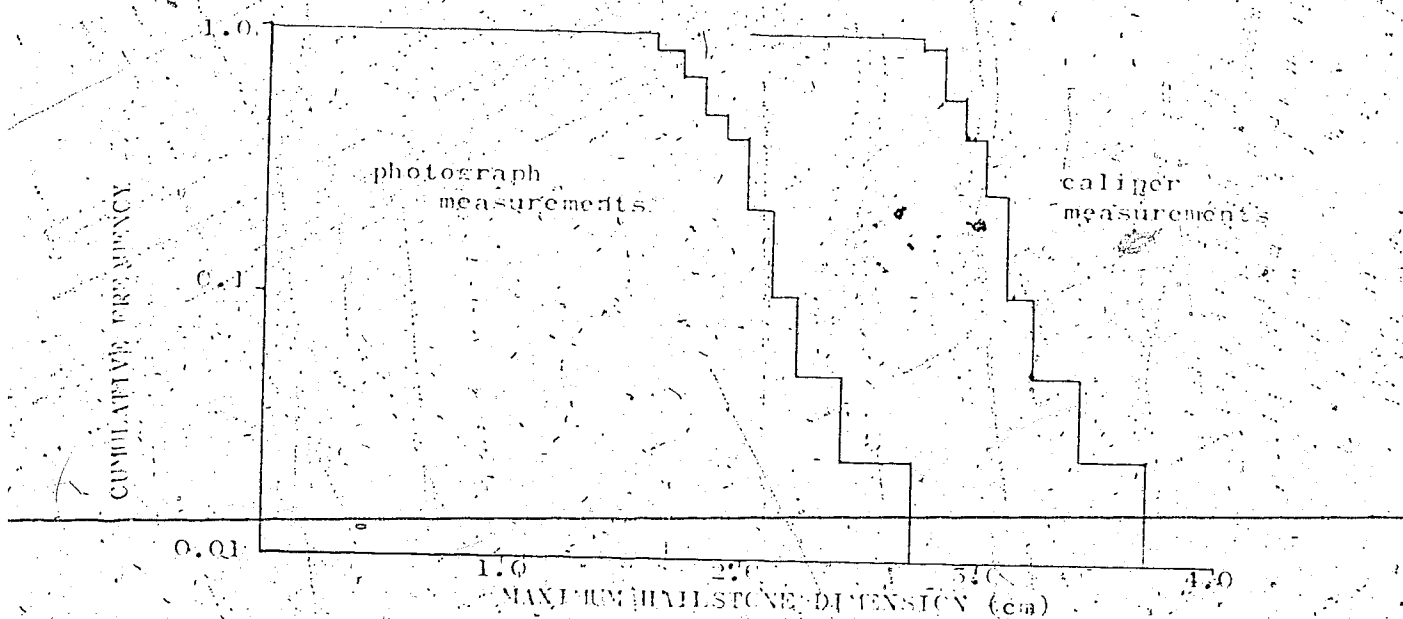


FIGURE 1. Histograms of the cumulative size distributions of a hail sample taken from the ground near Forestdale, Alberta, on 22 July 1971. The caliper-measured histogram is displaced to the right a distance of 1.0 cm along the x axis.

Knowing the accuracy of the measurements obtained using the projected images, the accuracy of the measurements obtained by using the computerized line-scanning system can now be estimated.

Figure 5 shows two histograms of hailstone size distributions for the same sample. One was obtained by measuring the photographic images manually, and the other was generated by the computerized line-scanning system. The same photographs were used in both cases.

The comparison is not very encouraging, because the total numbers and the modal sizes do not agree. The discrepancy is largely attributable to the overlapping of the hailstones, resulting in a large number of hailstones with a diameter of around 0.7 cm being counted as a smaller number of hailstones with diameters from 1.0 to 1.1 cm, by the computer. The larger numbers of particles in the 0 to 0.2 cm range counted by the scanning system are still ice fragments and frost particles that can be recognized and discounted when working manually. The number of hailstones counted by the scanning system was 111, while there were 179 counted by hand. These errors were discovered quite late in this work, and could not be corrected due to the poor focussing and lack of contrast in the photographs of the samples.

Consequently, the size distributions for 1973 should be viewed with caution.

In some cases, the samples were too conglomerated with frozen rainwater to permit separation of all the hailstones.

When this happened, as many hailstones as possible were separated and photographed. The mass of the separated hailstones was then

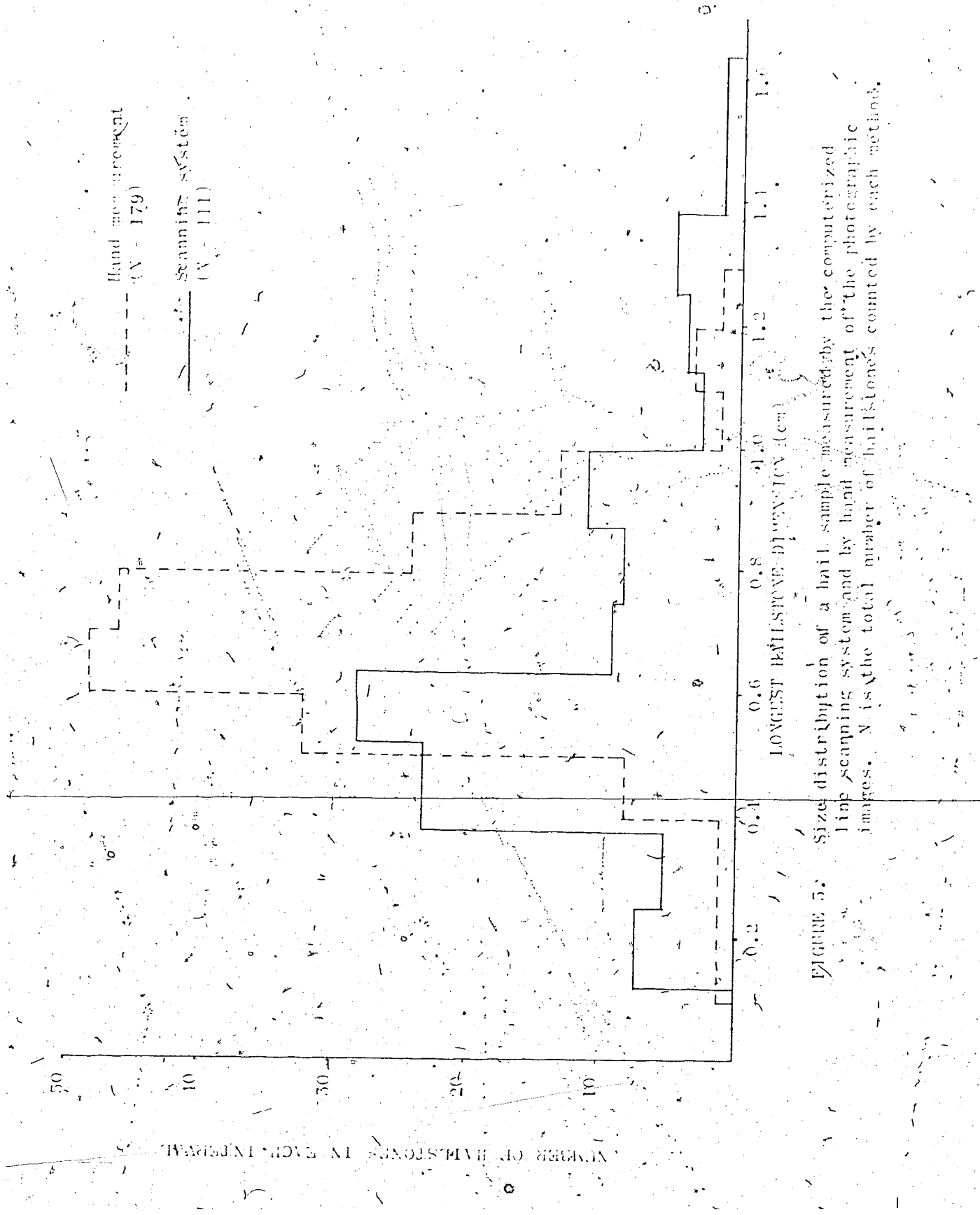


FIGURE 5: Size distribution of a hail sample measured by the computerized line scanning system and by hand measurement of the photographic images. N is the total number of hailstones counted by each method.

measured as well as the total sample mass. The final number of hailstones in each size category was then estimated using the formula:

$$N_d = N_{dp} \cdot \frac{M_s}{M_p} \quad (7)$$

where

N_d is the estimated number of hailstones of diameter $d-1$ to d in the entire sample.

N_{dp} is the number of separated and photographed hailstones in the diameter interval $d-1$ to d .

M_s is the measured mass of the total sample.

M_p is the measured mass of the separated and photographed hailstones.

This was not an entirely satisfactory procedure, because the frozen conglominate consisted largely of rainwater and the smaller hailstones, while the larger hailstones with less mutual contact area would be less likely to stick together and would therefore predominate in the separated hailstones. Thus, the estimated distribution is likely to have an excess of large hailstones, but no way was seen to correct for this. In some cases, the procedure adopted was to prepare a few cross sections of the lump, and to measure the sizes of the individual hailstone cross-sections.

Although the slice may not have passed through the center of all the hailstones in the section, enough embryos were recognizable to indicate many hailstones that had been cut close to their center. Using these hailstones with recognizable embryos,

reasonable size distribution could be obtained. Of course, this procedure does not give the number of hailstones in the entire sample, but an estimate can be made based on the sample mass provided there is not too much rainwater in it. The samples from 9 July 1971 were those most affected by large amounts of rainwater.

There are two conclusions from this chapter that are important for the following work. First, the hail catcher and subsequent storage and analysis can produce results in hail size distributions comparable to those from hailpads. Secondly, the diameters of hailstones may be represented by their longest dimensions without unreasonable errors. For the remainder of this work, the term diameter will be used to mean the longest dimension of a hailstone.

CHAPTER 4. SIZE DISTRIBUTIONS

4.3 Exponential Distributions

One way of representing size distributions of precipitation particles is by means of an exponential density function of the form:

$$N(D) \delta D = N_0 e^{-\Lambda D} \delta D \quad (8)$$

For example, Marshall and Palmer (1948) found, for rainfall:

$$N(D) \delta D = 0.08 e^{-\Lambda D} \delta D$$

$$\Lambda = 41 R^{-0.21} \text{ cm}^{-1} \quad (9)$$

where R is the rainfall rate in mm hr⁻¹.

If the density function is integrated, a cumulative distribution function is the result:

$$N(D) = \int_D^{\infty} N(\mu) d\mu = \frac{N_0}{\Lambda} e^{-\Lambda D} \quad (10)$$

where

$N(D)$ is the number of particles with diameter $\geq D$

$N_T = N_0 / \Lambda$ is the total number of particles in the sample.

This is also an exponential distribution. The average diameter

of the sample is given by:

$$D = \int_0^{\infty} (DN(D) \delta D) / \left[\int_0^{\infty} N(D) \delta D \right] \quad (11)$$

The mean volume is given by:

$$\bar{V} = \frac{\pi}{4} \frac{W^3}{A^3} \quad (92)$$

This is the volume of a spherical storm diameter, the volume from diameter D is given by (Warrich et al., 1973):

$$2 \int_0^{D_0} D^3 N(D) \delta D = \int_0^{\infty} D^3 N(D) \delta D \quad (13)$$

The size distribution of all the rainstorms collected in the sequential samples of the two summers is represented by the graph in Figure 6. This overall distribution is not representative either of an entire storm or of all the storms during a single summer; however, it is probably a fair estimate of the "representative" rainfall spectra for Central Alberta. A straight line was fitted to the measured points of the distribution by the method of least squares giving the following parameters for the cumulative exponential distribution:

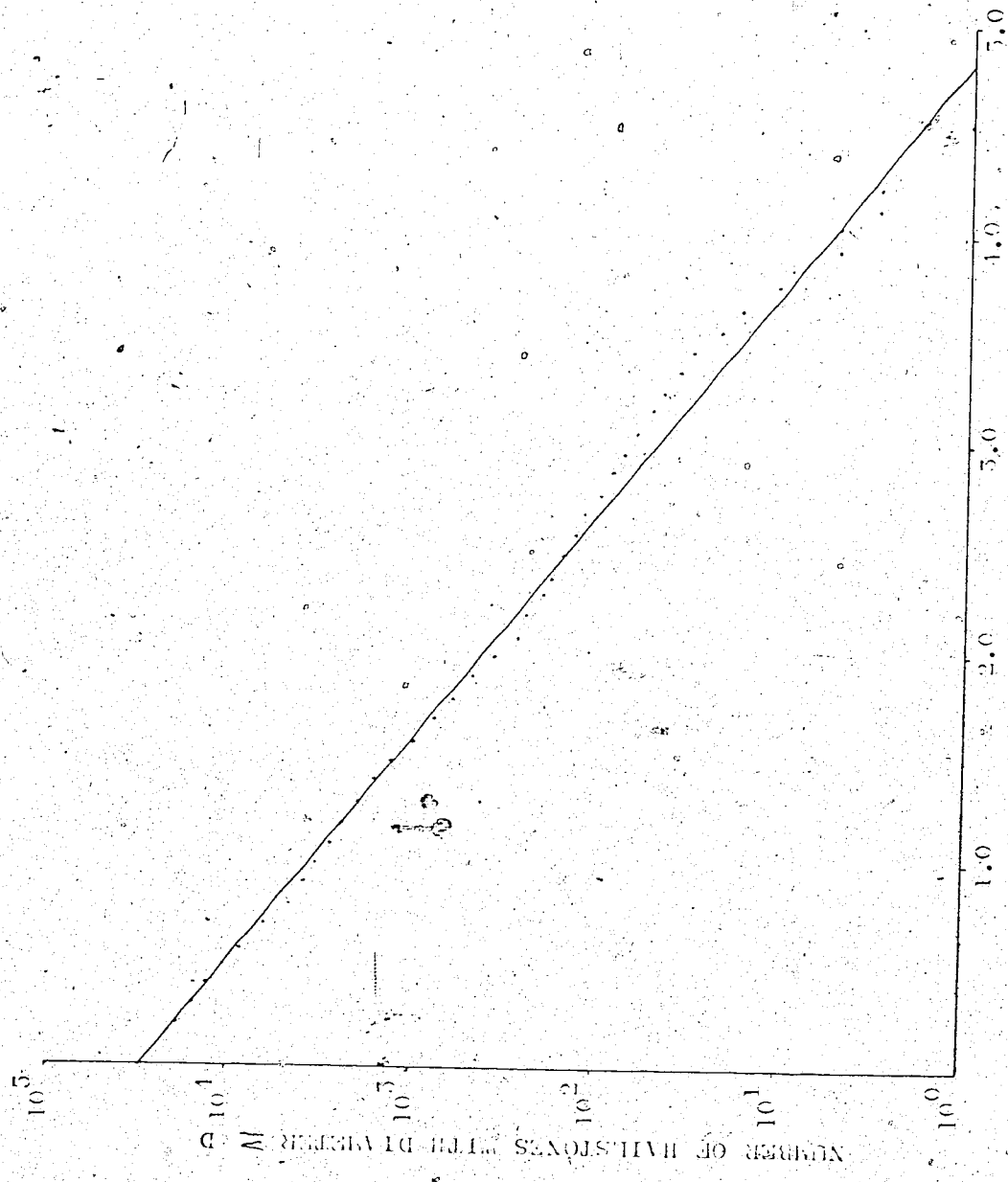


FIGURE 6. Bouldere size distribution for all sequential samples collected during 1975 and 1971. The points are the collected samples. The straight line is the best-fit to an exponential distribution.

$$N_0 = 28,239$$

$$\Delta = 2.0 \text{ cm}^{-1}$$

The total number of hailstones in the sequential samples is then

$$N_t = N_0 / \Delta \approx 14.056 \quad (14)$$

The variance of the collected sample distribution from the cumulative exponential straight line was calculated using the formula:

$$s^2 = \frac{\sum_{i=1}^n [(Y_i - \bar{Y}) - \hat{B}(D_i - \bar{D})]^2}{n-2} \quad (15)$$

where

$$Y_i = \log_{10} N(D)$$

$$\bar{Y} = \frac{1}{n} \sum_{i=1}^n Y_i$$

$$\hat{B} = \Delta / \ln 10$$

and n is the number of size categories. The denominator $(n-2)$ is used to obtain an unbiased estimate of s^2 in the case where two parameters, \hat{B} and $\hat{\Delta} = \bar{Y} - \hat{B}\bar{D}$ are estimated. The resulting variance was $s^2 = 0.0199$.

The main discrepancy between the least squares line and the sample points in Figure 6 occurs for diameters greater than about 2.5 cm.

There are several possibilities for this discrepancy, assuming that an exponential distribution represents the "true" distribution of the hailstones from which the sample was drawn.

1. Assuming that an individual sample has a double exponential size distribution, the oscillations may have been caused by the summation of several samples with different values of Δ . This is illustrated in Figure 7. The narrow distributions may occur for individual hailfalls and will be discussed later.

2. Because of the smaller numbers of the larger hailstones, random fluctuations in the numbers collected would produce relatively larger errors than for the smaller hailstones. But fluctuations in the numbers collected do not appear to be random at diameters greater than 2.5 cm. Instead, there is almost a continuous wave.

3. Almost all of the larger hailstones came from two sampling locations of 18 August 1974. On both of those occasions, the catcher net was torn, and some of the hailstones, both large and small, could have been lost. The collecting area lost due to the tears was probably less than 40 percent.

An exponential distribution was fitted to the samples for each year and for each sampling location with the results shown in Table 6 and in Figure 8. The maximum size of hailstone collected in 1974 was about twice that of 1973, while the total number of hailstones collected during 1973 was almost three times

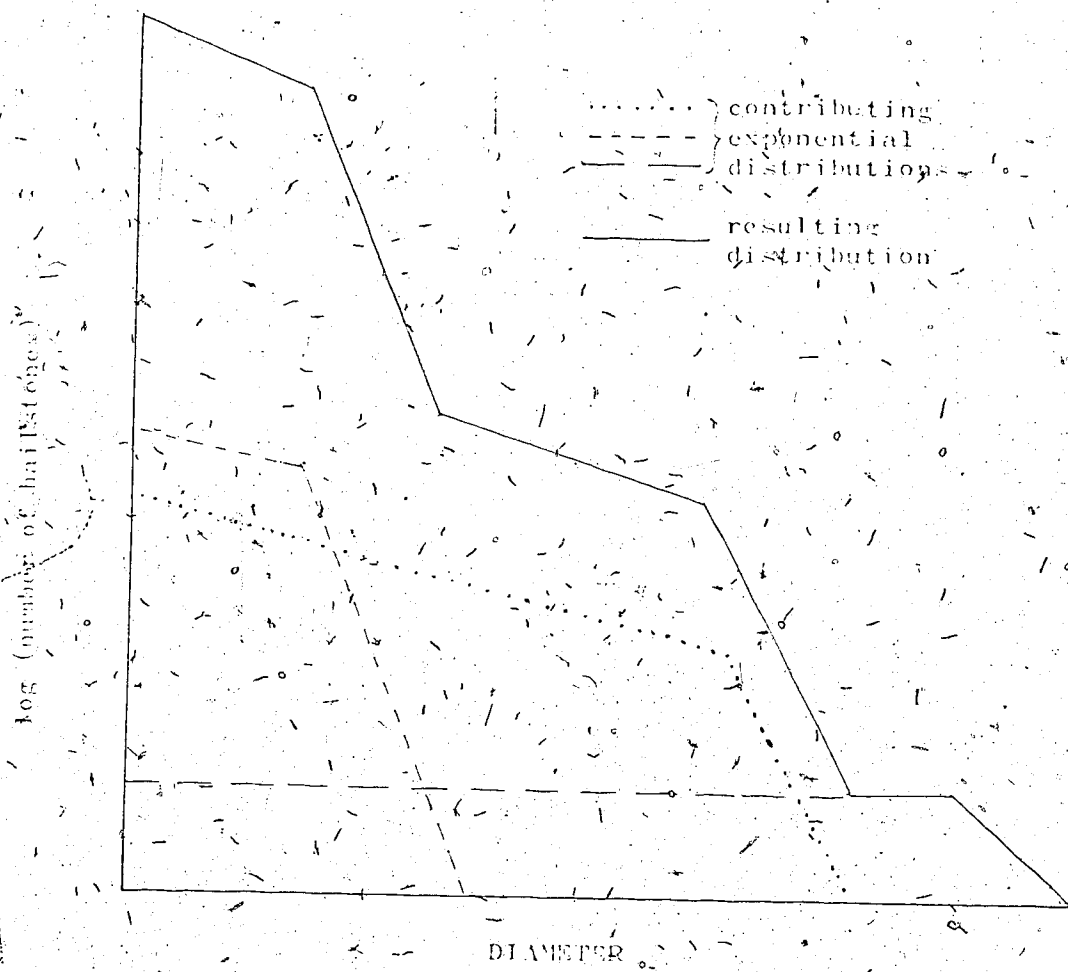


FIGURE 7. Oscillation of a cumulative exponential distribution caused by the superposition of several distributions of differing characteristics.

TABLE 6. Parameters of the best-fitting cumulative exponential distributions for hailstone samples collected from individual storms during 1973 and 1974.

SAMPLE DATE	N _T	(cm ⁻¹)	γ_0 (cm ⁻¹)	VARIANCE
ALL	14,056	2.01	—	28.329
1973	16,383	5.25	—	58.967
1974	5,823	1.75	—	6.127
23 July 1973	970	4.61	—	40.05
25 Aug. 1973	3,311	3.52	—	6.062
27 Aug. 1973	8,099	3.5	11.765	0.027
21 June 1974	147	2.85	—	0.002
2 July 1974	132	1.08	—	0.097
5 July 1974	712	5.85	—	5.58
9 July 1974	210	5.57	—	0.95
18 Aug. 1974	512	1.08	4.177	0.61
18 Aug. 1974	22,317	2.49	5.53	0.02
			15.099	0.083
			15.099	0.09

TABLE 6. Parameters of the best-fitting cumulative exponential distributions for hailstone samples collected from individual storms during 1973 and 1974.

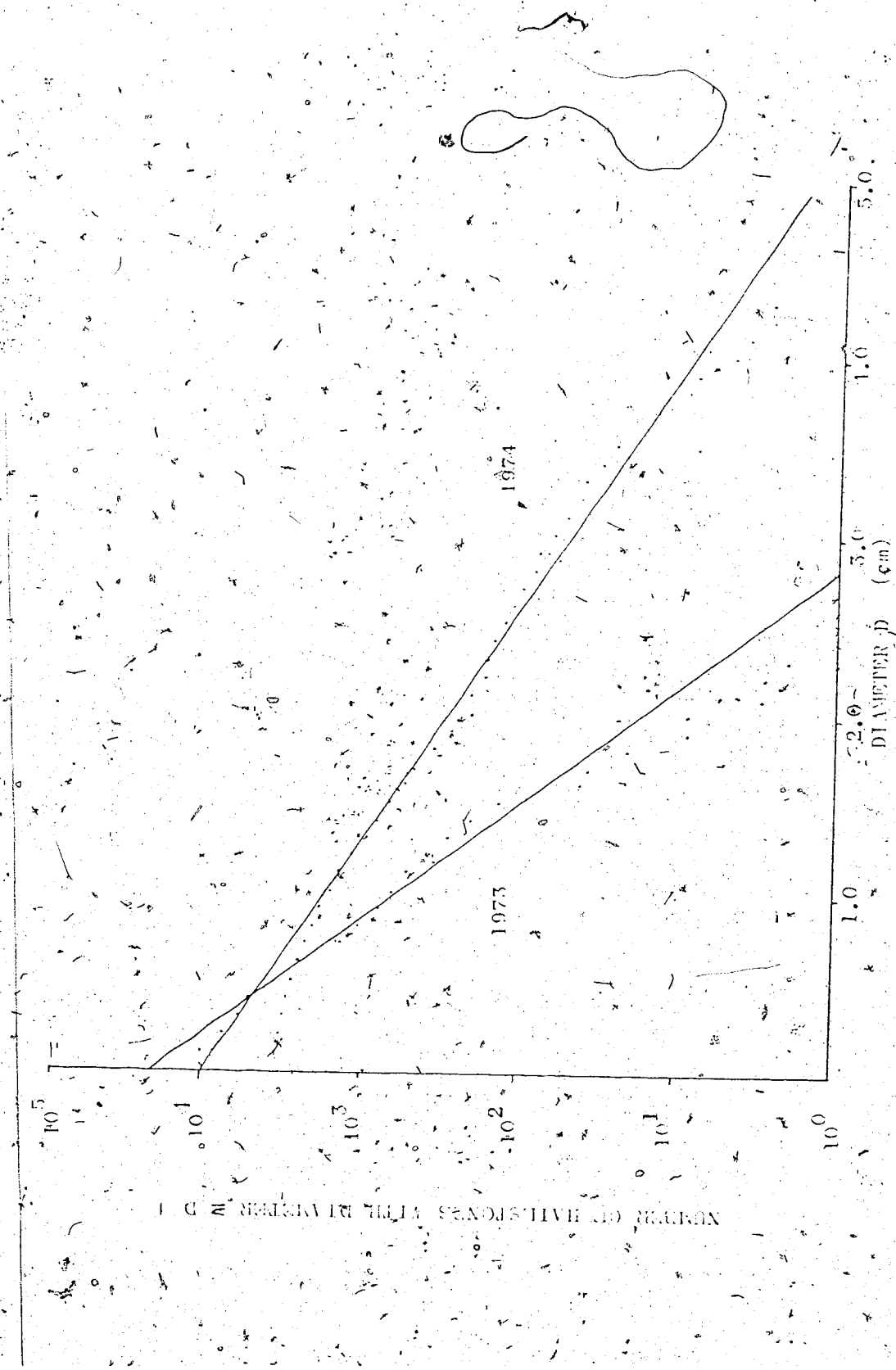
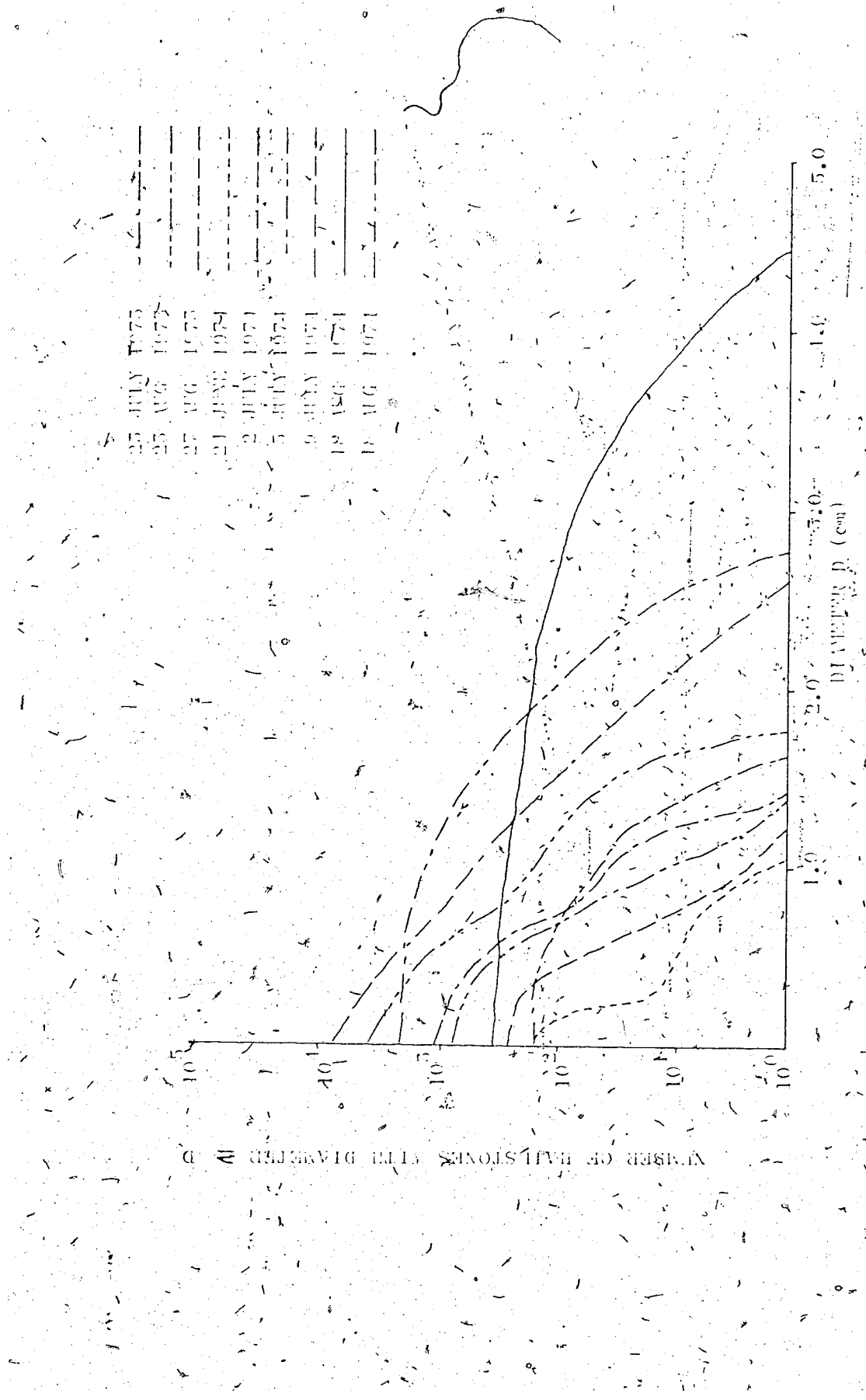


FIGURE 8. Hailstone size distributions for years 1973 and 1974 individually. The points indicate the collected samples. The lines are the best-fitting exponential distributions.

that collected in 1971. These differences can be attributed mostly to chance variations in the sampling occurrences and locations, rather than to climatological factors.

The results for the samples taken at single sampling sites in individual storms are also shown in Table 6. The values of Δ are generally greater in individual samples than they are for the total samples or for the yearly samples. This indicates that the size spectrum tends to be narrower for a single sampling location in an individual storm than it is for all the samples taken together. This fact is also pointed out by Auer and Marwitz (1972), who say: "...the size distribution of hail at a point from an individual storm is relatively narrow (almost monodisperse). . . . the Marshall-Palmer type of size distribution should not be expected throughout the storm." The cases observed in this work tend to corroborate the observations of Auer and Marwitz. The variance of the individual point samples from an exponential distribution is greater than that for the entire sample. This suggests, in agreement with Auer and Marwitz, that a cumulative exponential distribution is not as representative of a single-storm point-size distribution as it is of a sum of several hail samples. The relatively large variances of 0.08 and 0.09 for 18 August 1971 are perhaps indicative of the small number of hailstones collected, or of sorting by size by the storm catcher. The value of 0.69 for 21 June 1971 does not seem to be an experimental error, as that was one sampling occasion when everything worked well. Referring to Figure 9, it can be seen that the large variance results principally from a decrease



High stone size distributions at single sampling sites in individual storms (075-194). The parameters of the best-fitting exponential distributions were available.

FIGURE 9.

in the number of hailstones from the expected exponential distribution number in the size categories from 0.3 to 0.6 cm.

One feature that may be seen from Figure 8 is the flattening of the 1971 distribution at the smallest sizes. This is also evident in the curves for the individual storm samples, shown in Figure 9. This feature is characteristic of many of the sample distributions and it is poorly described by the cumulative exponential distribution. Reasons for the absence of smaller hailstones were offered in Chapter 5. From personal observation, there seems to be a relative scarcity of the smaller hailstones at the ground. A possible explanation of the absence of small hailstones is melting below the freezing level of the storm.

This hypothesis is considered in detail in Appendix 2. The conclusion is that melting can indeed remove some of the smaller hailstones from an initial exponential distribution at the freezing level. This also results in a change in the shape of the observed distribution.

Comparing the numbers of hailstones for each sample would be useful for estimating the relative intensities of different hailfalls during the sampling period. However, comparison of the total numbers is not very meaningful because the sampling times vary. This complication can be avoided by considering the mean flux density I of each sample:

$$I(D) = N(R)/A \delta t \quad (16)$$



where

$N(D)$ is the number of hailstones of diameter $D - \delta D$ to D collected in a sampling time δt .

A is the collector aperture area.

Values for A and δt are given in Chapter 2 and in Appendix 3.

The calculated values for the flux density of each sample are given in Appendix 3 and will be considered in detail in Chapter 5.

Exponential distributions were fitted to the flux density values using the least squares method. The parameters of these exponential distributions are given in Appendix 3. These results indicate a range of flux densities of over two orders of magnitude up to almost $10^4 \text{ m}^{-2} \text{ min}^{-1}$.

The mean concentration C of hail (number per cubic meter) is given by:

$$C(D) = I(D)/V_T(D) \quad (17)$$

where

$I(D)$ is the flux density calculated using Equation 16

$V_T(D)$ is the terminal velocity of hailstones of diameter D .

The terminal velocity of a hailstone can be estimated by equating the drag force and the weight of the hailstone:

$$V_T(D) = \left(\frac{4\pi g}{3C_D \rho_A} \right)^{\frac{1}{2}} D^{\frac{1}{2}} \quad (18)$$

where

ρ_h is the density of the hailstone

g is the acceleration of gravity

C_D is the drag coefficient of the hailstone

ρ_A is the density of air.

Values used in this work were $\rho_h = 0.89 \text{ g cm}^{-3}$, $g = 981 \text{ cm}$
 sec^{-2} , $C_D = 0.5$, and $\rho_A = 1.05 \times 10^{-3} \text{ g cm}^{-3}$. According to
Strong (private communication) these are "representative" values
for Central Alberta. This equation assumes spherical homogeneous
hailstones. The concentration distributions at the ground for
each sample are given in Appendix 3. The results for individual
samples will be considered in Chapter 4.

An exponential distribution of hail concentration with size
for a severe storm in England was found by Ludlam and Macklin
(1959), who estimated size spectra from photographs of hail lying
on the ground following the storm. Their equation for the
concentration distribution in the air at ground level was:

$$N(D) = 40 e^{-2.15 D}$$

Because the hailstones may have melted on the ground before being
photographed, tending to reduce the proportion of smaller hail-
stones, this equation may have a flatter slope than the true value.

Douglas (1963) also gives an exponential size distribution
for hailstones collected in several Alberta hailstorms. His
sampling techniques, however, tended to emphasize the larger

hailstones in a sample. Consequently, the slope he derived,

($\Delta = 2.93 \text{ cm}^{-1}$) may be smaller than the actual value which occurred in his sampling occasions.

4.2 Log-normal Distributions

Another distribution used to describe collections of particles is the log-normal distribution, given by:

$$P(D) = \frac{1}{\sqrt{2\pi}} \int_{-\infty}^{u(D)} \exp\left(-\frac{u^2}{2}\right) du \quad (19)$$

where

$P(D)$ is the probability that a particle in the distribution has a diameter $\leq D$.

$$u = \frac{y - \bar{y}}{\sigma_y}$$

is the standard normal variable.

$$y = \log_{10} D$$

$$\sigma_y = \left(\frac{\sum_{i=1}^n (Y_i - \bar{Y})^2}{n-1} \right)^{\frac{1}{2}}$$

is the standard deviation of the y 's.

Figure 10 shows the total sample population plotted on log-normal graph paper. The graph shows that 16 percent of the collected hailstones were smaller than 0.1 cm in diameter,

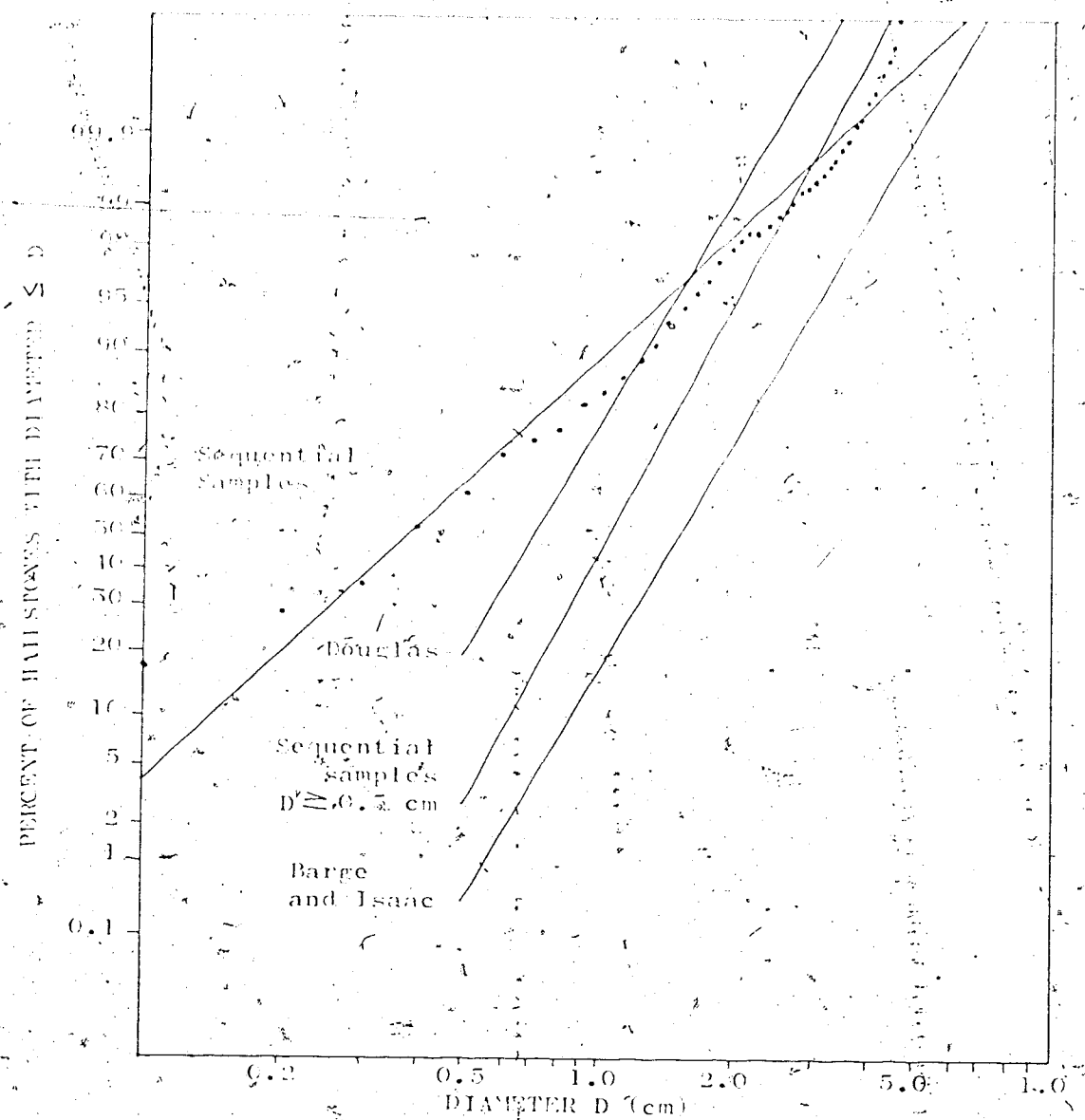


FIGURE 10.

Log-normal size distributions of hail samples collected during 1973 and 1974, and by Douglas (1960) and by Barge and Isaac (1973). Also shown is the distribution of the hailstones from the sequential samples with diameters greater than 0.5 cm.

50 percent were smaller than 0.33 cm (the median size) and 90 percent were smaller than 1.2 cm. Corresponding to the observations of the curve in Figure 6, there is a "kink" in the graph for larger hailstones, in this case at a diameter of 2.0 cm. The graph seems to consist of two curved segments that approach some maximum diameter asymptotically. It should be emphasized that for $P \geq 99.9$ percent on the graph only ten or fewer hailstones are involved with the result that this part of the graph is not as reliable as the rest.

Also included in Figure 10 are log-normal distributions of other Alberta hailstorm samples. That due to Douglas consists of 67 hailstone samples (Barne & Isaac, 1973). The distribution due to Barne and Isaac (1973) was derived from 1920 hailstones collected from S-Alberta hailsforms during the summer of 1969. If the hailstone samples of this work are reconsidered allowing only hail with a diameter greater than 0.5 cm (MANCBS), a distribution comparable to those of Douglas, and Barne and Isaac results.

Log-normal graphs of the sample size distributions of individual sampling occasions are shown in Appendix 4. Most of the graphs resemble Figure 10 in that they appear to consist of two curves connected at a kink. Some information about the hail sizes for each sampling location is given in Table 7. Particles smaller than 0.1 cm appeared in the samples on all but three occasions. The fraction of particles less than 0.1 cm in diameter usually varied between 0 and about one fourth of the total collected samples.

SAMPLE DATE	MINIMUM DIAMETER (cm)	MAXIMUM DIAMETER (cm)	FRACTION COLLECTED ≤ 0.1 cm	MEDIAN DIAMETER (cm)	MEDIAN VOLUME (cm ³)	90% DIAMETERS (cm)
ML	0.1	0.17	0.57	1.12	1.12	1.2
6 July 1973	0.1	0.22	0.51	1.07	0.71	
8 July 1974	0.4	0.05	0.81	1.34	1.7	
25 July 1973	0.1	0.14	0.55	1.07	0.57	
25 Aug. 1973	0.1	0.20	0.28	1.01	0.77	
24 June 1974	0.5	0	0.75	1.21	1.10	
2 July 1974	0.1	0.58	0.07	0.20	0.20	
5 July 1974	0.1	0.04	0.51	1.06	0.65	
9 July 1974	0.1	0.05	0.26	0.91	0.55	
18 Aug. 1974	0.4	0	1.9	1.28	3.3	
18 Aug. 1974	0.4	0	1.1	1.21	1.7	

TABLE 7. Log-normal distribution parameters for individual sampling locations.
The 90% diameter is the diameter greater than or equal to 90% of the collected sample.

The probabilities and diameters of the cumulative size distributions of the samples were transformed to two new variables, X and Y , using:

$$X := \log_{10} D$$

$$Y = \frac{1}{\sqrt{2\pi}} \int_{-\infty}^u \exp\left(-\frac{u^2}{2}\right) du.$$

(20)

$$u = \frac{X - \bar{X}}{\sigma_X}$$

The transformed data were used to generate least-squares fits to the graphs of Figure 10 and Appendix 4 in order to determine the parameters of the log-normal distribution most closely approximated by the data points. Table 8 gives the results of the calculations. The table shows that the slopes are not constant. According to List et. al. (1972), a constant slope means a constant standard deviation of the samples. This illustrates the lack of similarity among the samples from each location. As will be shown in Chapter 5, the standard deviation also varies during a haulfall. The two samples with the closest fit to a log-normal distribution (minimum variance from a log-normal distribution) are that of 9 July and the second sampling location of 18 August 1974. On these two occasions, rather large problems arose in the collection of the samples. (n)

SAMPLE DATE	SLOPE (cm^{-1})	$P(D \leq D_{\text{crit}})$	VARIANCE
ALL	5.054	0.04	0.055
1973	2.994	0.0578	0.120
1974	5.728	0.0009	0.116
25 July 1973	3.794	0.0162	0.115
25 Aug 1973	3.194	0.112	0.159
27 Aug 1973	3.445	0.0592	0.112
24 June 1974	7.559	0	0.262
2 July 1974	2.276	0.5918	0.195
5 July 1974	4.967	0.0080	0.169
9 July 1974	4.505	0.0707	0.018
18 Aug 1974	4.471	0	0.416
18 Aug 1974	7.095	0	0.687

TABLE 8 Least squares fits for log-normal hail size distributions at individual sampling locations. $P(D \leq D_{\text{crit}})$ is the probability that a hailstone will have a diameter less than D_{crit} cm.

9 July 1974 large quantities of rainwater were collected along with the hail, and on 18 August 1974 the catcher net was torn. Collected rainwater would melt the collected hailstones slightly, with the smaller hailstones the most affected. The torn catcher net should not have had any effect on the size distribution, since all sizes should have been more or less equally lost.

4.5 Power Law Distributions

Some authors (Tribarne and de Pena, 1962; and Sulakvelidze, 1967) suggest that the size distribution of hail in a storm obeys a power law of the form:

$$C(D) = k D^{-\alpha} \quad (21)$$

where

$C(D)$ is the concentration per m^3 in the diameter interval $D-\delta D$ to D .

D is the diameter of the hail in cm.

k and α are constants.

This distribution is not a cumulative distribution like the previous ones, but a density function. Sulakvelidze has suggested a value of 3 for α . Some values of k and α for Equation 21 are given in the literature. Auer (1972) gives

$$C = 561.3 D^{-3.4} \quad (22)$$

for hail and graupel from a convective cloud system over the High Plains. Auer and Marwitz (1972) give

$$C = 616.5 D^{-3.5} \quad (23)$$

for hail and graupel in the air near a thunderstorm updraft.

Power law distributions were fitted to the calculated concentrations using a least squares method. The results are given in Table 9. The concentration for each size increment has been divided by the total concentration, so that k is less than 1.

This procedure allows a comparison of the calculated variance to that for the other distributions.

The results indicate that the power law does not describe the storm samples very well, since the variance is about twice as large as for a log-normal distribution. Also, the slopes differ greatly from the Sulakvelidze value of 3. Figure 1k shows a log-log plot for the samples of 1974. On this graph, those hailstones with a diameter greater than about 1 cm match a distribution of the type

$$C = k D^{-3} \quad (24)$$

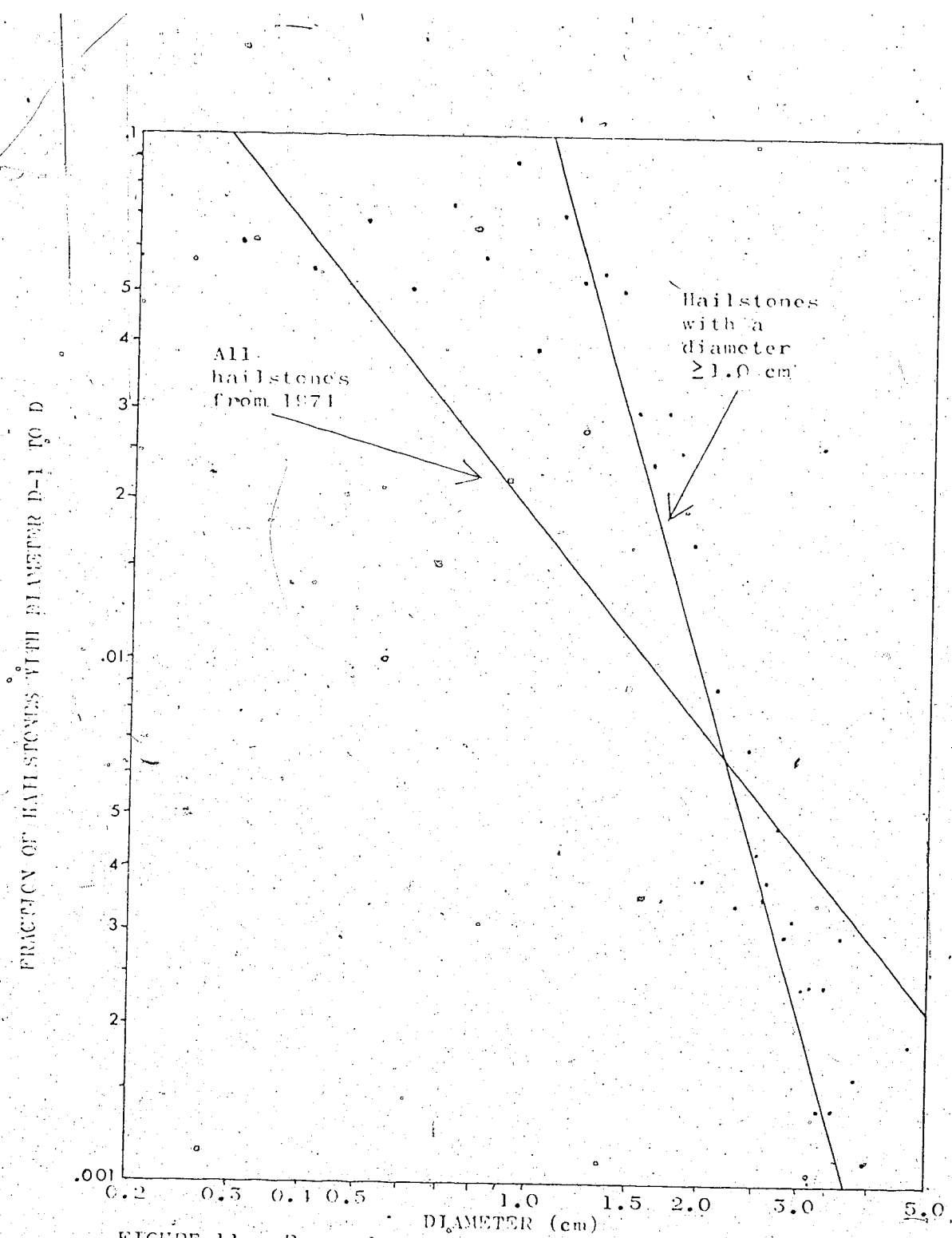


FIGURE 11. Power law size distribution of sequential hailstone samples from 1974. The two lines indicate the best-fitting distributions for all 1974 hailstones, and those greater than 1.0 cm respectively.

quite well. Apparently, the discrepancies from this distribution are caused by the smaller hailstones. Knowing this, the least-squares were recalculated using subsets of the samples with some of the smaller hailstones eliminated. Table 9 shows the results of the calculations on these truncated samples.

These results are more encouraging. The slopes for the individual storms tend to be both larger and smaller than 3. The large "averaged" sample of 1974 has the slope closest to 3, suggesting that $\alpha = 3$ is reasonable. In the cases where the smaller hailstones are neglected, the variance of the sample from a power law distribution is also reduced, as shown in

Table 9.

MINIMUM
DIAMETER
= 1.0 cm
= 1.5 cm

ALL
HAILSTONES

SAMPLE DATE	ALPHA	K _a	s ²	ALPHA	K	s ²	ALPHA	K	s ²
1973	1.827	0.012	0.094	5.630	0.027	0.094	7.107	0.073	0.137
1974	1.353	0.619	0.186	3.746	0.115	0.070	4.015	0.159	0.171
23 July 1973	1.741	0.011	0.180	1.211	0.666	0.694	-	-	-
23 Aug. 1975	1.736	0.012	0.090	1.614	0.009	0.029	-	-	-
27 Aug. 1975	1.803	0.015	0.088	5.062	0.0292	0.075	-	-	-
24 Aug. 1974	0.155	0.675	0.105	6.907	0.151	0.062	-	-	-
2 July 1974	1.892	0.005	0.195	-	-	-	-	-	-
5 July 1974	1.641	0.011	0.383	5.149	0.006	0.049	-	-	-
9 July 1974	1.257	0.018	0.248	-	-	-	-	-	-
18 Aug. 1974	0.542	0.0024	0.140	1.252	0.058	0.091	1.453	0.056	0.105
18 Aug. 1974	0.998	0.039	0.195	4.691	0.193	0.085	6.042	0.852	0.054

TABLE 9. Power law least squares fits for subsets of the concentrations of collected hailstones at the ground level. The two sets of figures to the right are for the truncated samples, from which hailstones smaller than MINIMUM DIAMETER have been excluded. The dashes indicate that the truncated sample contained no hailstones, hence no calculations were possible.

CHAPTER 5. TIME-VARYING PROPERTIES

The detailed study of the time-varying properties of hailfalls will be based mainly on three storm sample sets.

The storms were subjectively judged to be of different severities, based on the criteria of hail amount, hail size, duration of hailfall, and whether rain was falling with the hail. The presence of rain during a hailfall may indicate that some of the small hail produced by the storm melted before reaching the ground. The three storms selected occurred on 9 July 1974, a "weak" storm; 21 June 1974, a "moderate" storm; and 18 August 1974, a "severe" storm. The information for other storm samples is included in Appendices 3 and 5.

5.1 Variation of Size Distributions with Time

Since hailstones of differing size generally have different terminal velocities, the measured values of number flux and concentration in the air at ground level are not the same as those aloft. In addition, vertical shear of the horizontal wind will cause horizontal sorting of hailstones according to size. For a stationary storm, if all the hailstones originated at one point and one time, the largest hailstones would reach the ground first, followed by the smaller ones. If the production of the hail continues with no change in the initial spectrum, then eventually the hail size distribution between the storm and the ground will

become homogeneous. If this storm now moves over a point on the ground, the initial hail collected at this point will consist partially of small hail as well as the large hail collected in the case of a stationary storm. Thus, the sequential samples for a moving storm may have an excess of small hailstones at the first of the sampling period compared to the sequential samples from a stationary storm. This result could be modified if different assumptions about the hailstone distribution within the storm are made.

Figures 12, 13 and 14 show the hailstone size spectra at ground level as a function of time for each of the three storms. Using these, an attempt was made to detect the sorting of the hail by size. The hailfall of 9 July 1974 (Figure 12) at the sampling site consisted of two events. The hailfall began with a fairly narrow size spectrum in the first two minutes, which broadened in the next two minutes. The hail had almost ceased by the third sample, from five to six minutes. In the fourth sample interval, from seven to eight minutes, the hail had started again, with another narrow spectrum. It then diminished in intensity for the final time, while the spectrum remained quite narrow.

The hail concentration of 24 June 1974 (Figure 13) was continuously decreasing in each sampling period. The beginning of the hailfall was not collected, which may explain the absence of a period of increasing hail concentration. The first sample had the broadest range of sizes, as well as the greatest concentration. The largest hailstones, those greater than about 1.0 cm in diameter, ceased falling the soonest, disappearing largely after the first sample interval. The smallest hail re-

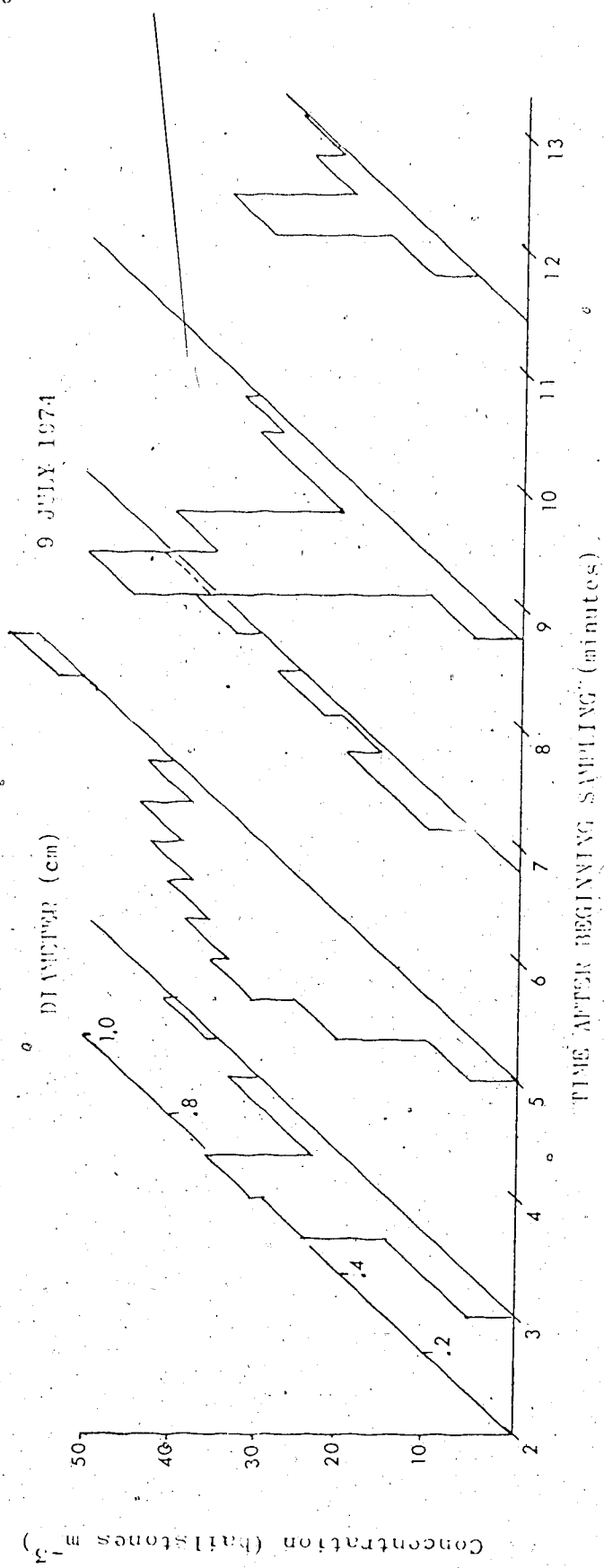


FIGURE 12. Hailstone concentration vs time and diameter. Each curve represents one sample and is located in time at the midpoint of the sampling interval. The first collected sample has been omitted because it contained no hailstones.

24 JUNE 1974

54

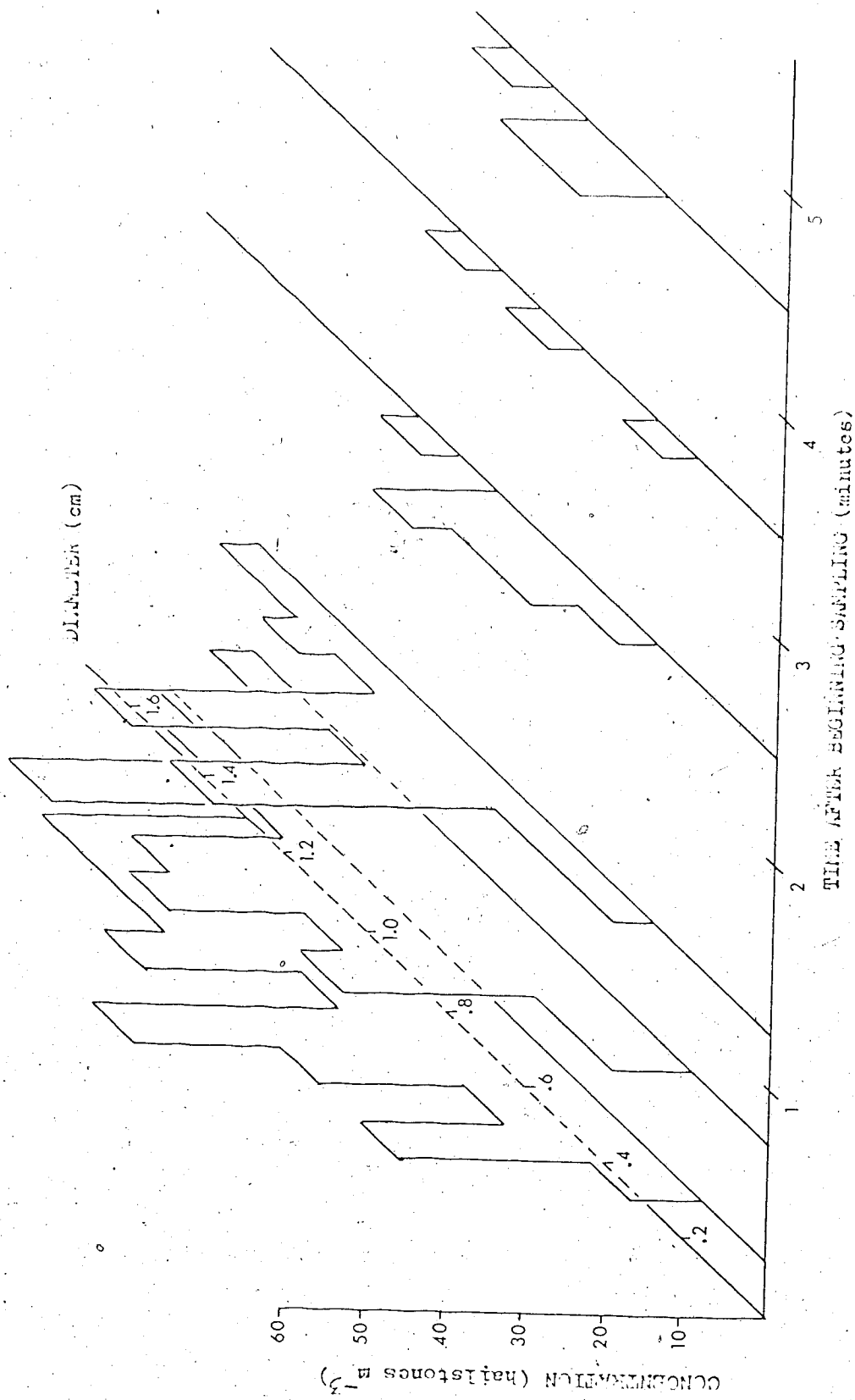


FIGURE 13. Hailstone concentration vs time and diameter. Each curve represents one sample and is located at the midpoint of the sampling interval.

mained the most constant in concentration throughout the sampling period. Because of the lesser requirements of updrafts and liquid water required for its growth, small hail can be expected to have a greater area of origin.

The hailfall of 18 August 1974 is shown in Figure 14. In this storm, the hailfall began with hail smaller than 1.0 cm. There was an abrupt drop in the concentration of the small hail as the larger (up to 2.0 cm) hailstones began to arrive. The largest hail came during the period from 9 minutes 20 seconds to 10 minutes, which almost coincides with the greatest concentration of all hail. The smallest and largest hail stopped falling between 10 minutes and 10 minutes 20 seconds, with the intermediate sizes continuing to the end of the shower with a reduced concentration.

Of the three storm samples, the one of 18 August, 1974 showed the greatest evidence of hail size sorting by the horizontal wind. The storm moved quite rapidly, with a speed of about 10 m s^{-1} . The storm of 21 June 1974 had a similar velocity, but the absence in the record of the first part of the hailfall makes it impossible to know whether there was an abundance of small hail in it also.

5.2 Variation of Other Parameters with Time

The onset time of hailfall at the collecting sites was estimated from the tape transcripts.

Q 18 AUGUST 1974

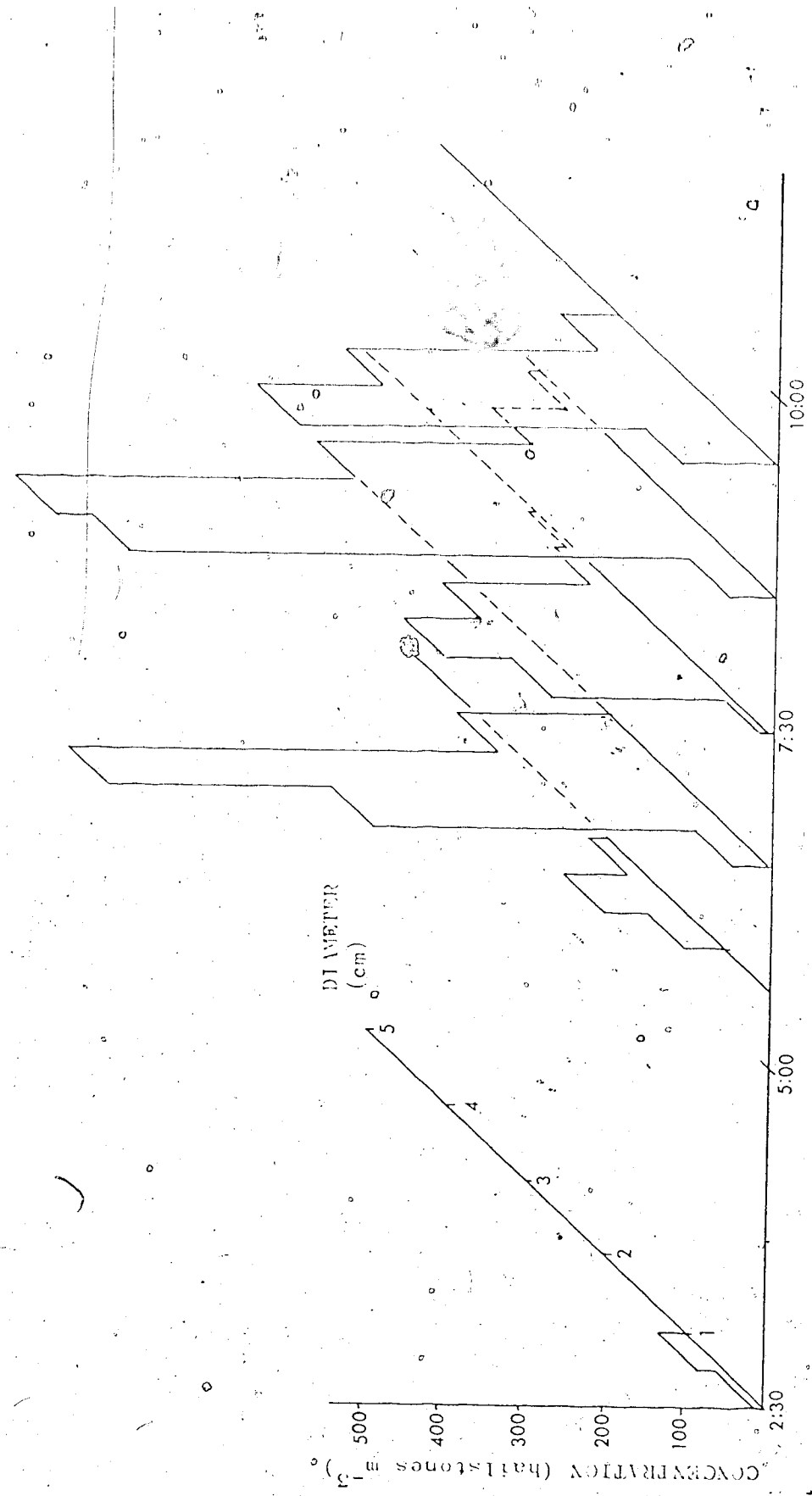


FIGURE 14. Hailstone concentration vs. time and diameter. Each curve represents one sample and is located at the midpoint of the sampling interval. The last two samples had very low concentrations and have therefore been omitted.

1. On 9 July 1971 the hail began approximately 2 minutes after beginning sampling. During the first 2 minutes of sampling, rain was falling.
2. On 21 June 1971 the hailfall began 1.5 minutes before sampling was started.
3. On 18 August 1971 the hailfall began at the same time as the sampling.

The samples were not of the same duration because the usual practice was to collect a sample sufficient to fill most of a sample container. The sampling intervals were therefore adjusted according to the rate of precipitation.

The errors indicated by the error bars in the following graphs come from three sources.

1. There is a possible 1 percent error in the measurement of the effective area of the hail catcher aperture. It is felt that losses due to bouncing and through the mesh holes probably contributed at most 5 percent error in the number.
2. Timing errors were introduced by approximate switching times and inaccurate clocks. For short samples of a duration of about 15 seconds, the maximum error is about 5 percent.
3. Errors in measuring the sizes and numbers of hailstones varied with the quality of the sample. These uncertainties ranged from greater than 100 percent for some of the samples of 9 July 1971 to 5 percent for some samples from 18 August 1971. These values were derived from repeated analyses of the same samples.

The time variation of hailfall flux density (number of hailstones per unit area per unit time) is shown in Figure 15.

The following features can be seen:

1. The point duration of hailfall varied from 6 minutes to 1785 minutes. All of these values are less than the modal value of about 20 minutes reported by Peili (1971). Peili's value came from hailcard information. Although the small number of hailstorms considered here is probably not a significant sample, the present results suggest that one should investigate the possibility that hailfall durations are overestimated on hailcards.
2. The hailfall occurs in bursts. Two bursts, at about 5 minutes and 10 minutes after the beginning of sampling are quite prominent on 9 July 1974.
3. The number flux of the hailfall may vary by a factor of ten during the time of "heavy" hailfall. Heavy hailfall here refers to number fluxes greater than 10 hailstones $m^{-2} \text{ min}^{-1}$.

Figure 16 shows the mass flux of ice as a function of time. Results for the storm of 9 July 1974 are not included, because the large amounts of collected rainwater obscured the mass measurements. The maxima and minima occur at the same times as those in Figure 15, but the relative maxima and minima are not as extreme as those for the number flux variations. Since the size distribution is such that the number of hailstones decreases as their diameter or mass increases, the greatest contributions to variations in number flux will come from small hailstones, which

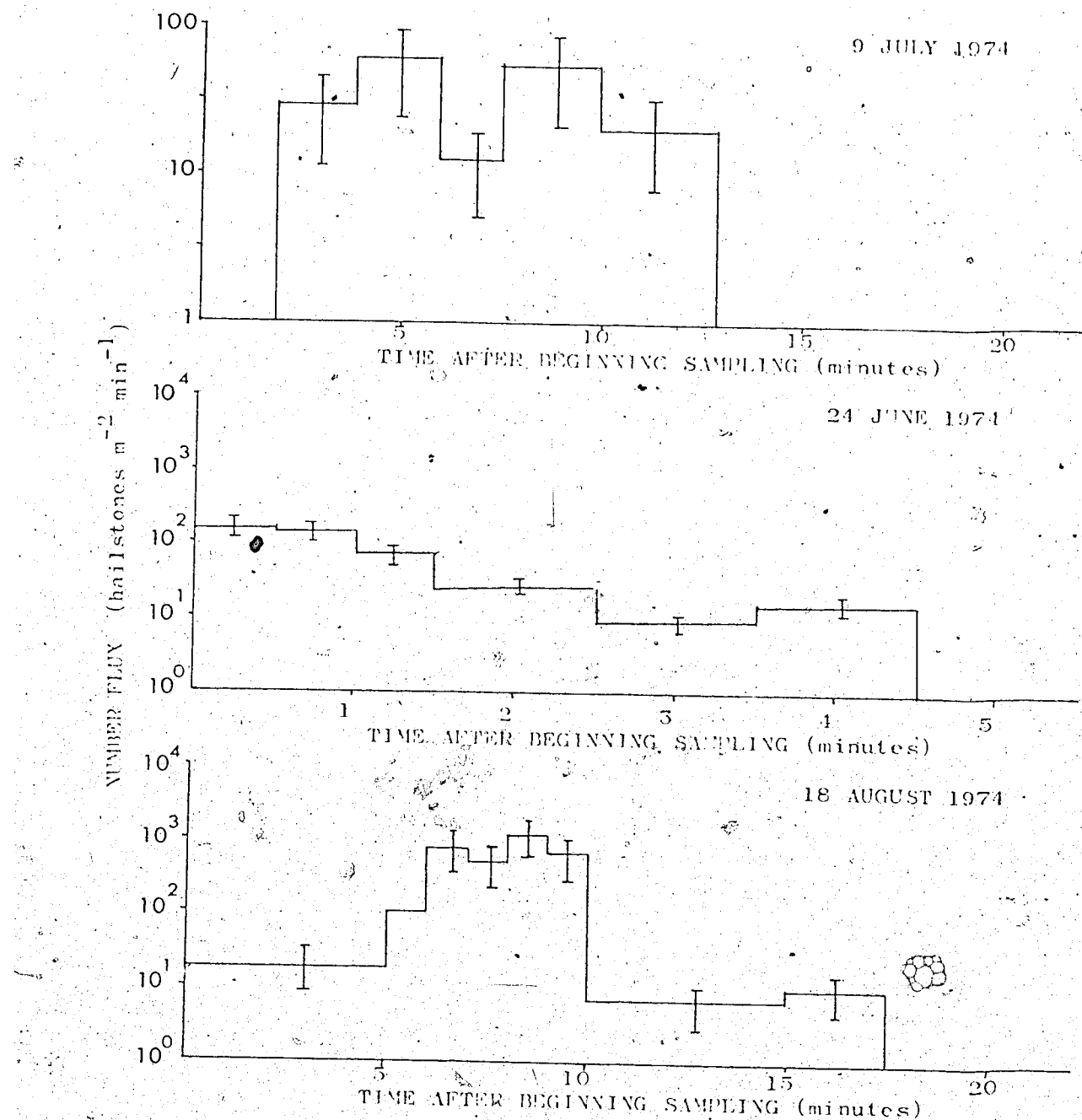


FIGURE 15. Number flux as a function of time. Each horizontal bar represents the number of hailstones collected $\text{m}^{-2} \text{min}^{-1}$. The error bars represent errors in timing, collection area and counting.

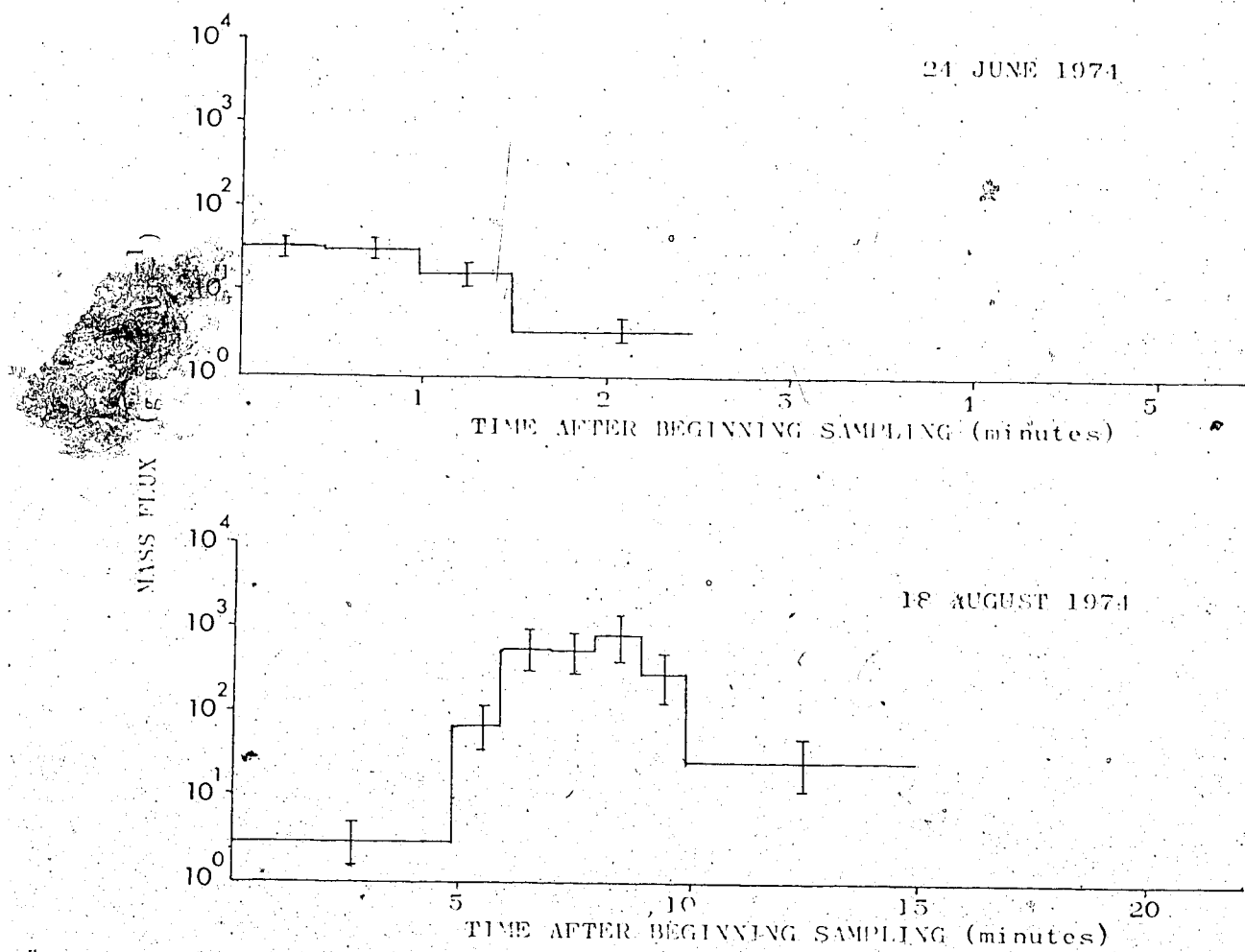


FIGURE 16. Mass flux as a function of time. The open ends of the graphs indicate that the subsequent samples were so small that contamination by collected rainwater made mass measurements invalid.

will cause smaller changes in mass flux.

Figure 17 shows the variation of the mean and median diameters of the samples, with time. The variation of the two parameters is similar. The mean diameter increases to a maximum during the hailfall, then decreases. To see whether these peaks correspond to those of number flux, the two variables, number flux and mean diameter, were correlated and the results are given in Table 10.

DATE OF SAMPLE	R
9 July 1974	-0.24
21 June 1974	0.59
18 August 1974	0.03

TABLE 10. Correlation coefficient, R, between number flux and mean diameter for three sets of storm samples.

There is no evident correlation between the number flux and mean hailstone diameter from these three examples. A qualitative comparison of the two graphs (Figures 15 and 17) reveals that the greatest discrepancies between the two variables occurs at the end of the hailfall, when the number fluxes are small. The first 1.5 minutes of hailfall on 21 June 1974 were not collected, so the high correlation in that case may indicate that the two variables correlate well during the more intense middle portions of a hailfall.

The hypothesis that the number flux is correlated with the maximum hailstone diameter of a sample was also tested. The

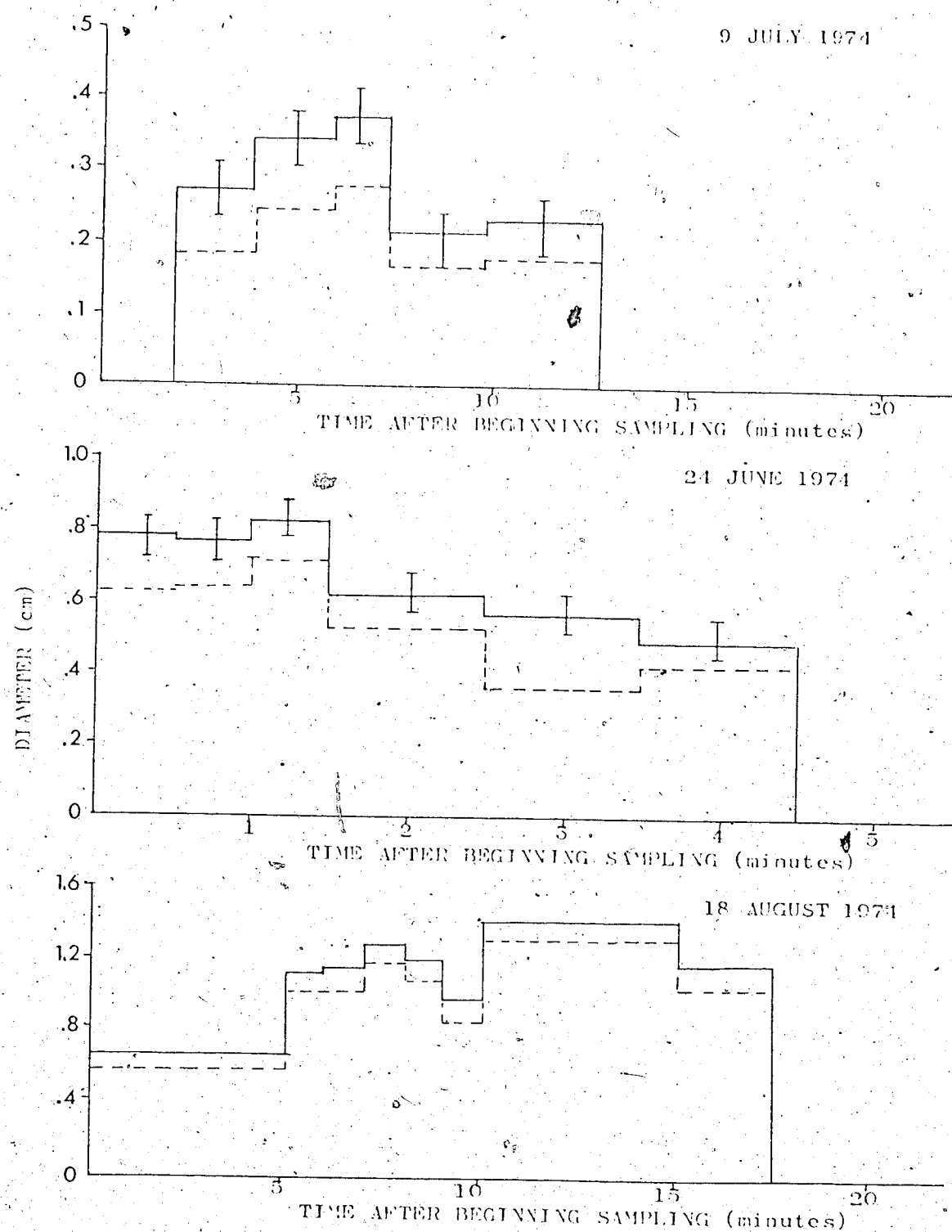


FIGURE 17. Mean and median diameter vs time. The solid line indicates mean diameter. The dashed line indicates median diameter.

results are given in Table 14.

DATE OF SAMPLE	R
9 July 1971	0.88
24 June 1971	0.70
18 August 1971	0.71

TABLE 14. Correlation coefficient R between number flux and maximum diameter for three sets of storm samples.

These results indicate a favorable correlation, suggesting that the conditions for large hail may be related to those for large quantities of hail.

Figure 18 shows the change in the variance of the number flux with time. Since the variance is defined here to be a measure of the deviation of the sample distribution from an exponential distribution, a low variance indicates that the hail-fall is approaching an exponential distribution. The graphs show a variance minimum at the times of the number flux maximum. If reductions in number flux are due in part to dispersion of hailstones by the winds below a storm cell, then periods of greater number flux would correspond to storm samples less disturbed from the actual distribution within the storm. If the size distribution of hail within the hailstorm is exponential, then the variance of the distribution at the ground would be smaller for greater number flux, as observed.

Figure 19 shows the variation with time of hailstone concentration, given by Equation 17. The features of the graph are similar to those of Figure 15, but the maxima and minima

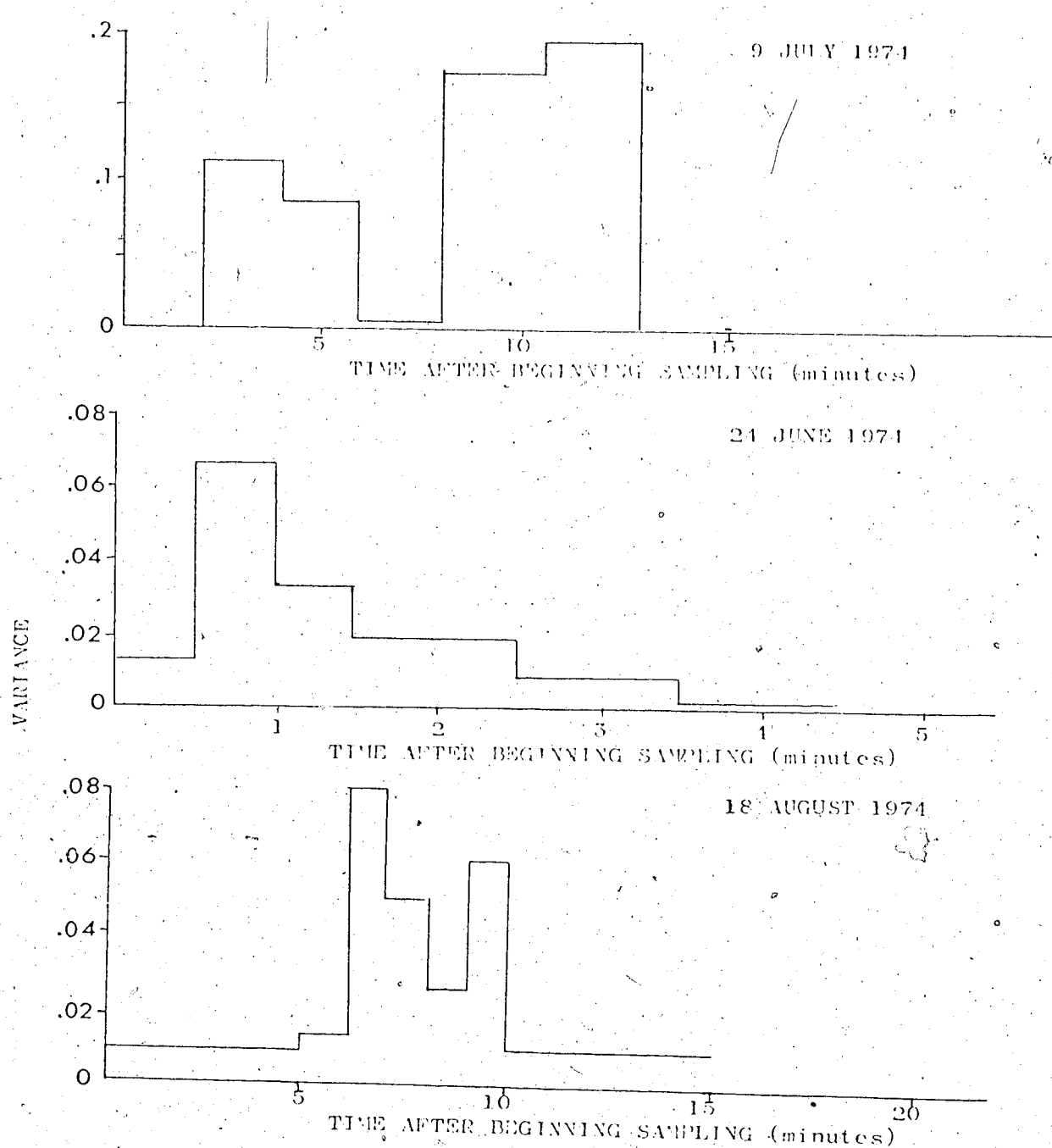


FIGURE 18. Variance of sample distributions from an exponential distribution. Open ends of the graphs indicate a sample too small to compute the variance (fewer than two hailstones).

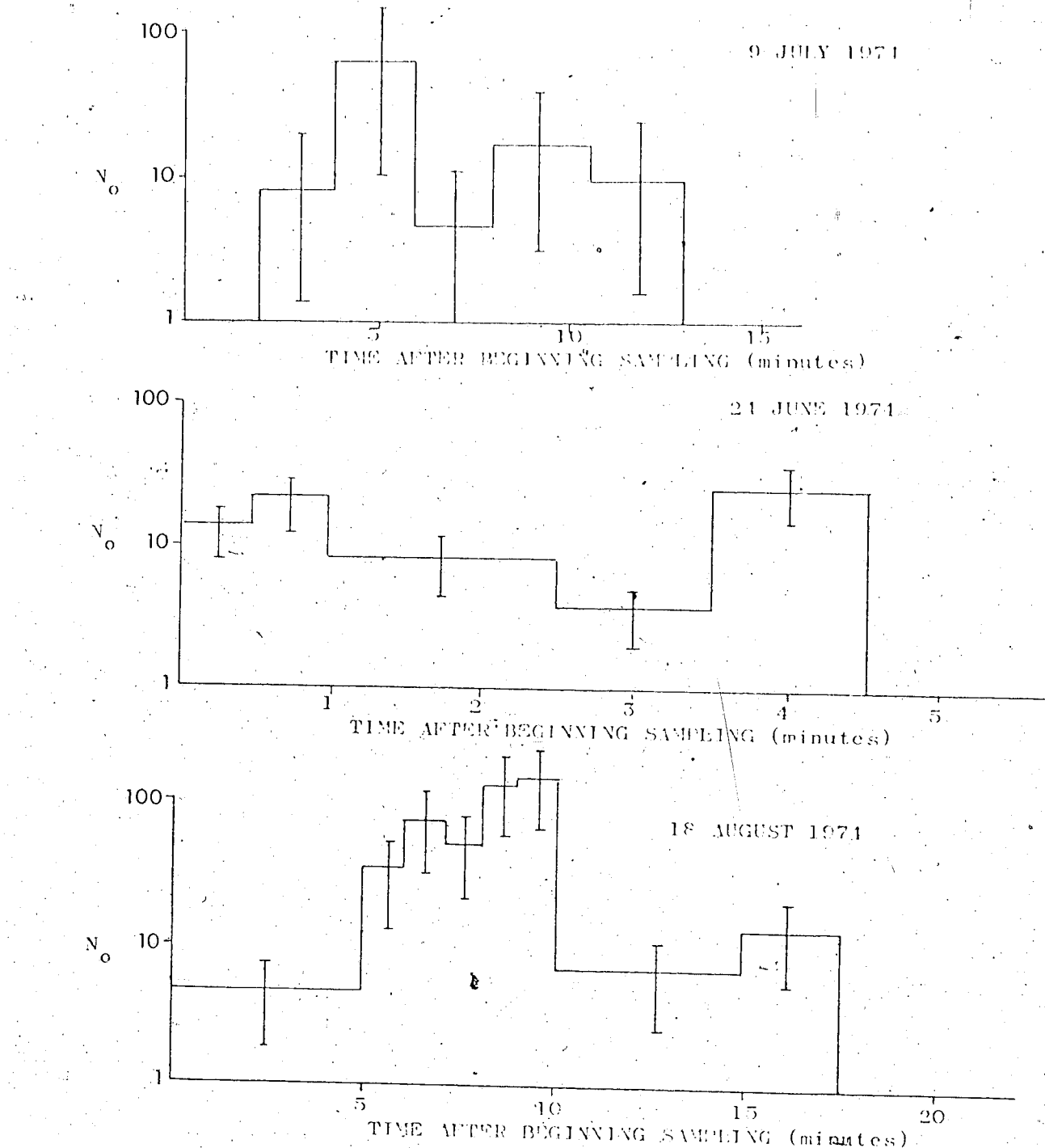


FIGURE 19. N_o of the best-fitting exponential distribution for concentration measurements. The error bars indicate accumulated errors in collection and analysis.

are more prominent. This is a consequence of the concentration being a function of the terminal velocity of the hailstones. Douglas (1964) gives $N_o = 3242 \text{ m}^{-3} \text{ cm}^{-1}$ for his exponential distribution for 67 hail samples collected from 1958 to 1964. For small samples, the present results show that N_o can vary either way by up to a factor of ten.

Ulbrich (1974) derived the two parameters, Δ and N_o , of an assumed exponential distribution along with the maximum diameter from the Doppler radar spectrum of falling hail. His use of a vertically pointing radar implied a sampling volume extending over the entire depth of the storm. Figure 20 shows the temporal changes of these parameters in a hailstorm on 10 August 1966.

Δ and N_o decrease with time, while the maximum diameter increases. Some of the values given for Δ and N_o are considerably larger than those found in the present work and in the literature (Douglas, 1964; and Atlas, 1965). This discrepancy seems to be caused by the rain also measured in the Doppler spectrum. Ulbrich states that the total hailstone concentration for all sizes decreases from 1000 m^{-3} to 10 m^{-3} and the median diameter increases from about 0.1 cm to 1.0 cm during the period of observation from 1502:39 to 1511:00. With regard to

Δ and N_o , he says "...the temporal behavior of N_o and Δ implies a size distribution which gradually broadens to hailstones of larger diameter and for which the number of smaller diameter stones is decreasing."

Another time variation study of the parameters N_o and Δ was performed by Federer and Malvogel (1975), for a hailstorm in

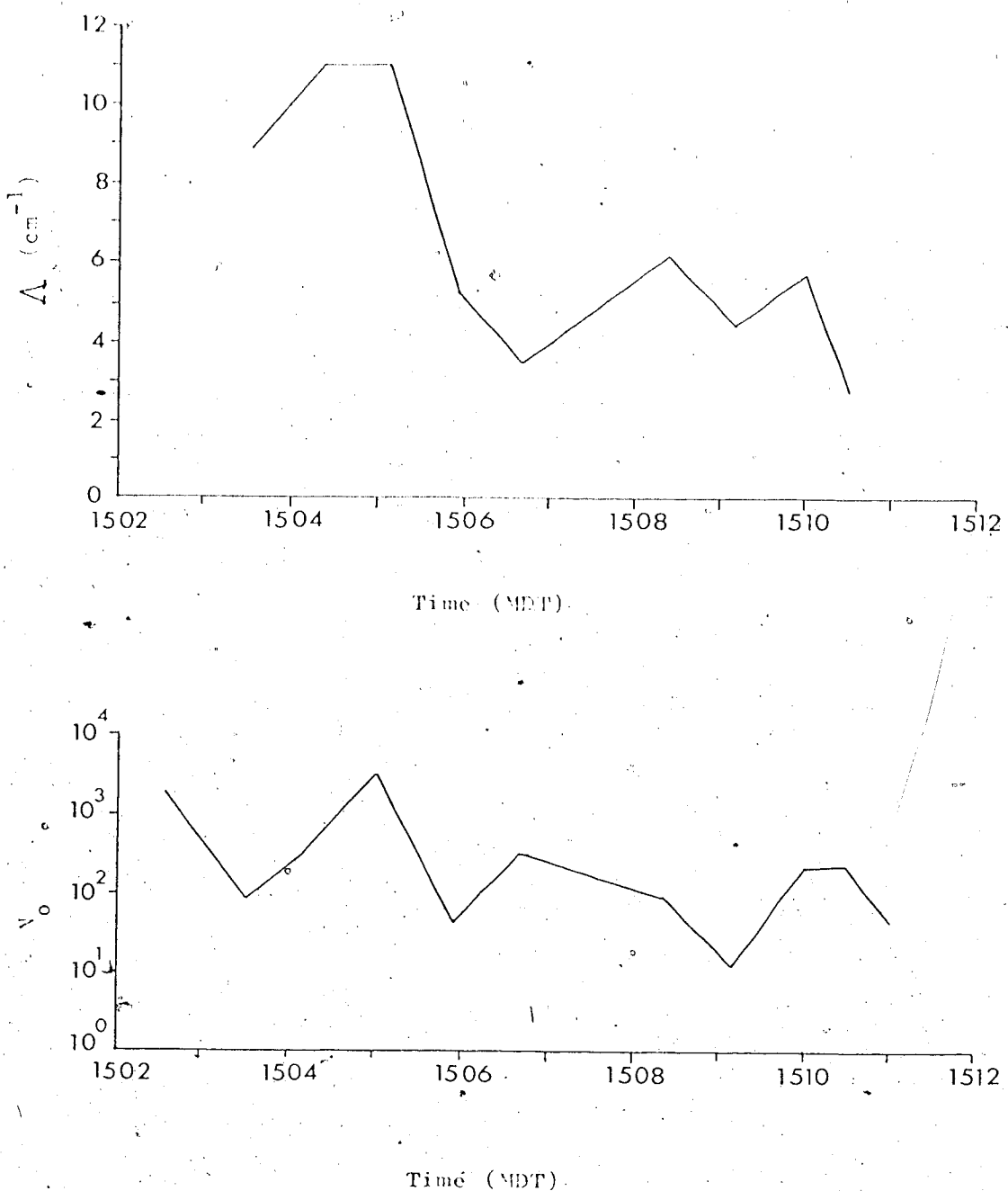


FIGURE 20 Change with time of ΔA and N in a hailstorm as observed by Doppler radar? (From Ulbrich, 1974).

Switzerland on 6 July 1975. They interpreted their results to show the passage of 4 different hail cells, each lasting for 2 to 3 minutes. At the beginning of each cell, mainly large hailstones were found, and smaller hailstones at the end of the passage of each hail cell. In that storm, the number flux and median diameter did not increase simultaneously toward the center of the hailfall, contrasted with the results of this study in Figures 1b and 17. Their results indicate that Δ showed an increasing trend during the passage of the four hail cells.

5.3 Statistical significance

Joss and Haldvoogel (1969) estimated the sample size required to make a good estimate of the parameters of an exponential distribution of precipitation particles. Their study applied to three cases of rainfall — drizzle, widespread rain, and thunderstorm rain. They determined the product of the sampling area A and the sampling time t that was required to approximate either the precipitation rate k or the radar reflectivity Z to the desired accuracy. As an example, to find an k or Z value with a probability of 95 percent which deviates less than 10 percent from the mean value, assuming a widespread rain of 1 mm hour^{-1} , the product At had to be at least $1.5 \text{ m}^2\text{s}$.

Their technique was adapted to hail, using precipitation rates from 1.0 to 100.0 mm hr^{-1} , which correspond to mass fluxes

of 17 to $1700 \text{ mm}^2 \text{ min}^{-1}$. The worst-case sample in this work is approximately a 10-second sample over an area of 0.58 m^2 in a precipitation rate of 1 mm hr^{-1} . For this sampling case, the exponential distribution parameters estimated from the sample would be within 5 percent of the mean value 95 percent of the time. Other samplers should give even better estimates. The conclusion is that, according to the dose and half-value criterion, the sampling times used in this experiment are long enough to give useful estimates of distribution parameters.

CHAPTER 6. HAILSHAFT MODELING

If the concentration-size spectrum of hail at the ground is known as a function of time, the concentration which occurred at upper levels can then be inferred by extrapolating backwards in time. The upper concentrations will be modified by horizontal and vertical winds, changing air density, and growth or melting of the hailstones, as well as by the differential motions of hailstones of varying sizes with respect to the air.

A simple two-dimensional model was developed to determine the previous concentrations of the hail samples. The model used the hail concentrations at the ground calculated from the sequential samples using Equation 17. The upper air concentrations can be evaluated completely only if the ground concentrations are known for many points. Several assumptions were made to simplify the treatment of the modifying processes mentioned above.

The hailstones were assumed neither to grow nor to melt. This assumption is not entirely unreasonable since there can be no growth below the freezing level, and, for hailstones with a radius greater than about 0.5 cm, melting will not be significant.

The hailstones were assumed to fall at their terminal velocity relative to the air. The terminal velocity is estimated by equation 16. The air density was determined from the hydrostatic equation and the ideal gas equation, assuming a constant lapse rate:

$$\rho_a(z) = \frac{\rho_s(T_s - \Gamma z)}{R T_s \frac{g}{\Gamma R} - 1} \quad (25)$$

where

$\rho_a(z)$ is the air density at z

ρ_s is the air density at the surface

T_s is the air temperature at the surface

Γ is the lapse rate

z is the altitude above the surface

g is the acceleration of gravity

R is the specific gas constant for dry air.

The following values were used in the model: $T_s = 200$, $\Gamma = 0.002$ $K km^{-1}$, $g = 980.0 cm s^{-2}$, $\rho_s = 1.05 \times 10^3 g cm^{-3}$. Using these values, the freezing level occurs at about 3.1 km above the surface.

Let the concentration of hailstones with diameter D at an altitude z at a horizontal distance from the sampling site x be $C(D, x, z, t)$. The collected samples correspond to $C(D, 0, 0, t_s)$, where t_s is the sample time. The model then calculates $C(D, x, z, t)$ for other values of x , z , and t .

The model begins with the hailstone concentration for the smallest diameter interval calculated from the last sample near the ground — $C(D_i, x_i, z_i, t_f)$,
where

$$D_i = 0.5 \text{ cm}$$

$$x_i = 0$$

$$z_i = 0$$

t_f = the midpoint of the last minute of sampling.

At the collection site the atmosphere is described by

$$T_s = \text{the surface temperature}$$

$$P_s = \text{the surface pressure}$$

ρ_s = the surface air density. The upper air conditions are then calculated by equation 25. This knowledge of upper air conditions allows the calculation of the terminal velocity of a falling hailstone at an altitude z using equation 18. A fixed time step of 1 minute is used to extrapolate the concentrations backward in time and space in a Lagrangian fashion.

This time step was chosen to correspond to the sampling interval used for most of the collected samples. Vectors representing the movement of a hailstone with diameter D at an altitude z were computed in the following ways. In the horizontal, the hailstone was assumed to move with the air velocity with respect to the ground. Hence the horizontal speed of any hailstone is given by

$$V_h(z) = \alpha z \quad (26)$$

where α is the wind shear. The form of α is given in Figure 21.

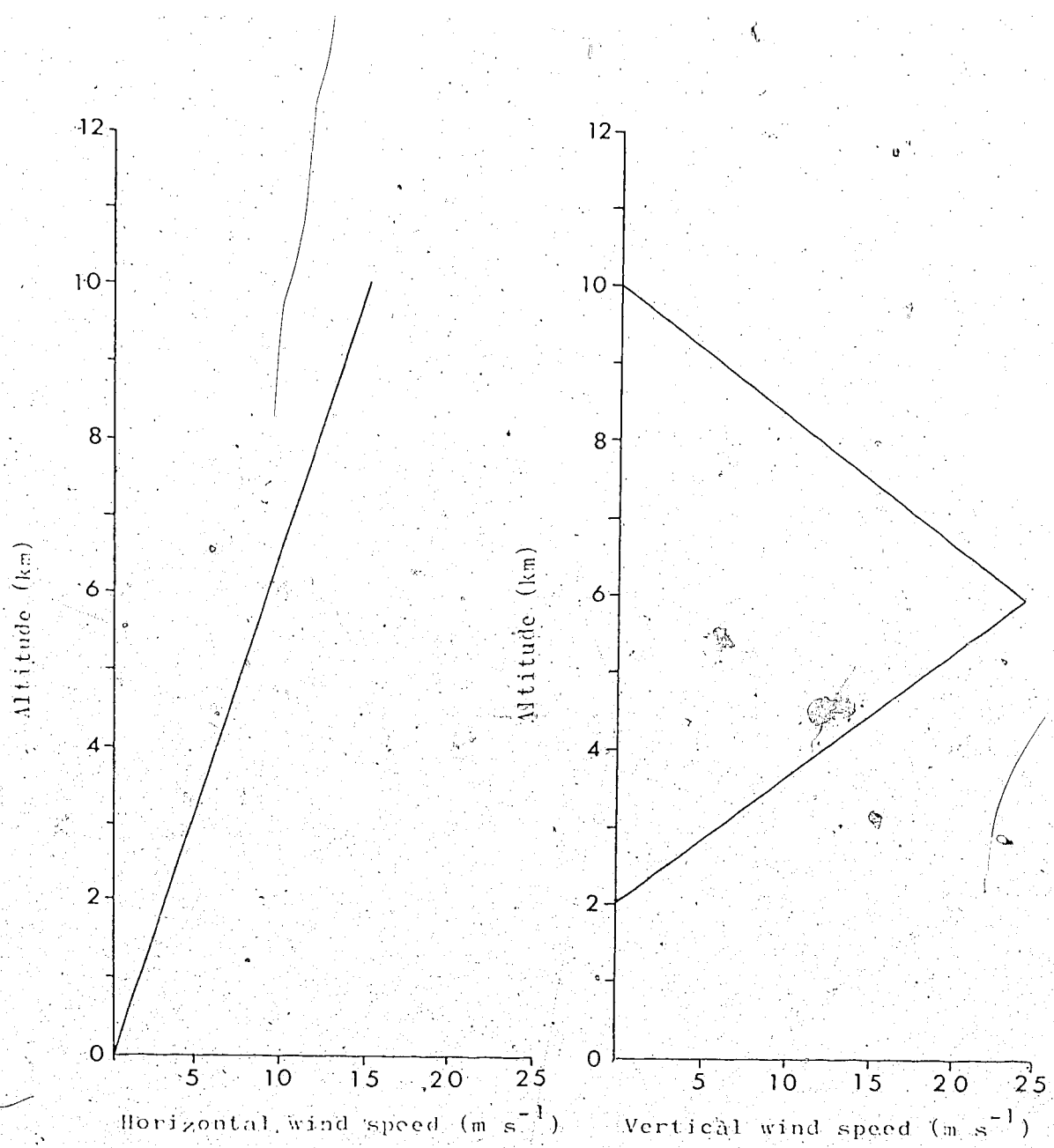


FIGURE 21. Wind shear and updraft profiles for the hailfall model.

In the vertical direction, the hailstones were assumed to fall with their terminal velocity with respect to the air. The assumed updraft profile is shown in Figure 21, with the maximum updraft velocity approximately equal to the terminal velocity of the largest collected hailstone. Then the vertical velocity of a hailstone with respect to the ground is given by:

$$V_v(z) = V_t(D, z) - V_u(z) \quad (27)$$

where $V_u(z)$ is the updraft velocity at z . $V_v(z)$ will be negative for hailstones falling with respect to the ground. Then during a small time step δt near an altitude z , a hailstone with diameter D will be displaced the following distances:

$$\delta z = V_v(D, z) \delta t \quad (28)$$

$$\delta x = V_h(D, z) \delta t$$

Then if the concentration at one point $C(D, x, z, t)$ is known, the concentration at another point at an earlier time, $t - \delta t$, can be determined by

$$C(D, x - \delta x, z + \delta z, t - \delta t) = \quad (29)$$

$$C(D, x, z, t) \cdot \frac{V_v(z)}{V_v(z + \delta z)}$$

This equation was evaluated at a grid of points separated by

thirty 100 m intervals in the horizontal, and fifty 200 m intervals in the vertical.

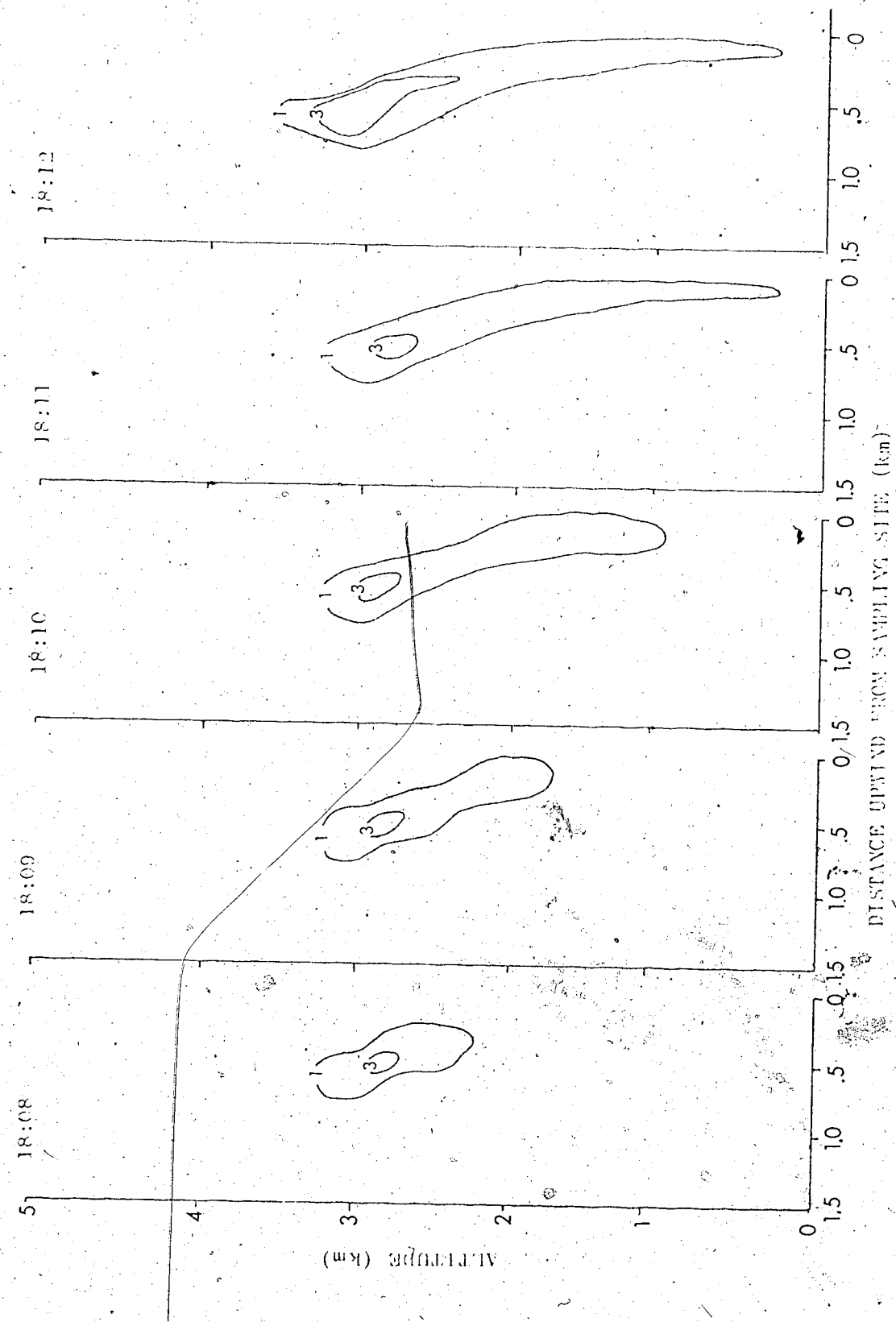
The updraft profile and the wind shear are approximations to the conditions which could have prevailed on 18 August 1974 at the sampling site and time. The wind shear was approximated from the storm velocity at 10,000 m as observed by the ALMAP radar. The updraft profile was made symmetrical, with a maximum velocity approximately equal to the terminal velocity of the largest collected hailstone. Both the wind shear and the updraft velocity profile would have been more complicated in the real storm. The sample hailstones were grouped into size categories 0.5 cm wide and all the hailstones within a size category were assumed to fall with the terminal velocity of a sphere with the average diameter for that category. The computed concentrations for the 12 minutes of model time are shown in Figure 22. The concentrations were computed backwards in time, so that the cumulative errors are greatest for the first minute, and decrease as time progresses. The sampling site is in the lower right hand corner. All times are MDT.

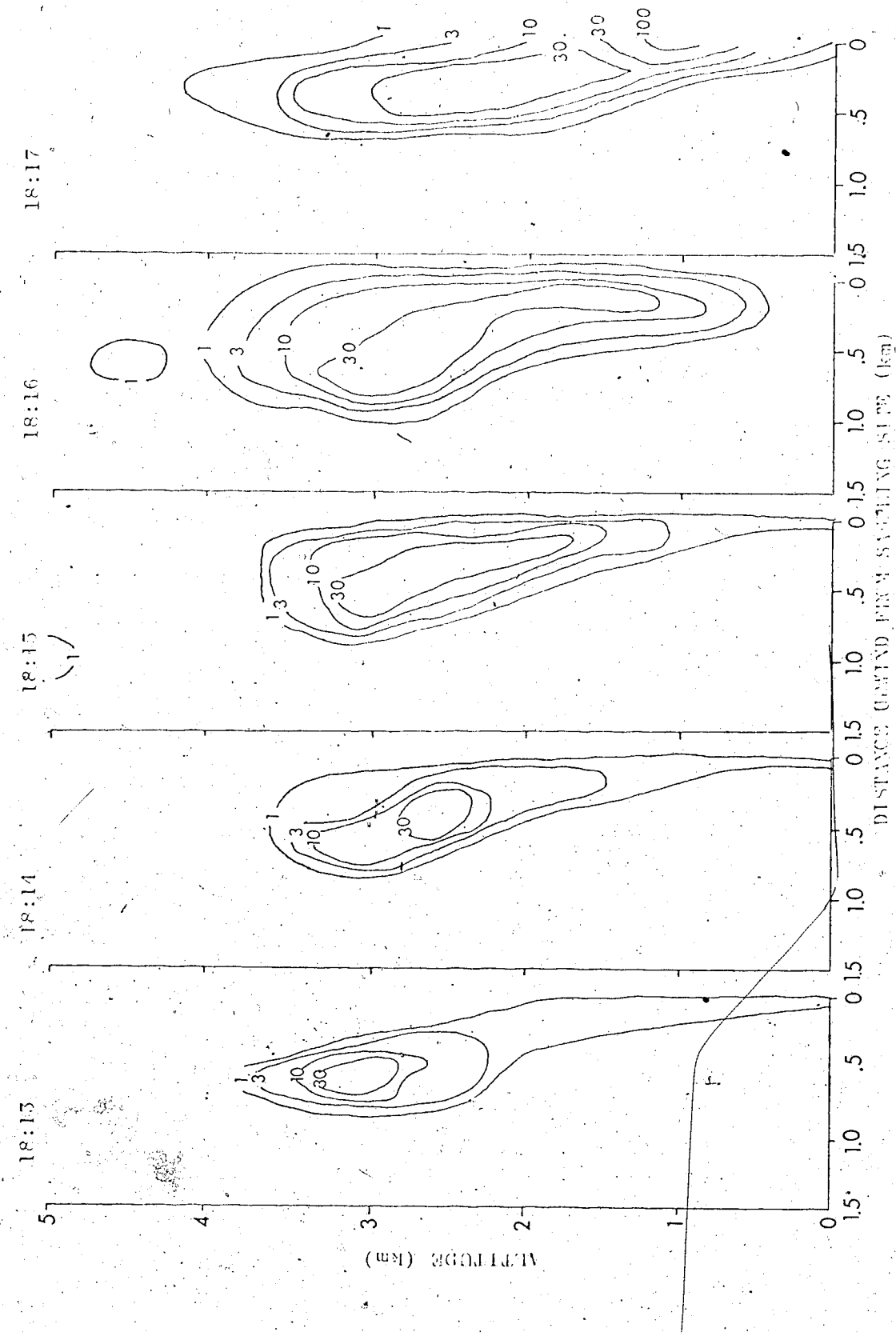
The model is limited in that the concentrations calculated represent only hail that fell at the sampling site. Other hailstones may be at the same point in space and time, but, if they have different sizes, they will fall elsewhere.

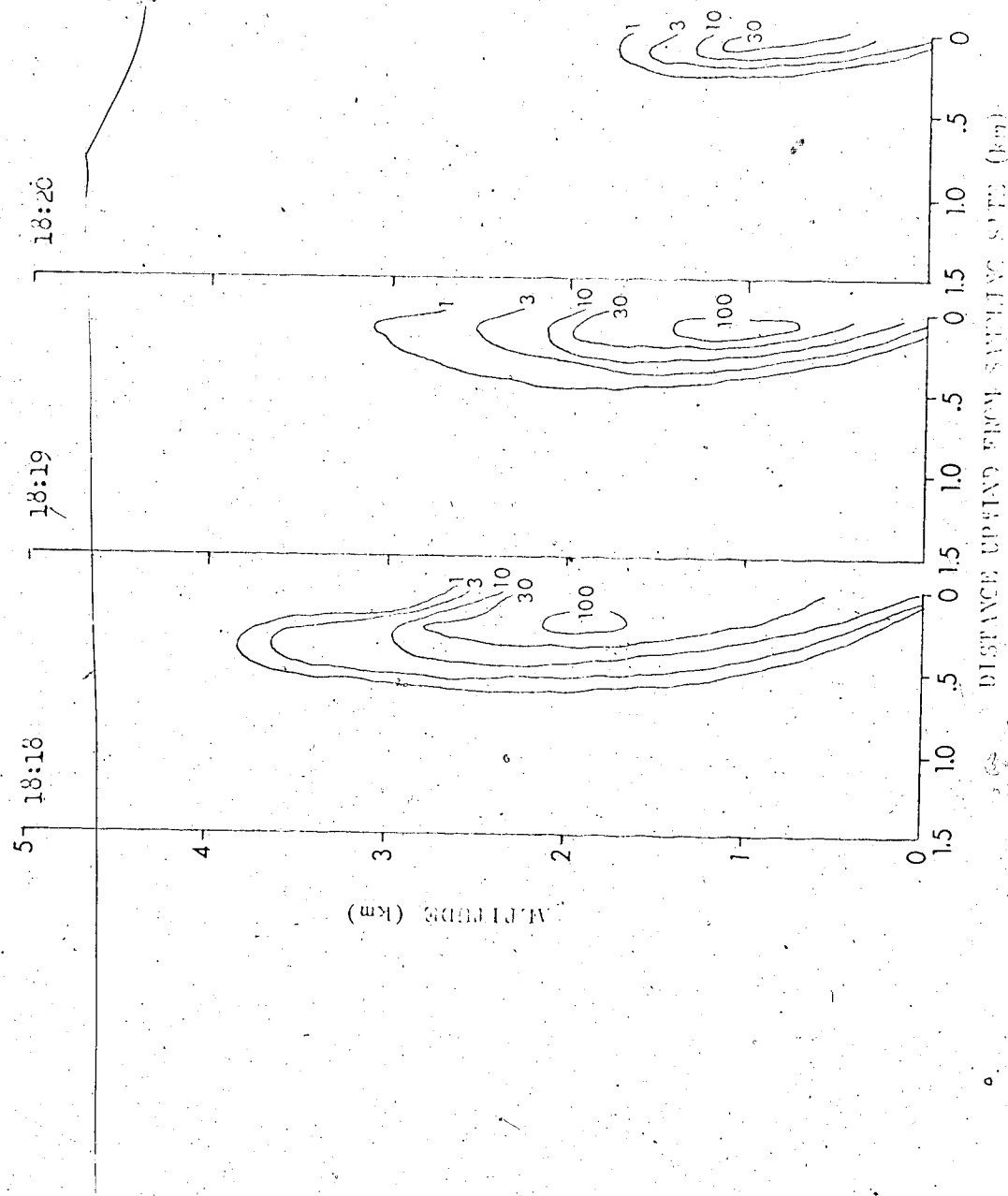
One feature of the results is the two separate areas of concentration maxima at 18:15 and 18:16. The upper region would consist of hailstones that are partially supported by the updraft. They first move into the area depicted in Figure 22 at about the level of the updraft maximum and fall with a velocity of 5 m.s^{-1} .

FIGURE 22.

Isolines of hailstone concentration produced by the hailfall model above and upstream of a hail sampling site. The samples used in the model were collected on 18 August 1974 beginning at 18:10 WDT. The isolines are at approximately logarithmic intervals and enclose areas of concentration in hailstones m^{-3} .







with respect to the ground. Because of the large terminal velocity and the small concentration, this isolated area seems to consist of large hailstones. As seen in Figure 14, large hail fell in the later stages of this hailfall. The existence of local areas of concentration maxima may be detected in another way. Examining the concentrations at the 3 km level, it may be seen that the concentration at the beginning time of 18:08 is 1 m^{-3} . This concentration increases to 3 m^{-3} at 18:12, then suddenly to 30 m^{-3} at 18:13. The concentration decreases to 10 m^{-3} at 18:14, then increases again to 30 m^{-3} at 18:15. This concentration is maintained until about 18:18, when the concentration begins diminishing to 0 at 18:20. These regions of local concentration maxima may be the result of the passage of more than one hail cell.

Another feature is the observation that hail which falls at a point comes from a region of greater horizontal extent in the upper levels. In this example, the collected hailstones extend over a distance of about 1 km horizontally at the 3 km level at 18:16. This point is relevant to comparing hail measured on the ground with radar measurements aloft.

The model is principally limited by not having a mechanism for the growth or melting of hail. Another improvement might be to use exponential distributions as the input, rather than the experimental results. This would give smoother concentration fields at the expense of greater deviations from the real situation.

CHAPTER 7. SUMMARY AND RECOMMENDATIONS

7.1 Summary

The field operations of the sequential sampling experiment were largely successful. Sequential hail samples were collected in three hailstorms in 1973 and six in 1974, indicating an improvement in hailstorm sampling ability partially due to increased experience. The best results were obtained when one person was able to devote most of his time to the sample collection. Collection of rainwater was the biggest difficulty with the equipment, but for the most severe storms, this problem was reduced. The large mesh size of the catcher netting did not appear to be a major factor in the non-capture of hail. Recording data on tape caused trouble on a few occasions.

The analysis techniques were less successful. The manual method of counting and measuring photographs of hailstones gives useful results, but is tedious. The computerized line scanning system is not much faster when all the necessary photographic steps are included, and it suffers from large calibration errors. Attempts at analyzing the internal structures of the hailstones were handicapped by the small hailstone sizes,

and by an inadequate hailstone sectioning method. The bandsaw used for sectioning could be used only on hailstones larger than about 1 cm in diameter, and the coarse teeth produced a rough surface.

The size distribution studies indicated that the hail was essentially exponentially distributed with size, with the degree of fit decreasing for smaller sizes. The dividing point for the accurate description by an exponential distribution is at about a diameter of 0.5 cm, corresponding to the MNOBS definition of hail. The exponential distribution of the total hail sample was given by

$$N(D) = 28,259 e^{-2.09 D}$$

where D is in cm. For samples from the individual storms, the coefficient of the exponent varied from 1.08 cm^{-1} to 5.83 cm^{-1} .

Log-normal distributions also approximate the observed size spectra of hail, but with deviations for both large and small diameters of hailstones. About 65 percent of the measured particles were less than 0.5 cm in diameter. The log-normal distributions were also approximated by straight lines, and the slopes of these lines showed variation from 2.28 to 7.54.

Power law distributions best fit the expected size distribution of

$$C(D) = k D^{-3} \quad (35)$$

when the sample considered was limited to hailstones with diameters greater than about 1.0 cm. When the smaller hailstones were included, the exponent tended to have a value around 1.5.

The time-dependent study did not permit generalizations to be made about falling hail, because of the small number of storm samples studied. However, interesting deductions can be made on the basis of this limited information. It was found that the greatest values of hailstone number flux, and mean hailstone diameter tended to occur in the middle of a fallfield at a point. Number fluxes and concentrations at the ground reached maximum values of about $1000 \text{ hailstones } m^{-2} \text{ min}^{-1}$ and $2000 \text{ hailstones } m^{-2}$. These numbers may show a variation of a factor of ten from one sample to the next, so the instantaneous values may be considerably higher than the values given for 1 minute averages. The size distribution of the hail is most nearly exponential during the times of greatest hailstone flux. The changes of the size distribution of the falling hail with time may be partly due to the sorting of the hail with respect to size by the vertical shear of the horizontal wind.

The modelling of the upper level concentration of the hail samples was limited by the simplicity of the model. It showed that for the particular case modelled, the collected hailstones may have come from more than one distinct storm region. It also showed that hail at a point on the ground may have arrived from a region of greater horizontal extent at upper levels.

7.2 Recommendations

The only major improvement needed for the field operation of the experiment is some method of separating hail from the rain. A lot of effort has been devoted to this problem by the author and by the personnel at ALHAP, but no satisfactory simple solution has been found. A centrifuge may work, but it seems unnecessarily complicated for such a simple problem. If the person concerned with operating the sampling system must devote a large part of his time to other matters, then an automatic sample container switcher would be a useful feature. If the sizes of the hail are the only interest, then the experiment could be considerably simplified by making the photographs of the hail in the field, by photographing a dark background that has been left out in the rainfall a known time. Schmenauer (1974) used a similar method for graupel. For internal analysis, the hailstones will have to be collected. Federer and Waldvogel (1975) give a brief description of a hailstone spectrometer used to collect sequential samples in Switzerland.

For the analysis of size distributions of collected hail, the greatest improvement would be to correctly calibrate the computer line scanning system. The problems of the system that were mentioned in Chapter 5 could be reduced by using sample sizes consisting of fewer hailstones. These smaller samples would be representative fractions of the collected samples.

Alternatively, the collected sample could be divided into sub-samples, each of which would be analyzed and then added together to give a total size distribution.

gether. A television camera could be used to photograph the hail samples and the resulting signal fed directly into the computer, thereby eliminating considerable noise and processing time.

In order to clarify the points raised in Chapter 5 about the time-dependent properties of falling hail, more sequential storm samples should be studied. The three cases studied were subjectively picked to cover a wide range of storm severities, but perhaps they were not representative of the full diversity of hailstorms. The variation with time of the correlation coefficients among various parameters should be studied in greater detail. In particular, it was suggested in Chapter 5 that hailstone number flux and mean diameter may correlate well only during the most intense hailfall. Although there is no reason for two parameters to be constantly correlated throughout a hailfall, there may exist correlations for part of the time.

The model of falling hail needs growth and melting processes included in its equations. In addition, a more detailed wind structure and temperature profile should be used, and may be available from mobile radiosonde soundings. The model uses the hailfall at one point only, so an estimate of the areal extent of the fallen hail could be used to calculate more realistic values of actual upper level concentrations. Alternatively, a set of sequential samples could be obtained from many points.

Analysis of other hailstone parameters, such as axis ratios, surface roughnesses, and internal structure, will depend largely on the availability of a suitable sample consisting of large, well-preserved hailstones. Measurements of the surface roughness and axis ratios would enable better estimates of drag coefficients as well as an evaluation of the factors used in the heat transfer equations used in the study of melting hailstones. The analysis of the internal structure of the hailstones may make it possible to determine the growth environment of the hailstones, but that will depend on the availability of suitable hailstones and analysis equipment.

BIBLIOGRAPHY

1. Atlas, D., 1963: Severe Local Storms. Meteorological Monographs, Vol. 5, 217 pp.
2. Atlas, D., and F. Ludlam, 1961: Multi-wavelength Radar Reflectivity of Hailstones. Quarterly Journal of the Royal Meteorological Society, 87, 523-531.
3. Auer, A., 1972: Distribution of Graupel and Hail with Size. Monthly Weather Review, 100, 525-528.
4. Auer, A., and J. Marwitz, 1972: Hail Encountered in the Vicinity of Thunderstorm Updrafts. Journal of Applied Meteorology, 11, 748-752..
5. Barge, B., and G. Isaac, 1973: The Shape of Alberta Hailstones. Journal de Recherches Atmosphériques, 7, 11-20.
6. Battan, L., and J. B. Theiss, 1972: Observed Doppler Spectra of Hail. Journal of Applied Meteorology, 11, 1001-1007.
7. Chapman, D. G., and R. A. Schaufele, 1970: Elementary Probability Models and Statistical Inference, Xerox Publishing, 358 pp.
8. Charlton, R. B., and R. List, 1972: Hail Size Distributions and Accumulation Zones. Journal of the Atmospheric Sciences, 29, 1182-1193.
9. Dennis, A. S., 1971: Hailstone Size Distributions and Equivalent Radar Reflectivity Factors Computed from Hailstone Momentum Records. Journal of Applied Meteorology, 10, 79-85.
10. Douglas, R. H., 1960: Size Distributions, Ice Contents, and Radar Reflectivities of Hail in Alberta. Nubila, 111, 5-11.
11. Douglas, R. H., 1963: Size Distributions of Alberta Hail Samples. Scientific Report MW-36, Stormy Weather Research Group, McGill University, Montreal, 55-701.

12. Douglas, R. H., 1961: Hail Size Distributions. Proceedings of the 1964 World Conference on Radar Meteorology, Boulder, Colorado, 146-149.
13. Federer, B., and A. Waldvogel, 1975: Hail and Raindrop Size Distributions From a Swiss Multicell Storm. Journal of Applied Meteorology, 14, 91-97.
14. Iribarne, J. and R. de Pena, 1962: The Influence of Particle Concentration on the Evolution of Hailstorms. Nubila, V, 7-30.
15. Joss, J., and A. Waldvogel, 1969: Raindrop Size Distributions and Sampling-Size Errors. Journal of the Atmospheric Sciences, 26, 566-569.
16. Knight, C. A., and N. C. Knight, 1968: The Final Freezing of Spongy Ice: Hailstone Collection Techniques and Interpretations of Structure. Journal of Applied Meteorology, 7, 875-881.
17. List, R., E. B. Charlton and P. Buttuls, 1968: A Numerical Experiment on the Growth and Feedback Mechanisms of Hailstones in a One-Dimensional Steady-State Model Cloud. Journal of the Atmospheric Sciences, 25, 1061-1074.
18. List, R., and J-G. Dussault, 1967: Quasi-Steady State Icing and Melting Conditions and Heat and Mass Transfer of Spherical and Spheroidal Hailstones. Journal of the Atmospheric Sciences, 24, 522-529.
19. List, R., W. A. Murray, and C. Dyck, 1972: Air Bubbles in Hailstones. Journal of the Atmospheric Sciences, 29, 916-920.
20. Lozowski, F. P., M. M. Oleskiw, and T. M. Morrow, 1975: Hail Photography: An Example of the Use of High-Speed Techniques Under Adverse Conditions. Journal of the Society of Motion Picture and Television Engineers, 84, 18-24.
21. Ludlam, F. and W. C. Macklin, 1960: Some Aspects of a Severe Storm in S. E. England. Nubila, 11, 38-50.
22. MANOBS: Manual of Standard Procedures for Surface Weather Observing and Reporting, Atmospheric Environment Service, Toronto, 307 pp.

23. Marshall, J. S., and W. McK. Palmer, 1948: The Distribution of Raindrops with Size. Journal of Meteorology, 5, 165-166.
24. Mason, B. J., 1956: On the Melting of Hailstones. Quarterly Journal of the Royal Meteorological Society, 82, 209-216.
25. Pell, J., 1971: Variations with Time of Six Alberta Hail Parameters. Proceedings of the Seventh Conference on Severe Local Storms, American Meteorological Society, Kansas City, 63-70.
26. Schemenauer, R. S., 1974: Size Distributions and Number Concentrations of Graupel from Alberta Showers. Preprint Volume, Conference on Cloud Physics, Tucson, Arizona, October 21-24, 1974. Published by the American Meteorological Society, Boston, MA.
27. Strong, G. S., 1974: The Objective Measurement of Alberta Hailfall, unpublished M. Sc. thesis, University of Alberta, 182 pp.
28. Sulakvelidze, G. K., 1967: Formation of Precipitation and Modification of Hail Processes, Israel Program for Scientific Translation, 207 pp.
29. Tsang, V., 1974: Determination of Hailpad Impression Size by Digital Picture Processing. Unpublished report to the Department of Computing Science, University of Alberta, 46 pp.
30. Ulbrich, C. W., 1974: Analysis of Doppler Radar Spectra of Hail. Journal of Applied Meteorology, 13, 387-396.
31. Ulbrich, C. W., D. Atlas and R. E. Rinehart, 1975: Hail Parameter Diagram. NIRE Symposium/Workshop on Hail, Estes Park, Colorado, September 21-28, 1975, Preprint Vol. 1.
32. Williams, G. N. and Douglas, R. H., 1963: Continuity of Hail Production in Alberta Storms. Scientific Report MW-36, Stormy Weather Research Group, McGill University, Montreal, 16-51.
33. Wisner, C., H. Orville and C. Myers, 1972: A Numerical Model of a Hail Bearing Cloud. Journal of the Atmospheric Sciences, 29, 1160-1181.

APPENDIX I

SAMPLING PROBLEMS

Various problems affected the collection of the sequential samples, thereby affecting the analyses. The troubles were the following ones.

1. 23 August 1973. Rain was collected along with hail in several of the samples, causing some melting and refreezing of the collected hailstones. This would alter the sample distribution leaving smaller hailstones overall, and fewer small hailstones than was actually the case.

2. 27 August 1973. Very soft, wet hail was collected, which was quite fragile in storage. Consequently, there was a lot of hailstone chipping and frost in the analyzed samples. The effect on the distribution would be to produce an excess of small hailstones.

3. 24 June 1974. The sampling location was on the edge of the storm and no samples were obtained from the area of the most intense hailfall. Consequently, the collected samples may have represented hailstones smaller than average for that storm.

4. 2 July 1974. The timing of the samples was not recorded. However, since the total time of sampling was recorded as 1 minute for four samples, each was assumed to be 15 seconds long.

5. 9 July 1974. Sampling took place in the final stages of the hailstorm. The samples collected consisted mostly of rainwater which melted the hailstones to some extent, and spoiled any mass measurements. The resulting distribution would have been altered in a fashion similar to that for 23 August 1973.

6. 18 August 1974. The catcher net was torn by the large

hair. The rips were so large that particular size categories were probably not preferentially lost through the holes in the catcher net. The collection efficiency of the catcher was probably reduced to about one half. Sample spectra were probably not significantly affected, but the flux densities would have been reduced.

APPENDIX II

THE MELTING OF FALLING HAILSTONES

The problem of the melting of a hailstone as it falls below the freezing level has been considered by several authors (Mason, 1956; and List and Dussault, 1957). Mason (1956)

gives the result that a particle with a radius of less than about 0.4 cm would melt completely on falling from a freezing level at 1 km above ground level in air with a lapse rate of $6.5 \text{ }^{\circ}\text{C km}^{-1}$.

A comprehensive treatment of the heat transfer between a hailstone and its environment is given by List and Dussault (1967). For a hailstone, there are four sources and sinks of heat, described by the following expressions.

1. Heat source from the freezing of accreted water.

$$Q_F = 0.785 \nu E W_f D R_e L_f I \quad (\text{A1})$$

2. Heat sink to warm the accreted cloud droplets.

$$Q_{CD} = -0.785 \nu E W_f D R_e \bar{c}_w (T_o - T_A) \quad (\text{A2})$$

3. Heat sink by evaporation, condensation and sublimation.

$$Q_{ES} = -C_{1,2} \theta D w_a T_A R_e^{-\frac{1}{2}} D (\bar{e}_{sh} - \bar{e}_v) \delta X \quad (\text{A3})$$

4. Rate of heat transfer between a hailstone and its environment by conduction and convection.

$$Q_{CC} = -1.68 \theta k R_e^{-\frac{1}{2}} D (T_o - T_A) \delta X \quad (\text{A4})$$

where

ν is the kinematic viscosity of air

E is the collection efficiency of the hailstone for cloud drops

w_f is the free liquid water content of the air

D is the major axis diameter of the hailstone (assumed oblate spherical)

Re is the Reynolds number

L_f is the latent heat of fusion at the deposit temperature

I is the fraction of accreted water which freezes

c_w is the specific heat of water averaged over the temperature range T_d to T_a

T_d is the deposit steady state temperature

T_a is the air temperature

C_{l2} is the latent heat of evaporation or sublimation

θ is the roughness factor

D_{wa} is the diffusivity of water vapor in air

c_{sh} is the saturation vapor pressure over the hailstone

c_v is the partial pressure of water vapor in ambient air

δ is the surface ratio of spheroid to a sphere

X is the heat transfer factor for a spheroid

k is the thermal conductivity of air.

When these equations are applied to melting, a few changes are required. The deposit temperature T_d remains constant at 0°C. Because any water drops that are shed will be warmed by the air and not the hailstone, Equation A2 becomes

$$Q_{cc} = 0 \quad (A5)$$

Equation A1 becomes

$$Q_M = -0.785 \nu W_f' D R e L_f \quad (A6)$$

where W_f' is the free liquid water produced in the wake of the hailstone by its melting. The collection efficiency, in this case represents the divergence of the water droplets and water vapor in the wake of the hailstone and is approximately equal to 1.

For a steady state the sum of the heat sources and sinks is zero, or

$$Q_M + Q_{ES} + Q_{cc} = 0 \quad (A7)$$

This formulation neglects the heat required to raise the temperature of the interior of the hailstone to 0°C. When Equations A3, A4, A5 and A6 are substituted into Equation A7, the thermodynamic state of a hailstone below the freezing level can be described by (List and Dussault, 1967)

$$\frac{1.68k(T_0 - T_A) + C_{1,2} D_{wa} T_A^{-1} (e_{sh} - e_v)}{0.785 \nu L_f} = W_f' \Phi \quad (A8)$$

where

$$\Phi = \frac{E R_e}{\theta \delta X} \quad (A9)$$

Thus, leads to the following equation relating the diameter and the auxiliary function ϕ below the freezing level:

$$\phi = 5933 D^{\frac{3}{2}} \quad (A10)$$

The "liquid water" content produced in the wake by the melting hailstone is given by

$$W_f = \frac{1.68k(T_a - T_0) + 6\mu_{in} D_w T_a^2 (\rho_{air} - \rho_{av})}{0.785 \times 5933 \sqrt{D}} \quad (A11)$$

The terminal speed of a falling spherical hailstone can be found by Equation 18. The air temperature is given by

$$T_a = T_s - \Gamma Z \quad (A12)$$

where Γ is the lapse rate, assumed constant at $0.5 \text{ } ^\circ\text{C km}^{-1}$, and T_s is the surface air temperature. Using the above equations, the mass melted from a hailstone in a time interval δt is given by

$$\delta M = \frac{\pi D^2}{4} V_t \delta t W_f \quad (A13)$$

The change in diameters δD is given by

$$\delta D = \frac{2\delta M}{\pi D^2 \rho_i} \quad (A14)$$

and the diameter after time δt , is given by

$$D_{\text{NEW}} = D_{\text{OLD}} - \delta D \quad (\text{A15})$$

This incremental procedure for the determination of the diameter of a melting hailstone as a function of time can be repeated until the hailstone either reaches the ground or melts completely.

Equations A11 to A16 were solved by computer with the following parameters. The air density was kept constant at a value of $\rho_A = 1.705 \times 10^{-3} \text{ g cm}^{-3}$. The effects of relative humidity or already present liquid water were ignored, which would increase the rate of melting. The hailstones were assumed to be smooth spheres with a drag coefficient of 0.5 and a density of 0.89 g cm^{-3} .

Table A1 shows the radius of the frozen part of a melting hailstone falling from the freezing level, upon reaching the ground.

	Initial radius (cm)				
	0.1	0.2	0.3	0.4	
Freezing level (km)	1.0	0	0.13	0.26	0.36
	2.0	0	0	0	0.22
	3.0	0	0	0	0
	4.0	0	0	0	0

TABLE A1 Radius of the frozen part of a melting hailstone at the ground level after falling from the freezing level

Table A1 shows that for a radius less than about 0.4 cm a hailstone will melt completely while falling 3 km below the freezing level. The effects of melting become less significant as the diameter increases because the increased terminal velocity results in less time being spent in the air, and the greater mass requires more latent heat to melt the ice.

The liquid water content of the air produced by the melting hail is an interesting by-product of the solution of the equations.

The values of w_f are summarized in Table A2.

Initial radius (cm)	2.5	2.0	1.5	1.0	0.9	0.8	0.7	0.6	0.5
w_f (g m ⁻³)	2.5	3.0	3.5	5.1	5.7	6.5	7.4	9.7	18.5

TABLE A2 Liquid water concentrations produced at the ground in the wakes of melting hailstones.

Table A2 applies only in the wake of the falling hailstones, and so will not directly give the total water content of the air. However, it does show that showers of small hail may produce high liquid water contents, and, hence, high rainfall rates.

The effect of melting on a cumulative exponential distribution is shown in Figure A1. The hail size distribution at the freezing level is assumed to be exponential. The change in the smaller diameters (less than 0.5 cm) is qualitatively in agreement with that observed in the individual collected hail samples.

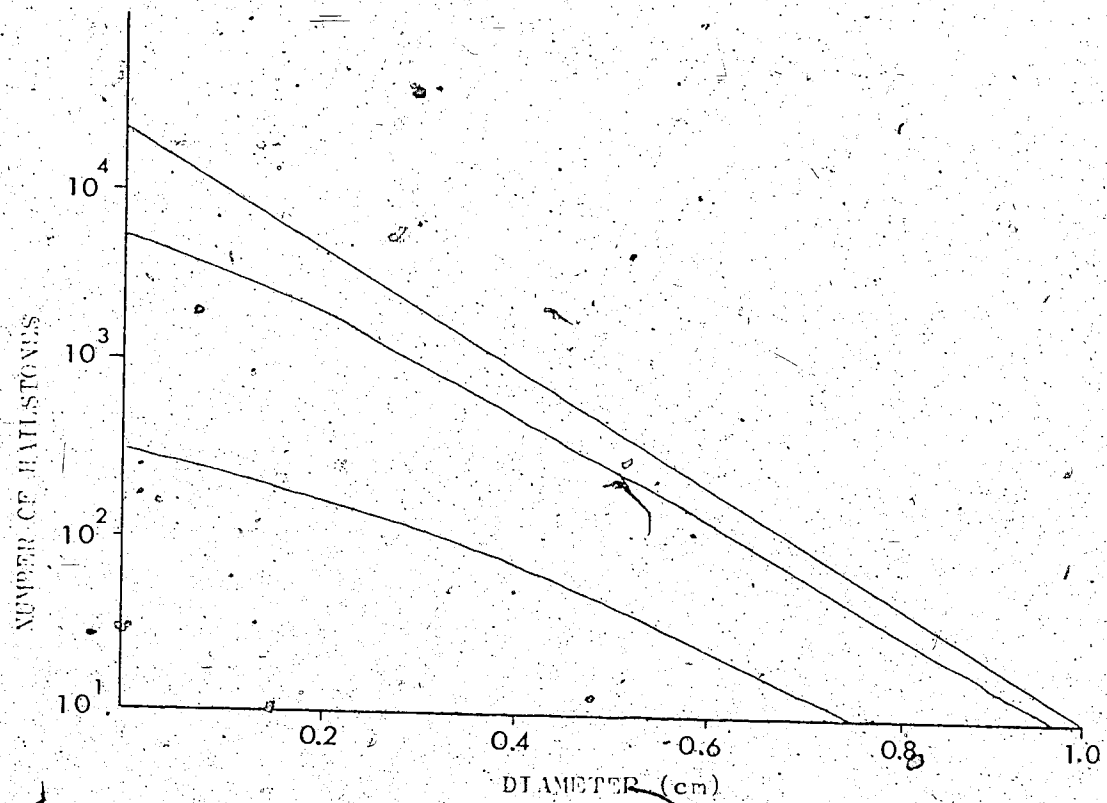


FIGURE Al. The effect of melting on a cumulative exponential distribution. The top curve is an initial distribution at the freezing level, assumed exponential. The middle curve is the resulting distribution if the freezing level is at 1.0 km, and the lower curve is the result if the freezing level is at 2.0 km.

APPENDIX III
INDIVIDUAL SAMPLES --
COLLECTION LOCATIONS AND TIMES,
SAMPLE DESCRIPTIONS AND
DISTRIBUTION PARAMETERS

LIN#	SAMPLING DATE	LOCATION	TIME OF SAMPLE CONTAINED START	TIME OF SAMPLE INTAKE END	SAMPLE CLASS	NUMBER OF STONES (G.)	MEAN DIAMETER (CM)
1	23 JUL 73	M4 S27T35E08	BOTTLE	19:41:00	19:43:00	2:00	45.6
2				19:43:00	19:45:04	2:00	-0.00
3	23 AUG 73	CF S33T35E04	BOTTLE	19:45:00	19:47:00	2:00	55.5
4				17:50:00	17:50:15	0:15	-0.30
5				17:50:15	17:50:30	0:15	415
6				17:50:30	17:50:45	0:15	40.0
7				17:50:45	17:51:15	0:15	112.8
8				17:51:15	17:51:45	0:15	133.1
9				17:51:45	17:52:15	0:30	152.5
10				17:52:15	17:52:45	0:30	110.4
11				17:52:45	17:53:15	0:30	110.4
12	27 AUG 73	CF S33T35E04	BOTTLE	19:23:00	19:23:20	0:20	-0.00
13				19:23:20	19:23:40	0:20	30.4
14				19:23:40	19:24:00	0:20	30.4
15				19:24:00	19:24:20	0:20	32.1
16				19:24:20	19:24:40	0:20	112.6
17				19:24:40	19:25:00	0:20	16.5
18				19:25:00	19:25:20	0:20	-0.00
19				19:25:20	19:25:40	0:20	-0.00
20				19:25:40	19:26:00	0:20	13.5
21				19:26:00	19:26:20	0:20	51.9
22				19:26:20	19:26:40	0:20	157
23				19:26:40	19:27:00	0:20	63.2
24				19:27:00	19:27:20	0:20	165
				19:27:20	19:27:40	0:20	-0.00
				19:27:40	19:28:00	0:20	26.1
				19:28:00	19:28:20	0:20	-0.00
				19:28:20	19:28:40	0:20	-0.00
				19:28:40	19:29:00	0:20	-0.00
				19:29:00	19:29:20	0:20	-0.00
				19:29:20	19:29:40	0:20	-0.00
				19:29:40	19:30:00	0:20	-0.00
				19:30:00	19:30:20	0:20	-0.00
				19:30:20	19:30:40	0:20	-0.00
				19:30:40	19:31:00	0:20	-0.00
				19:31:00	19:31:20	0:20	-0.00
				19:31:20	19:31:40	0:20	-0.00
				19:31:40	19:32:00	0:20	-0.00
				19:32:00	19:32:20	0:20	-0.00
				19:32:20	19:32:40	0:20	-0.00
				19:32:40	19:33:00	0:20	-0.00
				19:33:00	19:33:20	0:20	-0.00
				19:33:20	19:33:40	0:20	-0.00
				19:33:40	19:34:00	0:20	-0.00
				19:34:00	19:34:20	0:20	-0.00
				19:34:20	19:34:40	0:20	-0.00
				19:34:40	19:35:00	0:20	-0.00
				19:35:00	19:35:20	0:20	-0.00
				19:35:20	19:35:40	0:20	-0.00
				19:35:40	19:36:00	0:20	-0.00
				19:36:00	19:36:20	0:20	-0.00
				19:36:20	19:36:40	0:20	-0.00
				19:36:40	19:37:00	0:20	-0.00
				19:37:00	19:37:20	0:20	-0.00
				19:37:20	19:37:40	0:20	-0.00
				19:37:40	19:38:00	0:20	-0.00
				19:38:00	19:38:20	0:20	-0.00
				19:38:20	19:38:40	0:20	-0.00
				19:38:40	19:39:00	0:20	-0.00
				19:39:00	19:39:20	0:20	-0.00
				19:39:20	19:39:40	0:20	-0.00
				19:39:40	19:40:00	0:20	-0.00
				19:40:00	19:40:20	0:20	-0.00
				19:40:20	19:40:40	0:20	-0.00
				19:40:40	19:41:00	0:20	-0.00
				19:41:00	19:41:20	0:20	-0.00
				19:41:20	19:41:40	0:20	-0.00
				19:41:40	19:42:00	0:20	-0.00
				19:42:00	19:42:20	0:20	-0.00
				19:42:20	19:42:40	0:20	-0.00
				19:42:40	19:43:00	0:20	-0.00
				19:43:00	19:43:20	0:20	-0.00
				19:43:20	19:43:40	0:20	-0.00
				19:43:40	19:44:00	0:20	-0.00
				19:44:00	19:44:20	0:20	-0.00
				19:44:20	19:44:40	0:20	-0.00
				19:44:40	19:45:00	0:20	-0.00
				19:45:00	19:45:20	0:20	-0.00
				19:45:20	19:45:40	0:20	-0.00
				19:45:40	19:46:00	0:20	-0.00
				19:46:00	19:46:20	0:20	-0.00
				19:46:20	19:46:40	0:20	-0.00
				19:46:40	19:47:00	0:20	-0.00
				19:47:00	19:47:20	0:20	-0.00
				19:47:20	19:47:40	0:20	-0.00
				19:47:40	19:48:00	0:20	-0.00
				19:48:00	19:48:20	0:20	-0.00
				19:48:20	19:48:40	0:20	-0.00
				19:48:40	19:49:00	0:20	-0.00
				19:49:00	19:49:20	0:20	-0.00
				19:49:20	19:49:40	0:20	-0.00
				19:49:40	19:50:00	0:20	-0.00
				19:50:00	19:50:20	0:20	-0.00
				19:50:20	19:50:40	0:20	-0.00
				19:50:40	19:51:00	0:20	-0.00
				19:51:00	19:51:20	0:20	-0.00
				19:51:20	19:51:40	0:20	-0.00
				19:51:40	19:52:00	0:20	-0.00
				19:52:00	19:52:20	0:20	-0.00
				19:52:20	19:52:40	0:20	-0.00
				19:52:40	19:53:00	0:20	-0.00
				19:53:00	19:53:20	0:20	-0.00
				19:53:20	19:53:40	0:20	-0.00
				19:53:40	19:54:00	0:20	-0.00
				19:54:00	19:54:20	0:20	-0.00
				19:54:20	19:54:40	0:20	-0.00
				19:54:40	19:55:00	0:20	-0.00
				19:55:00	19:55:20	0:20	-0.00
				19:55:20	19:55:40	0:20	-0.00
				19:55:40	19:56:00	0:20	-0.00
				19:56:00	19:56:20	0:20	-0.00
				19:56:20	19:56:40	0:20	-0.00
				19:56:40	19:57:00	0:20	-0.00
				19:57:00	19:57:20	0:20	-0.00
				19:57:20	19:57:40	0:20	-0.00
				19:57:40	19:58:00	0:20	-0.00
				19:58:00	19:58:20	0:20	-0.00
				19:58:20	19:58:40	0:20	-0.00
				19:58:40	19:59:00	0:20	-0.00
				19:59:00	19:59:20	0:20	-0.00
				19:59:20	19:59:40	0:20	-0.00
				19:59:40	19:50:00	0:20	-0.00
				19:50:00	19:50:20	0:20	-0.00
				19:50:20	19:50:40	0:20	-0.00
				19:50:40	19:51:00	0:20	-0.00
				19:51:00	19:51:20	0:20	-0.00
				19:51:20	19:51:40	0:20	-0.00
				19:51:40	19:52:00	0:20	-0.00
				19:52:00	19:52:20	0:20	-0.00
				19:52:20	19:52:40	0:20	-0.00
				19:52:40	19:53:00	0:20	-0.00
				19:53:00	19:53:20	0:20	-0.00
				19:53:20	19:53:40	0:20	-0.00
				19:53:40	19:54:00	0:20	-0.00
				19:54:00	19:54:20	0:20	-0.00
				19:54:20	19:54:40	0:20	-0.00
				19:54:40	19:55:00	0:20	-0.00
				19:55:00	19:55:20	0:20	-0.00
				19:55:20	19:55:40	0:20	-0.00
				19:55:40	19:56:00	0:20	-0.00
				19:56:00	19:56:20	0:20	-0.00
				19:56:20	19:56:40	0:20	-0.00
				19:56:40	19:57:00	0:20	-0.00
				19:57:00	19:57:20	0:20	-0.00
				19:57:20	19:57:40	0:20	-0.00
				19:57:40	19:58:00	0:20	-0.00
				19:58:00	19:58:20	0:20	-0.00
				19:58:20	19:58:40	0:20	-0.00
				19:58:40	19:59:00	0:20	-0.00
				19:59:00	19:59:20	0:20	-0.00
				19:59:20	19:59:40	0:20	-0.00
				19:59:40	19:50:00	0:20	-0.00
				19:50:00	19:50:20	0:20	-0.00
				19:50:20	19:50:40	0:20	-0.00
				19:50:40	19:51:00	0:20	-0.00
				19:51:00	19:51:20	0:20	-0.00
				19:51:20	19:51:40	0:20	-0.00
				19:51:40	19:52:00	0:20	-0.00
				19:52:00	19:52:20	0:20	-0.00
				19:52:20	19:52:40	0:20	-0.00
				19:52:40	19:53:00	0:20	-0.00
				19:53:00	19:53:20	0:20	-0.00
				19:53:20	19:53:40	0:20	-0.00
				19:53:40	19:54:00	0:20	-0.00
				19:54:00	19:54:20	0:20	-0.00
				19:54:20	19:54:40	0:20	-0.00
				19:54:40	19:55:00	0:20	-0.00
				19:55:00	19:55:20	0:20	-0.00
				19:55:20	19:55:40	0:20	-0.00
				19:55:40	19:5		

DATE	LOCATION	CAPTION	SAMPLE CONTAINER	TYPE OF SAMPLE	TIME OF SAMPLE	SAMPLE NUMBER	MEAN DURATION	MASS END (g.)	HAILSTONES (CM)
25					15:27:20	15:27:40	0:20	147.5	4.0
26					15:27:40	15:28:00	0:20	77.0	2.97
27					15:28:00	15:28:20	0:20	97.5	5.0
28					15:28:20	15:28:40	0:20	92.7	2.12
29					15:28:40	15:29:00	0:20	112.2	4.1
30					15:29:00	15:29:20	0:20	122.1	4.4
31					15:29:20	15:29:40	0:20	75.6	4.3
32					15:29:40	15:30:00	0:20	103.1	4.0
33					15:30:00	15:30:20	0:20	93.1	3.3
34	24 JUL 74	NF S09T31E63	BOTTLE	15:55:30	15:56:00	3:30	11.4	4.1	5.3
35					15:56:00	15:56:30	3:30	17.6	7.9
36					15:56:30	15:57:00	3:30	16.1	5.9
37					15:57:00	15:58:30	1:30	1.0	2.5
38					15:58:30	15:59:00	1:30	0.9	0.3
39					15:59:00	16:00:00	1:00	0.0	0.2
40	02 JUL 74	SF S26T34E03	BOTTLE	17:25:30	17:25:15	0:15	99.5	3	5.7
41					17:25:15	17:25:30	0:15	1.0	0.3
42					17:25:30	17:25:45	0:15	1.0	4.4
43					17:25:45	17:26:00	0:15	1.0	1.6
44	05 JUL 74	NW S36T34E02	BOTTLE	16:47:00	16:48:30	1:30	4.0	1.1	4.4
45					16:48:30	16:50:30	2:00	1.0	1.2
46					16:50:30	16:51:40	1:10	0.2	0.56
47					16:51:40	16:53:40	2:00	0.1	0.45
48					16:54:05	16:54:00	1:55	1.0	2.4
49					16:56:00	16:57:00	1:00	1.1	1.59
								1.1	0.48
								1.1	3.55
								1.1	1.10

LIN#	SAMPLING DATE	LOCATION	SAMPLE CONTAINER START	TYPE OF SAMPLE	TIME OF SAMPLE START	SAMPLE END	TIME OF SAMPLE END	IRRADIATION FNU.	SAMPLE MASS (G.)	NUMBER OF HATCHES	MEAN DIAMETER OF HATCHES (CM)
50	14 JUL74	NW	\$36T33P02	HATCHES	22:03:00	22:05:00	22:06:00	-0.0	-0.0	-0.0	-0.00
51					22:05:00	22:07:00	2:00	50.0	34	34	
52					22:07:00	22:09:00	2:00	50.0	72	43	
53					22:09:00	22:10:30	1:30	50.0	14	47	
54					22:10:30	22:13:00	2:30	50.0	81	26	
55					22:15:10	22:16:00	3:00	50.0	37	30	
56	18 AUG74	SW	\$24T34H01	HAG	17:21:00	17:24:15	3:15	355.0	122	205	
57					17:24:15	17:24:15	2:00	560.0	50	225	
58					17:26:15	17:27:15	1:00	242.0	36	312	
59					17:27:15	17:28:15	1:00	122.2	24	275	
60					17:28:15	17:29:15	1:00	53.3	41	149	
61					17:29:23	17:30:37	1:00	12.4	25	102	
62					17:30:15	17:32:45	3:30	-0.0	14	80	
63	18 AUG74		\$36T33P28	HAG	17:44:00	17:51:00	2:00	-0.0	20	85	
64					17:51:00	17:54:00	3:00	-0.0	-9	0.00	
65	18 AUG74	SW	\$23T33H26	HAG	18:10:00	18:15:00	5:00	-0.0	73	70	
66					18:15:00	18:16:00	1:00	49.6	70	115	
67					18:16:00	18:17:00	1:00	347.5	49.7	118	
68					18:17:00	18:18:00	1:00	341.4	283	133	
69					18:18:00	18:19:00	1:00	652.7	739	122	
70					18:19:00	18:20:00	1:00	147.1	395	99	
71					18:20:00	18:25:00	5:00	42.0	31	146	
72					18:25:00	18:27:30	2:30	12.0	14	20	
73	18 AUG74		\$0LT33P25	HAG	18:42:30	18:44:30	2:00	-0.0	13	113	
74					18:49:30	18:50:30	1:00	-0.0	-0	-0.00	

EXPONENTIAL HISTOGRAM

EXponential DISTRIBUTION

CUMULATIVE EXPONENTIAL		EXPONENTIAL		CUMULATIVE EXPONENTIAL		EXPONENTIAL	
LAMPRA	(Cr-1)	LAMPRA	(Cr-1)	LAMPRA	(Cr-1)	LAMPRA	(Cr-1)
1	-0	-0.100	-0.60	-0	-0.000	-0	-0.000
2	411	3.649	2.10	79	2.624	43	2.22
3	407	4.373	2.60	57	2.610	54	2.22
4	6591	4.048	4.82	1564	3.724	17.54	2.22
5	6251	3.330	2.70	1040	2.724	10.14	2.22
6	5909	3.346	2.62	1137	3.015	11.36	2.22
7	-1	-0.660	-0.16	-0	-0.000	-0	-0.000
8	121	1.034	1.63	6	2.60	4.23	1.45
9	-0	-0.610	-0	-0	-0.000	-0	-0.000
10	574	3.729	54	54	1.630	5.22	5.1
11	-0	-1.010	-0.64	-0	-0.000	-0	-0.000
12	1150	4.578	1.36	294	3.232	2.05	1.937
13	-0	-0.600	-0.09	-0	-0.000	-0	-0.000
14	-6	-0.600	-0.50	-0	-0.000	-0	-0.000
15	-0	-0.610	-0.00	-0	-0.000	-0	-0.000
16	-0	-0.600	-0.00	-0	-0.000	-0	-0.000
17	1078	4.682	2.31	164	3.253	16.60	1.819
18	1134	6.371	3.55	267	4.605	4.41	1.921
19	2921	2.305	2.87	342	1.619	4.30	4.894
20	2678	4.531	0.72	446	3.739	3.11	3.534
21	1653	4.124	1.25	125	3.234	4.44	2.768
22	1749	4.000	3.15	340	3.712	4.85	2.971
23	3042	2.512	1.63	163	1.64	1.82	2.10
24	2389	3.445	1.36	403	2.403	2.743	2.61

LINE	FLUX DENSITY EXPONENTIAL DISTRIBUTION	CUMULATIVE EXPONENTIAL									
		LAMBDA (CM-1)	N (CM-1)								
25	2074	3.654	•30	4.29	3.113	4.05	3.459	3.668	3.30	7.22	3.143
26	1395	2.540	1.16	1.87	1.448	6.32	2.348	2.579	1.31	314	1.971
27	2489	3.307	1.72	4.17	2.641	5.11	4.142	3.307	1.72	665	2.641
28	1590	3.624	2.76	2.39	6.785	4.16	2.694	3.972	3.03	402	2.821
29	2415	3.264	1.02	4.23	2.776	5.27	4.074	3.445	1.11	719	2.821
30	3194	3.143	1.43	5.70	2.887	18.83	5.313	3.148	1.44	951	2.905
31	3311	3.408	1.65	5.92	3.171	25.50	5.504	3.410	1.67	99	3.196
32	2693	2.046	1.59	4.41	2.335	1.69	4.566	3.015	1.79	749	2.372
33	406	4.410	4.64	5	-3.91	13.43	6.87	4.605	4.51	8	-1.431
34	394	2.257	1.31	7	-8.47	3.44	6.46	2.254	1.32	15	-7.452
35	634	3.442	6.62	14	-2.30	10.55	1.049	3.454	6.42	24	3.49
36	456	3.759	3.24	5	-1.16	16.27	75.3	3.751	3.23	9	-2.251
37	163	4.667	1.81	5	-1.59	7.55	26.2	4.552	1.70	9	-1.113
38	14	2.130	.89	2	0.009	0.09	24	2.130	.59	4	0.000
39	98	5.816	0.3	1.9	3.625	.97	14.9	5.646	.62	28	2.815
40	415	11.680	9.49	20.9	11.775	26.43	6.92	15.551	11.68	35.0	11.625
41	113	3.212	3.37	10	-4.31	7.62	1.87	3.210	5.33	16	-4.25
42	-0	-0.000	-0.06	-0	-0.000	-0.60	-0	-0.000	-0.00	-9	-0.000
43	-0	-0.000	-0.00	-0	-0.000	-0.00	-0	-0.000	-0.00	-9	-0.000
44	127	4.133	4.64	5	-0.18	12.35	21.0	4.198	5.08	7	-0.044
45	362	5.046	5.07	21.	-1.257	23.54	6.07	5.165	5.38	35	1.326
46	84	6.281	.54	26	3.933	5.43	1.38	6.383	.67	43	4.114
47	319	4.757	2.31	36	2.713	4.62	5.29	4.812	2.42	69	2.275
48	334	6.652	3.99	39	3.493	23.25	5.63	7.014	4.25	66	3.661
49	-0	-0.000	-0	-0	-0.000	-0	-0.000	-0.000	-0	-0.000	-0.000

FLUX OR SIGHT EXPONENTIAL DISTRIBUTION

EXPONENTIAL DISTRIBUTION

CUMULATIVE EXPONENTIAL EXPONENTIAL

LINF	N	LAMM	S	LAMM	CUMULATIVE EXPONENTIAL EXPONENTIAL	
					LAMM	S
50	-0	-0.000	-0.000	-0	-0.000	-0
51	44	5.548	3.32	4	0.458	11.57
52	94	3.864	1.57	10	1.366	8.13
53	16	2.927	1.19	3	0.817	2.81
54	75	6.717	1.66	10	2.494	17.33
55	60	9.220	5.43	6	1.436	19.41
56	85	8.03	0.82	2	-0.85	2.50
57	187	8.54	3.90	4	-0.87	1.37
58	3144	1.656	3.65	3	-0.207	6.97
59	264	1.418	2.66	2	0.000	0.60
60	203	1.902	3.63	4	0.004	3.13
61	1	363	3.021	5	-0.404	4.46
62	-0	-0.600	-0.00	6	-0.600	4.32
63	2601	8.524	2.02	38	3.465	4.04
64	0	-0.600	-0.600	0	-0.600	-0
65	75	3.233	0.97	3	-0.600	-0.600
66	915	2.765	1.65	21	0.365	1.55
67	4097	2.747	8.02	46	0.364	0.94
68	2739	2.305	5.03	33	0.437	0.45
69	4344	2.612	2.63	50	0.470	1.41
70	3080	2.837	9.24	49	0.459	1.52
71	0	-0.600	-0.600	0	-0.600	-0
72	7681	6.265	1.06	1	0.600	2.07
73	22	1.665	0.60	1	-0.854	3.3
74	-0	-0.700	-0.60	4	-0.606	0.60

LINEAR DISTRIBUTION PARAMETERS

LINE	SLOPE $D < 0.1 \text{ cm}$	PROBABILITY $P(D < 0.1 \text{ cm})$	\bar{D}	RELATIONSHIP BETWEEN \bar{D} AND D_{MAX}	
				D_{MAX}	D_{MAX}^2
1	-0.70	-0.60	13.3	13.3	-0.000
2	3.32	0.9	13.4	25.6	-0.000
3	4.34	0.02	13.3	24.9	-0.000
4	3.64	0.09	19.2	24.3	-0.000
5	3.06	0.13	17.2	23.4	-0.000
6	3.10	0.14	14.3	22.5	-0.000
7	6.69	20.0	10.0	10.0	-0.000
8	6.24	0.00	24.6	7.52	-0.000
9	-0.60	-0.00	26.0	-0.065	-0.000
10	13.55	0.00	27.7	-0.000	-0.000
11	-0.40	-0.00	17.9	-0.000	-0.000
12	3.47	0.14	17.9	20.2	-0.000
13	-5.09	-0.00	16.0	-0.000	-0.000
14	-6.06	-0.00	10.0	-0.000	-0.000
15	-9.65	-0.00	10.0	-0.000	-0.000
16	-0.50	-0.00	16.0	-0.000	-0.000
17	3.46	0.04	13.1	22.2	-0.000
18	4.15	Y1	13.8	25.9	-0.000
19	3.68	0.00	14.6	25.0	-0.000
20	3.43	0.13	13.0	21.4	-0.000
21	3.61	0.17	11.6	26.2	-0.000
22	3.50	0.65	19.0	24.9	-0.000
23	3.52	0.02	11.4	17.1	-0.000
24		0.05		23.0	-0.000

LOG-NORMAL DISTRIBUTION PARAMETERS

LINE SLOPE PROBABILITY
 D < 0.1 cm D < 0.1 cm

LINE	SLOPE	PROBABILITY D < 0.1 cm	VARIANCE D < 0.1 cm	MEDIAN DIAMETER (cm)
25	3.38	2.02	7.5	22.6
26	3.18	.05	12.5	33.1
27	3.13	.10	20.5	25.8
28	3.70	.04	23.0	24.9
29	3.66	.04	7.9	31.6
30	3.87	.11	10.3	25.4
31	2.17	.22	12.1	15.1
32	3.43	.04	21.7	33.7
33	11.61	0.00	36.3	36.3
34	6.51	0.00	45.7	45.7
35	7.11	0.00	25.1	25.7
36	9.27	0.00	22.8	22.8
37	12.03	0.00	20.9	20.9
38	7.65	0.00	20.0	20.0
39	15.97	0.00	10.8	10.8
40	7.17	.40	19.4	19.4
41	6.20	0.00	16.6	16.6
42	-9.00	-0.00	10.0	10.0
43	-9.00	-0.00	10.0	10.0
44	5.62	0.00	22.3	22.3
45	5.36	.17	15.2	15.2
46	4.76	0.00	32.6	32.6
47	4.62	.02	31.4	31.4
48	4.77	.03	30.5	30.5
49	-0.00	-0.00	10.0	10.0

THE INFLUENCE OF INSTRUMENTATION ON PREDICTION

LINE	SLOPE	PERMEABILITY $D < 0.1 \text{ cm}$	WATER C _E	WATER C _E
1	0.0000	0.0000	0.0000	0.0000
2	-0.0001	0.0001	0.0001	0.0001
3	-0.0002	0.0002	0.0002	0.0002
4	-0.0003	0.0003	0.0003	0.0003
5	-0.0004	0.0004	0.0004	0.0004
6	-0.0005	0.0005	0.0005	0.0005
7	-0.0006	0.0006	0.0006	0.0006
8	-0.0007	0.0007	0.0007	0.0007
9	-0.0008	0.0008	0.0008	0.0008
10	-0.0009	0.0009	0.0009	0.0009
11	-0.0010	0.0010	0.0010	0.0010
12	-0.0011	0.0011	0.0011	0.0011
13	-0.0012	0.0012	0.0012	0.0012
14	-0.0013	0.0013	0.0013	0.0013
15	-0.0014	0.0014	0.0014	0.0014
16	-0.0015	0.0015	0.0015	0.0015
17	-0.0016	0.0016	0.0016	0.0016
18	-0.0017	0.0017	0.0017	0.0017
19	-0.0018	0.0018	0.0018	0.0018
20	-0.0019	0.0019	0.0019	0.0019
21	-0.0020	0.0020	0.0020	0.0020
22	-0.0021	0.0021	0.0021	0.0021
23	-0.0022	0.0022	0.0022	0.0022
24	-0.0023	0.0023	0.0023	0.0023
25	-0.0024	0.0024	0.0024	0.0024
26	-0.0025	0.0025	0.0025	0.0025
27	-0.0026	0.0026	0.0026	0.0026
28	-0.0027	0.0027	0.0027	0.0027
29	-0.0028	0.0028	0.0028	0.0028
30	-0.0029	0.0029	0.0029	0.0029
31	-0.0030	0.0030	0.0030	0.0030
32	-0.0031	0.0031	0.0031	0.0031
33	-0.0032	0.0032	0.0032	0.0032
34	-0.0033	0.0033	0.0033	0.0033
35	-0.0034	0.0034	0.0034	0.0034
36	-0.0035	0.0035	0.0035	0.0035
37	-0.0036	0.0036	0.0036	0.0036
38	-0.0037	0.0037	0.0037	0.0037
39	-0.0038	0.0038	0.0038	0.0038
40	-0.0039	0.0039	0.0039	0.0039
41	-0.0040	0.0040	0.0040	0.0040
42	-0.0041	0.0041	0.0041	0.0041
43	-0.0042	0.0042	0.0042	0.0042
44	-0.0043	0.0043	0.0043	0.0043
45	-0.0044	0.0044	0.0044	0.0044
46	-0.0045	0.0045	0.0045	0.0045
47	-0.0046	0.0046	0.0046	0.0046
48	-0.0047	0.0047	0.0047	0.0047
49	-0.0048	0.0048	0.0048	0.0048
50	-0.0049	0.0049	0.0049	0.0049
51	-0.0050	0.0050	0.0050	0.0050
52	-0.0051	0.0051	0.0051	0.0051
53	-0.0052	0.0052	0.0052	0.0052
54	-0.0053	0.0053	0.0053	0.0053
55	-0.0054	0.0054	0.0054	0.0054
56	-0.0055	0.0055	0.0055	0.0055
57	-0.0056	0.0056	0.0056	0.0056
58	-0.0057	0.0057	0.0057	0.0057
59	-0.0058	0.0058	0.0058	0.0058
60	-0.0059	0.0059	0.0059	0.0059
61	-0.0060	0.0060	0.0060	0.0060
62	-0.0061	0.0061	0.0061	0.0061
63	-0.0062	0.0062	0.0062	0.0062
64	-0.0063	0.0063	0.0063	0.0063
65	-0.0064	0.0064	0.0064	0.0064
66	-0.0065	0.0065	0.0065	0.0065
67	-0.0066	0.0066	0.0066	0.0066
68	-0.0067	0.0067	0.0067	0.0067
69	-0.0068	0.0068	0.0068	0.0068
70	-0.0069	0.0069	0.0069	0.0069
71	-0.0070	0.0070	0.0070	0.0070
72	-0.0071	0.0071	0.0071	0.0071
73	-0.0072	0.0072	0.0072	0.0072
74	-0.0073	0.0073	0.0073	0.0073
75	-0.0074	0.0074	0.0074	0.0074
76	-0.0075	0.0075	0.0075	0.0075
77	-0.0076	0.0076	0.0076	0.0076
78	-0.0077	0.0077	0.0077	0.0077
79	-0.0078	0.0078	0.0078	0.0078
80	-0.0079	0.0079	0.0079	0.0079
81	-0.0080	0.0080	0.0080	0.0080
82	-0.0081	0.0081	0.0081	0.0081
83	-0.0082	0.0082	0.0082	0.0082
84	-0.0083	0.0083	0.0083	0.0083
85	-0.0084	0.0084	0.0084	0.0084
86	-0.0085	0.0085	0.0085	0.0085
87	-0.0086	0.0086	0.0086	0.0086
88	-0.0087	0.0087	0.0087	0.0087
89	-0.0088	0.0088	0.0088	0.0088
90	-0.0089	0.0089	0.0089	0.0089
91	-0.0090	0.0090	0.0090	0.0090
92	-0.0091	0.0091	0.0091	0.0091
93	-0.0092	0.0092	0.0092	0.0092
94	-0.0093	0.0093	0.0093	0.0093
95	-0.0094	0.0094	0.0094	0.0094
96	-0.0095	0.0095	0.0095	0.0095
97	-0.0096	0.0096	0.0096	0.0096
98	-0.0097	0.0097	0.0097	0.0097
99	-0.0098	0.0098	0.0098	0.0098
100	-0.0099	0.0099	0.0099	0.0099
101	-0.0100	0.0100	0.0100	0.0100
102	-0.0101	0.0101	0.0101	0.0101
103	-0.0102	0.0102	0.0102	0.0102
104	-0.0103	0.0103	0.0103	0.0103
105	-0.0104	0.0104	0.0104	0.0104
106	-0.0105	0.0105	0.0105	0.0105
107	-0.0106	0.0106	0.0106	0.0106
108	-0.0107	0.0107	0.0107	0.0107
109	-0.0108	0.0108	0.0108	0.0108
110	-0.0109	0.0109	0.0109	0.0109
111	-0.0110	0.0110	0.0110	0.0110
112	-0.0111	0.0111	0.0111	0.0111
113	-0.0112	0.0112	0.0112	0.0112
114	-0.0113	0.0113	0.0113	0.0113
115	-0.0114	0.0114	0.0114	0.0114
116	-0.0115	0.0115	0.0115	0.0115
117	-0.0116	0.0116	0.0116	0.0116
118	-0.0117	0.0117	0.0117	0.0117
119	-0.0118	0.0118	0.0118	0.0118
120	-0.0119	0.0119	0.0119	0.0119
121	-0.0120	0.0120	0.0120	0.0120
122	-0.0121	0.0121	0.0121	0.0121
123	-0.0122	0.0122	0.0122	0.0122
124	-0.0123	0.0123	0.0123	0.0123
125	-0.0124	0.0124	0.0124	0.0124
126	-0.0125	0.0125	0.0125	0.0125
127	-0.0126	0.0126	0.0126	0.0126
128	-0.0127	0.0127	0.0127	0.0127
129	-0.0128	0.0128	0.0128	0.0128
130	-0.0129	0.0129	0.0129	0.0129
131	-0.0130	0.0130	0.0130	0.0130
132	-0.0131	0.0131	0.0131	0.0131
133	-0.0132	0.0132	0.0132	0.0132
134	-0.0133	0.0133	0.0133	0.0133
135	-0.0134	0.0134	0.0134	0.0134
136	-0.0135	0.0135	0.0135	0.0135
137	-0.0136	0.0136	0.0136	0.0136
138	-0.0137	0.0137	0.0137	0.0137
139	-0.0138	0.0138	0.0138	0.0138
140	-0.0139	0.0139	0.0139	0.0139
141	-0.0140	0.0140	0.0140	0.0140
142	-0.0141	0.0141	0.0141	0.0141
143	-0.0142	0.0142	0.0142	0.0142
144	-0.0143	0.0143	0.0143	0.0143
145	-0.0144	0.0144	0.0144	0.0144
146	-0.0145	0.0145	0.0145	0.0145
147	-0.0146	0.0146	0.0146	0.0146
148	-0.0147	0.0147	0.0147	0.0147
149	-0.0148	0.0148	0.0148	0.0148
150	-0.0149	0.0149	0.0149	0.0149
151	-0.0150	0.0150	0.0150	0.0150
152	-0.0151	0.0151	0.0151	0.0151
153	-0.0152	0.0152	0.0152	0.0152
154	-0.0153	0.0153	0.0153	0.0153
155	-0.0154	0.0154	0.0154	0.0154
156	-0.0155	0.0155	0.0155	0.0155
157	-0.0156	0.0156	0.0156	0.0156
158	-0.0157	0.0157	0.0157	0.0157
159	-0.0158	0.0158	0.0158	0.0158
160	-0.0159	0.0159	0.0159	0.0159
161	-0.0160	0.0160	0.0160	0.0160
162	-0.0161	0.0161	0.0161	0.0161
163	-0.0162	0.0162	0.0162	0.0162
164	-0.0163	0.0163	0.0163	0.0163
165	-0.0164	0.0164	0.0164	0.0164
166	-0.0165	0.0165	0.0165	0.0165
167	-0.0166	0.0166	0.0166	0.0166
168	-0.0167	0.0167	0.0167	0.0167
169	-0.0168	0.0168	0.0168	0.0168
170	-0.0169	0.0169	0.0169	0.0169
171	-0.0170	0.0170	0.0170	0.0170
172	-0.0171	0.0171	0.0171	0.0171
173	-0.0172	0.0172	0.0172	0.0172
174	-0.0173	0.0173	0.0173	0.0173
175	-0.0174	0.0174	0.0174	0.0174
176	-0.0175	0.0175	0.0175	0.0175
177	-0.0176	0.0176	0.0176	0.0176
178	-0.0177	0.0177	0.0177	0.0177
179	-0.0178	0.0178	0.0178	0.0178
180	-0.0179	0.0179	0.0179	0.0179
181	-0.0180	0.0180	0.0180	0.0180
182	-0.0181	0.0181	0.0181	0.0181
183	-0.0182	0.0182	0.0182	0.0182
184	-0.0183	0.0183	0.0183	0.0183
185	-0.0184	0.0184	0.0184	0.0184
186	-0.0185	0.0185	0.0185	0.0185
187	-0.0186	0.0186	0.0186	0.0186
188	-0.0187	0.0187	0.0187	0.0187
189	-0.0188	0.0188	0.0188	0.0188
190	-0.0189	0.0189	0.0189	0.0189
191	-0.0190	0.0190	0.0190	0.0190
192	-0.0191	0.0191	0.0191	0.0191
193	-0.0192	0.0192	0.0192	0.0192
194	-0.0193	0.0193	0.0193	0.0193
195	-0.0194	0.0194	0.0194	0.0194
196	-0.0195	0.0195	0.0195	0.0195
197	-0.0196	0.0196	0.0196	0.0196
198	-0.0197	0.0197	0.0197	0.0197
199	-0.0198	0.0198	0.0198	0.0198
200	-0.0199	0.0199	0.0199	0.0199
201	-0.0200	0.0200	0.0200	0.0200
202	-0.0201	0.0201	0.0201	0.0201
203	-0.0202	0.0202	0.0202	0.0202
204	-0.0203	0.0203	0.0203	0.0203
205	-0.0204	0.0204	0.0204	0.0204
206	-0.0205	0.0205	0.0205	0.0205
207	-0.0206	0.0206	0.0206	0.0206
208	-0.0207	0.0207	0.0207	0.0207
209	-0.0208	0.0208	0.0208	0.0208
210	-0.0209	0.0209	0.0209	0.0209
211	-0.0210	0.0210	0.0210	0.0210
212	-0.0211	0.0211	0.0211	0.0211
213	-0.0212	0.0212	0.0212	0.0212
214	-0.0213	0.0213	0.0213	0.0213
215	-0.0214	0.0214	0.0214	0.0214
216	-0.0215	0.0215	0.0215	0.0215
217	-0.0216	0.0216	0.0216	

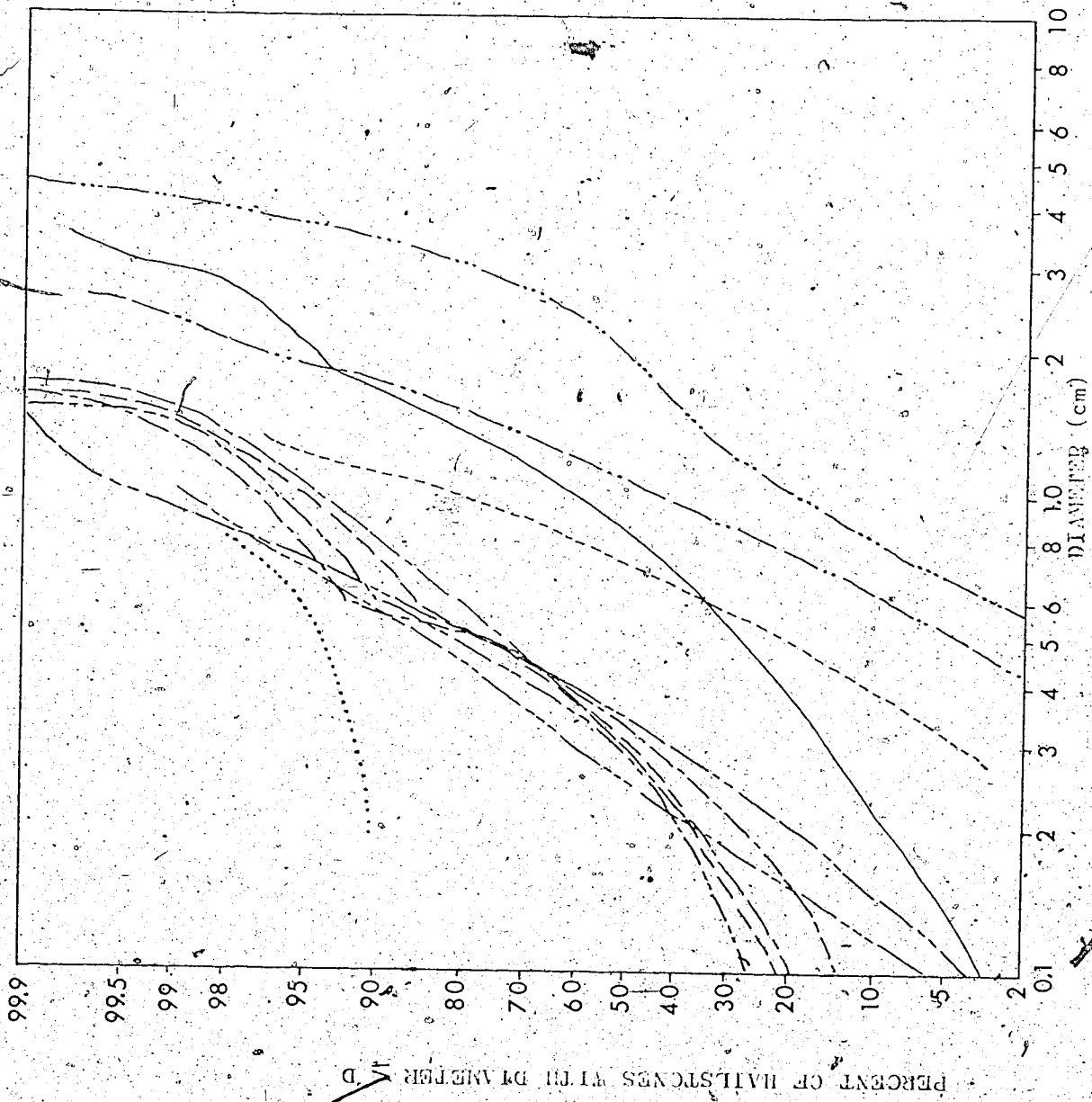
50	-9.00
51	4.63
52	-4.62
53	5.86
54	5.56
55	7.437
56	5.16
57	5.77
58	13.82
59	7.45
60	23.64
61	13.65
62	8.52
63	10.63
64	-0.00
65	6.54
66	2.52
67	8.63
68	7.76
69	6.71
70	7.65
71	14.95
72	17.48
73	12.02
74	-6.60

APPENDIX IV

LOG-NORMAL DISTRIBUTIONS
FOR INDIVIDUAL STORM SAMPLES

FIGURE A2. Log-normal size distributions of the hail collected at individual sample sites. The lines correspond to the following sampling occasions.

— 1973
— 1974
— · — 23 July 1973
— · — 23 August 1973
— · — 27 August 1973
· · · · · 2 July 1974
· · · · · 24 June 1974
— · — 5 July 1974
— · — 9 July 1974
· · · · · 18 August 1974
· · · · · 18 August 1974



APPENDIX V
FLUX DENSITY,
CONCENTRATION
AND SIZE SPECTRA
OF SEQUENTIAL HAIL SAMPLES

PLASTIC LIGAMENT (mm)

	1	2	3	4	5	6	7	8	9	10	11	12	13	14	15
1.	0	0	0	0	0	0	0	0	0	0	0	0	0	0	0
2.	71	54	60	59	37	46	5	5	3	1	2	4	0	0	0
3.	1120	1013	672	1146	714	554	43	117	48	48	26	37	16	20	20
4.	1902	561	689	605	602	922	37	55	48	40	53	53	53°	37	64
5.	1674	730	654	1477	614	304	74	138	23	42	5	37	74	42	42
6.	0	0	0	0	0	0	0	0	0	0	0	0	0	0	0
7.	0	0	0	0	0	0	0	0	0	0	0	0	0	0	0
8.	0	0	0	0	0	0	0	0	0	0	0	0	0	0	0
9.	0	0	0	0	0	0	0	0	0	0	0	0	0	0	0
10.	0	0	0	0	0	0	0	0	0	0	0	0	0	0	0
11.	0	0	0	0	0	0	0	0	0	0	0	0	0	0	0
12.	255	226	149	96	60	54	28	12	8	16	8	4	0	0	0
13.	0	0	0	0	0	0	0	0	0	0	0	0	0	0	0
14.	0	0	0	0	0	0	0	0	0	0	0	0	0	0	0
15.	0	0	0	0	0	0	0	0	0	0	0	0	0	0	0
16.	0	0	0	0	0	0	0	0	0	0	0	0	0	0	0
17.	60	124	68	133	48	72	68	48	8	8	4	0	0	0	0
18.	145	222	157	24	52	5	0	0	4	0	0	0	0	0	0
19.	0	177	184	0	164	133	0	153	0	149	133	0	02	0	52
20.	472	165	327	146	141	49	68	24	32	0	12	4	4	0	0
21.	169	226	157	88	101	30	60	12	20	20	4	3	0	0	0
22.	153	274	133	177	121	72	32	20	4	4	0	0	0	0	0
23.	0	62	212	6	113	26	0	56	0	32	32	0	24	0	12
24.	315	254	161	149	163	113	105	95	30	32	48	24	48	12	12

THE TESTIMONY OF THE TEMPLARS (M.W.)

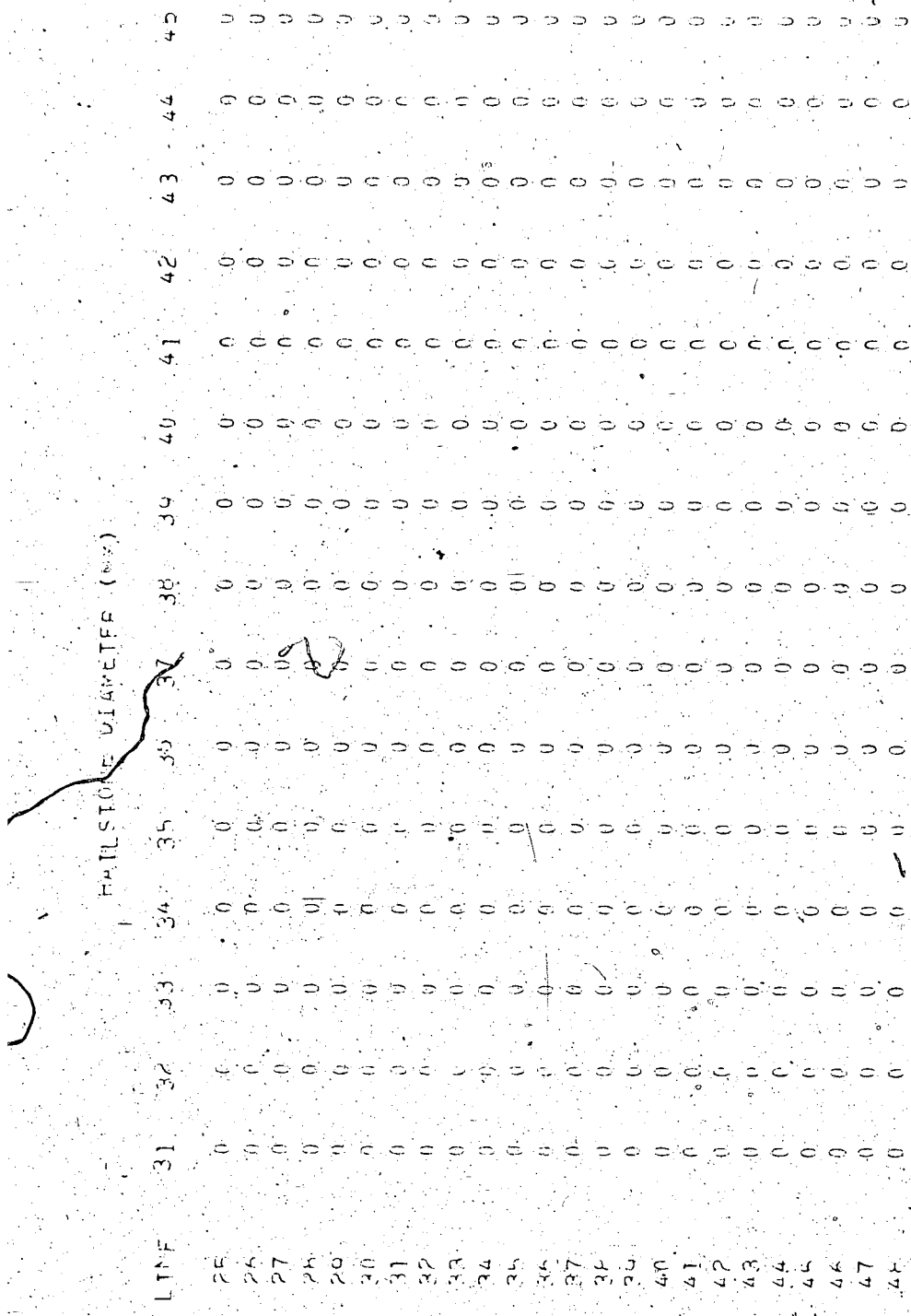
HAILSTONE DIAMETER (MM)

1	0
2	0
3	0
4	0
5	0
6	0
7	0
8	0
9	0
10	0
11	0
12	0
13	0
14	0
15	0
16	0
17	0
18	0
19	0
20	0
21	0
22	0
23	0
24	0
25	0
26	0
27	0
28	0
29	0
30	0
31	0
32	0
33	0
34	0
35	0
36	0
37	0
38	0
39	0
40	0
41	0
42	0
43	0
44	0
45	0

MARLSTONE DIAMETER (mm)

LINE	1	2	3	4	5	6	7	8	9	10	11	12	13	14	15
25	252	311	274	282	278	40	36	40	36	12	16	4	12	6	
26	137	157	311	133	72	50	68	92	25	4	24	0	12	12	
27	514	275	286	285	91	165	45	119	18	64	27	15	9	9	
28	146	165	129	64	9145	121	52	10	40	32	12	4	0	0	
29	17	240	230	426	145	135	113	72	52	32	52	12	0	4	
30	723	467	161	423	404	351	32	76	36	20	4	36	8	8	
31	1301	676	313	141	161	727	10	44	24	4	32	56	4	4	
32	242	277	0	242	214	202	113	101	76	0	60	24	24	24	
33	6	6	6	4	9	12	4	12	4	0	0	0	0	0	
34	0	0	6	20	10	20	10	20	13	24	20	20	0	0	
35	0	0	0	6	20	20	17	21	24	13	27	10	3	0	
36	0	0	0	0	3	3	3	3	10	24	3	6	3	0	
37	0	0	0	0	3	7	7	7	10	0	3	0	0	0	
38	0	0	0	0	0	3	0	3	6	0	0	0	0	0	
39	0	0	0	0	0	7	7	0	3	0	0	0	0	0	
40	137	151	137	151	13	0	0	0	0	0	0	0	0	0	
41	0	26	6	6	6	6	6	0	20	6	0	0	0	0	
42	0	0	0	0	0	0	0	0	0	0	20	0	0	0	
43	393	117	0	0	0	0	0	0	0	0	0	0	0	0	
44	1	1	2	4	10	11	11	3	6	1	2	0	0	0	
45	3	16	34	36	37	25	13	6	1	2	0	0	0	0	
46	26	65	17	4	7	0	0	0	0	0	0	0	0	0	
47	1	19	19	18	31	18	14	4	5	0	0	0	0	0	
48	5	22	53	34	24	7	2	2	0	0	0	0	0	0	

ESTATE PLANNING (REV.)



11

THE JOURNAL OF THE AMERICAN ECONOMIC ASSOCIATION

HISTOGRAMMEN (S. 72).

ESTATE PLANNING (1985)

ESTATE PLANNING

ESTATE PLANNING

HAIL STONE DIAMETER (mm)

	1	2	3	4	5	6	7	8	9	10	11	12	13	14	15
25	4.34	5.12	4.56	3.70	4.63	1.50	5.6	6.0	5.6	6.0	2.6	1.3	6	2.0	
26	2.25	2.61	5.16	2.21	1.26	1.00	1.13	1.53	6.0	4.6	3.3	4.0	0	0	2.0
27	8.56	4.65	4.43	4.43	1.61	2.75	7.5	1.95	3.0	1.05	4.5	5.0	7.5	1.5	
28	2.44	3.05	2.15	1.06	2.41	2.91	8.6	2.6	6.6	5.3	2.0	1.3	6	0	
29	3.22	4.63	3.53	7.13	2.41	2.21	1.88	1.20	8.6	5.3	2.0	1.3	0	0	6
30	1.205	7.13	2.55	1.205	6.73	5.65	5.3	1.26	5.0	3.5	6	6.0	1.5	9.3	1.3
31	2.258	11.36	5.31	2.35	2.68	1.271	2.5	7.3	4.0	6	5.3	6	4.0	4.0	
32	4.03	4.63	0	4.03	3.46	3.30	1.88	1.63	1.26	0	1.00	4.6	4.6	4.0	-3.2
33	0	6.	0	6.	6.	2.0	4.6	5.6	2.0	6	0	0	0	0	0
34	0	0	0	1.0	3.3	1.6	3.3	5.1	2.1	4.0	3.3	3.3	0	0	0
35	0	0	0	1.0	1.6	3.3	2.7	4.5	4.0	2.1	4.5	1.1	2.1	1.6	5.
35	0	0	0	0	2	5	7	4.0	1.6	4.0	5	1.0	5	5	0
37	0	0	0	0	4	1.1	1.1	1.9	0	5	0	0	0	0	0
38	0	0	0	0	5	0	0	5	0	0	0	0	0	0	0
39	0	0	0	0	0	1.1	1.1	0	0	0	0	0	0	0	0
40	2.25	2.61	2.1	0	0	0	0	0	0	0	0	0	0	0	0
41	0	0	3.3	1.0	1.0	1.0	1.0	1.3	1.0	0	0	0	0	0	0
42	0	0	0	0	0	0	0	0	0	0	0	0	0	0	0
43	6.65	1.95	0	0	0	0	0	0	0	0	0	0	0	0	0
44	1	1	3	6	1.6	1.6	1.6	1.6	5	1.3	0	0	0	1	0
45	6	2.6	5.6	6.0	6.1	4.3	2.1	1.0	3.0	1	0	0	0	0	0
45	3.3	4.1	2.8	6	1.1	0	0	0	0	0	0	0	0	0	0
47	1	3.1	31	5.1	39	23	6	8	0	0	0	0	0	0	0
48	1.0	7.0	8.8	5.6	4.9	1.1	3	0	1	0	0	0	0	0	0

CHILD STONE - 01 AUGUST (200)

HATSTONÉ DIAMETER (mm)

HALL STONE DIALECTS (WV.)

130 a.

LIMESTONE DIAMETERED (in.)

1	18	17	16	15	14	13	12	11	10	9	8	7	6	5	4	3	2	1	24	25	26	27	28	29	30
29	40	41	42	43	44	45	46	47	48	49	50	51	52	53	54	55	56	57	58	59	60	61	62	63	64
65	66	67	68	69	70	71	72	73	74	75	76	77	78	79	80	81	82	83	84	85	86	87	88	89	90
91	92	93	94	95	96	97	98	99	100	101	102	103	104	105	106	107	108	109	110	111	112	113	114	115	116
117	118	119	120	121	122	123	124	125	126	127	128	129	130	131	132	133	134	135	136	137	138	139	140	141	142

2

HALSTON DIAMETEP (m)

45	44	43	42	41	40	39	38	37	36	35	34	33	32	31	30	29	28	27	26	25	24	23	22	21	20	19	18	17	16	15	14	13	12	11	10	9	8	7	6	5	4	3	2	1	0
45	44	43	42	41	40	39	38	37	36	35	34	33	32	31	30	29	28	27	26	25	24	23	22	21	20	19	18	17	16	15	14	13	12	11	10	9	8	7	6	5	4	3	2	1	0
45	44	43	42	41	40	39	38	37	36	35	34	33	32	31	30	29	28	27	26	25	24	23	22	21	20	19	18	17	16	15	14	13	12	11	10	9	8	7	6	5	4	3	2	1	0
45	44	43	42	41	40	39	38	37	36	35	34	33	32	31	30	29	28	27	26	25	24	23	22	21	20	19	18	17	16	15	14	13	12	11	10	9	8	7	6	5	4	3	2	1	0
45	44	43	42	41	40	39	38	37	36	35	34	33	32	31	30	29	28	27	26	25	24	23	22	21	20	19	18	17	16	15	14	13	12	11	10	9	8	7	6	5	4	3	2	1	0

HANDBLOCK DIATETES (66)

LINE	1	2	3	4	5	6	7	8	9	10	11	12	13	14	15
1	0	0	0	0	0	0	0	0	0	0	0	0	0	0	0
2	107	71	78	124	41	35	10	5	2	4	7	2	5	3	0
3	27	51	71	84	55	72	4	2	2	3	6	7	1	3	5
4	210	166	126	215	134	134	22	5	7	10	10	10	7	12	0
5	353	94	122	161	113	113	15	9	4	10	10	10	7	14	0
6	314	137	104	277	115	115	14	26	10	0	0	0	0	0	0
7	0	6	0	9	0	0	0	0	0	0	0	0	0	0	0
8	70	6	0	3	0	0	2	2	1	0	0	0	0	0	0
9	0	6	0	6	0	0	0	0	0	0	0	0	0	0	0
10	0	0	0	0	0	0	0	0	0	0	0	0	0	0	0
11	0	0	0	0	0	0	0	0	0	0	0	0	0	0	0
12	0	0	0	0	0	0	0	0	0	0	0	0	0	0	0
13	0	0	0	0	0	0	0	0	0	0	0	0	0	0	0
14	0	0	0	0	0	0	0	0	0	0	0	0	0	0	0
15	0	0	0	0	0	0	0	0	0	0	0	0	0	0	0
16	0	0	0	0	0	0	0	0	0	0	0	0	0	0	0
17	15	32	22	33	12	11	17	1	2	2	2	2	0	0	0
18	45	22	55	34	17	13	2	0	1	0	0	0	0	0	0
19	31	44	47	6	42	33	0	34	0	0	0	0	0	0	0
20	117	42	96	37	45	12	22	6	0	3	3	3	2	1	0
21	42	56	56	39	22	22	9	15	3	5	5	5	1	2	0
22	35	65	53	44	30	13	5	5	5	1	1	0	0	0	0
23	0	23	0	26	14	0	14	0	8	8	8	8	0	6	0
24	24	78	63	45	37	40	23	25	24	9	9	9	12	0	0

HATLICHTENBERG (1981)

MILLSTONE DISTANCE (ft.)

31	0
32	0
33	0
34	0
35	0
36	0
37	0
38	0
39	0
40	0
41	0
42	0
43	0
44	0
45	0
46	0
47	0
48	0
49	0
50	0
51	0
52	0
53	0
54	0
55	0
56	0
57	0
58	0
59	0
60	0
61	0
62	0
63	0
64	0
65	0
66	0
67	0
68	0
69	0
70	0
71	0
72	0
73	0
74	0
75	0
76	0
77	0
78	0
79	0
80	0
81	0
82	0
83	0
84	0
85	0
86	0
87	0
88	0
89	0
90	0
91	0
92	0
93	0
94	0
95	0
96	0
97	0
98	0
99	0
100	0
101	0
102	0
103	0
104	0
105	0
106	0
107	0
108	0
109	0
110	0
111	0
112	0
113	0
114	0
115	0
116	0
117	0
118	0
119	0
120	0
121	0
122	0
123	0
124	0

ESTATE PLANNING (M)

HAILSTORM DOWNTIME (hrs)

ILLUSTRATION OF AN ETP (M)

FILE LIST (See [FILE INDEX](#))

HALLSTONE DIAMETERS (28)

HALLSTON PLATE. (1880)